U.S. Department
of Transportation
National Highway
Traffic Safety
Administration

NHTSA

DOT HS 812 997

February 2021

Occupant Dynamics During Crash Avoidance Maneuvers

DISCLAIMER

This publication is distributed by the U.S. Department of Transportation, National Highway Traffic Safety Administration, in the interest of information exchange. The opinions, findings and conclusions expressed in this publication are those of the authors and not necessarily those of the Department of Transportation or the National Highway Traffic Safety Administration. The United States Government assumes no liability for its contents or use thereof. If trade or manufacturers' names are mentioned, it is only because they are considered essential to the object of the publication and should not be construed as an endorsement. The United States Government does not endorse products or manufacturers.

NOTE: This report is published in the interest of advancing motor vehicle safety research. While the report may provide results from research or tests using specifically identified motor vehicle models, it is not intended to make conclusions about the safety performance or safety compliance of those motor vehicles, and no such conclusions should be drawn.

Suggested APA Format Citation:

Reed, M. P., Ebert, S. M., Jones, M. L. H., & Park, B.-K. (2021, February). *Occupant dynamics during crash avoidance maneuvers* (Report No. DOT HS 812 997). National Highway Traffic Safety Administration.

Technical Report Documentation Page

1. Report No. DOT HS 812 997	2. Government Accession No.	3. Recipient's Catalog No.	
4. Title and Subtitle Occupant Dynamics During Crash Avoidance Maneuvers		5. Report Date February 2021	
		6. Performing Organization Code	
7. Authors Matthew P. Reed, Sheila M. Ebert, Monica L.H. Jones, and Byoung-keon D. Park		8. Performing Organization Report No.	
9. Performing Organization Name and Address University of Michigan Transportation Research Institute 2901 Baxter Rd. Ann Arbor MI 48109		10. Work Unit No. (TRAIS)	
		11. Contract or Grant No.	
12. Sponsoring Agency Name and Address National Highway Traffic Safety Administration 1200 New Jersey Avenue SE Washington, DC 20590		13. Type of Report and Period Covered	
		14. Sponsoring Agency Code	
15. Supplementary Notes			

16. Abstract

A test-track study assessed effects of initial posture and position on head motions of front-seat passengers in abrupt vehicle maneuvers. A 12-participant pilot study in a sedan, a minivan, and a pickup truck assessed whether head excursions differed across vehicles. With each experiencing two abrupt braking events, two lane changes, and turn-and-brake maneuvers. Head position was tracked and head center of gravity was estimated from landmarks on a three-dimensional scan of each participant's head and face. Forward head excursion was slightly smaller in the passenger car than in the other two vehicles. No explanation for this finding was apparent; the vehicle kinematics were similar. A larger study with 90 participants was then conducted using a passenger sedan and an SUV with a range of age and body size assigned to blocks of initial conditions. Factors investigated were seat position, foot placement, seat back recline angle, retractor locking, vehicle differences, and effects of leaning inboard on the console armrest or leaning forward while reaching. All 90 experienced two braking events, a right-going lane change, a left-going lane change, and a turn-and-brake maneuver. The two vehicles and the acceleration profiles were similar to both the pilot study and a 2018 study. A functional regression analysis of head CG trajectories on the primary axes of motion provided insight into effects of test and occupant variables on head motion. Parametric corridors were developed that can be used to tune and validate computational models of occupant responses in pre-crash maneuvers. Overall, the results suggest that a range of occupant head locations can be produced by abrupt vehicle maneuvers.

17. Key Words motor vehicle occupants, passengers, behaviors, posture, motion, pre-crash		18. Distribution Statement Document is available to the public from the National Technical Information Service, www.ntis.gov.	
19. Security Classif. (of this report)	20. Security Classif. (of this page)	21. No. of Pages 123	22. Price

Form DOT F 1700.7 (8-72) Reproduction of completed page authorized

TABLE OF CONTENTS

FIGURES

TABLES

ABSTRACT

A test-track study was conducted to assess the effects of initial posture and position on the head motions of front-seat passengers in abrupt vehicle maneuvers. A pilot study with 12 participants was conducted in a sedan, a minivan, and a pickup truck to assess whether head excursions differed across vehicles. Each participant experienced two abrupt braking events, two lane changes, and turn-and-brake maneuvers. Peak vehicle accelerations were about 1 g and 0.7 g in the braking and lane-change events, respectively. Head position was tracked using a custom, semi-automated system that uses a single depth camera. Head center-of-gravity (CG) location was estimated from landmarks identified on a three-dimensional scan of the participant's head and face. Forward head excursion was slightly smaller in the passenger car than in the other two vehicles. No explanation for this finding was apparent; the vehicle kinematics were similar.

A larger study was then conducted using a passenger sedan and an SUV. Ninety men and women with a wide range of age and body size were assigned to test-condition blocks that addressed a variety of initial conditions. The factors investigated were seat position, foot placement, seat back recline angle, retractor locking, vehicle differences, and the effects of leaning inboard on the console armrest or leaning forward while reaching. Each participant experienced two braking events, a right-going lane change, a left-going lane change, and a turn-and-brake maneuver. The two vehicles performed similarly, and the acceleration profiles were similar to both the pilot study and a 2018 study at the same facility.

Greater forward head excursion relative to the seat was observed when the seat was further rearward or reclined, or the feet were placed flat rather than resting on the heels. No difference in forward excursion was noted across vehicles. Forward leaning reduced forward head excursion during braking events, but the head position was more forward than when starting from a standard posture. Younger participants exhibited slightly larger forward excursions, but overall anthropometric effects were small.

Forward lean produced much larger lateral excursions than the standard posture. Recline reduced lateral excursions, as did resting the feet on the heels rather than flat on the soles. Greater outboard excursion was observed in the SUV during the left lane change, possibly because greater space was available than in the sedan. Higher BMI and younger age were associated with slightly larger lateral excursions in some conditions, but anthropometric effects were small compared with the effects of test conditions.

A functional regression analysis of head CG trajectories on the primary axes of motion was conducted. The results provide insight into the effects of test and occupant variables on head motion. Parametric corridors were developed that can be used to tune and validate computational models of occupant responses in pre-crash maneuvers. Overall, the results suggest that a wide range of occupant head locations can be produced by abrupt vehicle maneuvers. More research is needed to assess the robustness of occupant protection systems to this wide range of postures.

1 INTRODUCTION

1.1 Background

Approximately 40-50 percent of crashes are preceded by some sort of vehicle maneuver related to the crash event, such as braking or steering (Stockman, 2016; Ejima et al., 2009). Scanlon et al. (2015) found that nearly 80 percent of drivers involved in intersection crashes performed an evasive maneuver involving steering, braking, or both. In these cases, the vehicle motion may cause occupants to move out of their initial positions, potentially into postures in which the occupant protection systems will be less effective in crashes. Current test procedures for a few extreme "out-of-position" scenarios provide occupant injury predictions for inadvertent air bag deployments in non-moving vehicles. Most current dynamic tests and restraint optimizations are performed using anthropomorphic test devices (ATDs) that are "in-position," i.e., seated nominally.

Abrupt vehicle maneuvers prior to crashes may become more common as crash avoidance technologies that intervene to change vehicle movements become standard equipment on many vehicles in the coming decade. Automated emergency braking (AEB) for frontal crash avoidance is already available on many models, and major manufacturers have announced their intent to include AEB across their fleets. Manufacturers and suppliers have also demonstrated more advanced systems that are capable of rapid steering maneuvers to avoid crashes.

Although the benefits of these technologies for crash reduction and mitigation are beginning to be understood from test-track performance and field data, the effects of these rapid vehicle motions on unaware vehicle occupants have not been well quantified. When the maneuvers are successful in avoiding the crash, the consequences for the occupants are likely to be minimal. However, if a crash occurs despite the crash avoidance intervention, changes in occupant posture and position that result from the maneuvers may influence the performance of the crash protection systems. Understanding the effects of changes in occupant posture that result from pre-crash maneuvers could have immediate benefit as driver-initiated maneuvers prior to crashes are already common.

Recently, NHTSA sponsored a study to examine how alternative starting postures affected crash injury predictions obtained using ATDs. The Advanced Adaptive Restraints Systems program demonstrated the potential to improve occupant protection in flat-frontal and oblique-frontal crashes by tailoring the restraint system performance based on the occupant's characteristics and position. In addition to nominal, in-position tests with small-female, midsize-male, and large-male ATDs, tests and simulations were conducted in three "out-of-position" conditions created by leaning the ATD forward, inboard, or outboard. In each case, the ATD head was shifted by about 100 to 150 mm from the nominal position by inclining the torso. Leaning generally increased the injury risk predicted from ATD responses, with inboard leaning in oblique conditions being particularly challenging for the restraint system.

Because the effects of pre-crash maneuvers on occupants could vary widely, methods for simulating these effects are needed. ATDs have been demonstrated to react unrealistically during vehicle motions typical of pre-crash maneuvers (e.g., Bohman et al., 2011). Consequently, computational human body models that are capable of representing a wide range of responses to

vehicle maneuvers, including the effects of human muscle activations, are being developed (e.g., Ejima et al., 2009; Östh et al., 2012, 2014; Iwamoto et al., 2012; Östhmann & Jakobsson 2016). To support human model development and application, the focus of empirical research in this area has been on the kinematics and muscle responses of human volunteers.

1.2 Previous Research

Several previous studies have gathered data on occupant responses to abrupt vehicle maneuvers. Morris and Cross (2005) conducted a test-track study to investigate the motions of 49 "unaware" front-seat passengers during hard braking, lane changes, and other maneuvers. The testing employed subterfuge and distraction to reduce the participants' awareness of the purpose of the testing. Video was recorded of participants' reactions to maneuvers that began with the participants in various prescribed starting postures. Quantitative analysis of motions was not provided, but the authors reported a strong influence of lower-extremity bracing availability based on pre-maneuver posture.

Ejima et al. (2009) examined muscle activity and associated kinematics in low-speed frontal impacts on a sled. Five young men were tested on a rigid seat with their hands on a steering wheel. Hault-Dubrulle (2011) conducted a driving simulation study to examine responses to an impending collision. The authors documented bracing behaviors prior to simulated crashes, with the occupants pushing against the steering wheel. These behaviors are not possible for passengers and may be unlikely for drivers operating in automated steering modes.

Bohmann et al. (2011) examined the responses of child passengers to vehicle maneuvers. The data demonstrated the strong influence of bracing with the feet on postural control. Schoeneburg et al. (2011) summarized passenger response data from a midsize male volunteer in hard braking. The level of awareness of the occupant was not reported.

Carlsson and Davidsson (2011) examined the responses of 17 men and women to hard braking as drivers and passengers. All were aware of the purpose of the study and had optical targets applied to their heads and chests. Forward excursions for passengers were similar for both automated and driver-initiated braking. The locking of the seatbelt approximately 500 ms into the event appeared to be the primary factor limiting torso and head movement. Peak head excursions were larger for women than for men at the same stature, but the range of responses was more than 100 percent of the mean.

Östh et al. (2013) and Ólafsdóttir et al. (2013) reported a large study of occupant responses to automated braking events of approximately 1.1g for both drivers and passengers, respectively. The bracing behaviors reduced excursions for drivers, and a seatbelt equipped with a reversible pre-tensioner reduced excursions for both drivers and passengers. The participants in this study were aware of the purpose of the testing and were instrumented for motion tracking and electromyography. The 11 men and 9 women who participated in the passenger trials were tested first in the driver seat. The data showed a large amount of variability in excursions due to braking. The range of peak head excursions was about 200 percent of the mean value.

Kirchbichler et al. (2014) measured front passenger motions in a range of braking and lane-change maneuvers with a total of 51 men and 6 women. The vehicle was equipped with a passive

optical motion capture system and participants wore a specially designed suit with markers. The first test series was conducted with a flat rigid seat and a lap belt only. The second series included a more realistic seat. Some trials are described as "unaware" in the sense that the participants were not explicitly warned that the maneuver was about to begin. However, the overall level of test preparation was high, so that the initial state of the participant may have been quite different from a typical vehicle passenger.

Huber et al. (2015) presented additional data from the Kirchbichler et al. test series, focusing on data from 19 men and 6 women in braking and lane-change-with-braking maneuvers. The data collection methods and limitations were the same as those presented by Kirchbichler the previous year. The data demonstrate a large amount of variability between individuals, such that the range ±1 standard deviation (SD) spans more than 50 percent of the mean forward excursion for hard braking events. For head angle change, 2 SD is greater than the mean change from the starting posture.

In 2017 our research group at UMTRI conducted the largest study to date of occupant responses to abrupt vehicle maneuvers (Reed et al., 2018, hereafter referred to as the 2018 study). The primary goals of the study were to (1) assess the differences in response between aware and unaware passengers by comparing the first exposure with subsequent exposures, and (2) gather data from a large, diverse sample that would enable the assessment of the effects of passenger characteristics on outcomes.

A total of 87 men and women with a wide range of body size and age from 18 to 70 were recruited from the local community. Informed consent was obtained with a protocol that emphasized subjective assessment of vehicle ride, obfuscating the primary objective. Standard anthropometric data was obtained from each participant and whole-body 3D surface data was captured using UMTRI's VITUS laser scanner. In-vehicle testing was conducted at Mcity, a University of Michigan test facility adjacent to UMTRI. Participants sat in the right front passenger seat of a 2015 Toyota Avalon with the seat positioned full rearward on the track and wore the safety belt in a prescribed, optimal position.

The vehicle was equipped with an inertial measurement unit to record vehicle accelerations and a novel motion-capture system developed at UMTRI that uses a single Microsoft Kinect version-2 sensor to obtain 3D motion data (Park et al., 2019). The Kinect V2 uses a time-of-flight laser system to obtain a fast, accurate depth field that is converted via a calibration to a dense 3D point cloud. The calibrated system has head tracking accuracy comparable to optical motion capture systems but requires no markers on the subject or manual post-processing (Figure 1). A 3D scan of the participant's head obtained prior to testing is fit to the 3D data from the sensor to obtain position and orientation. Root-mean-square-error values relative to benchmark video tracking are between 1.5 and 3 mm depending on the distance to the sensor.

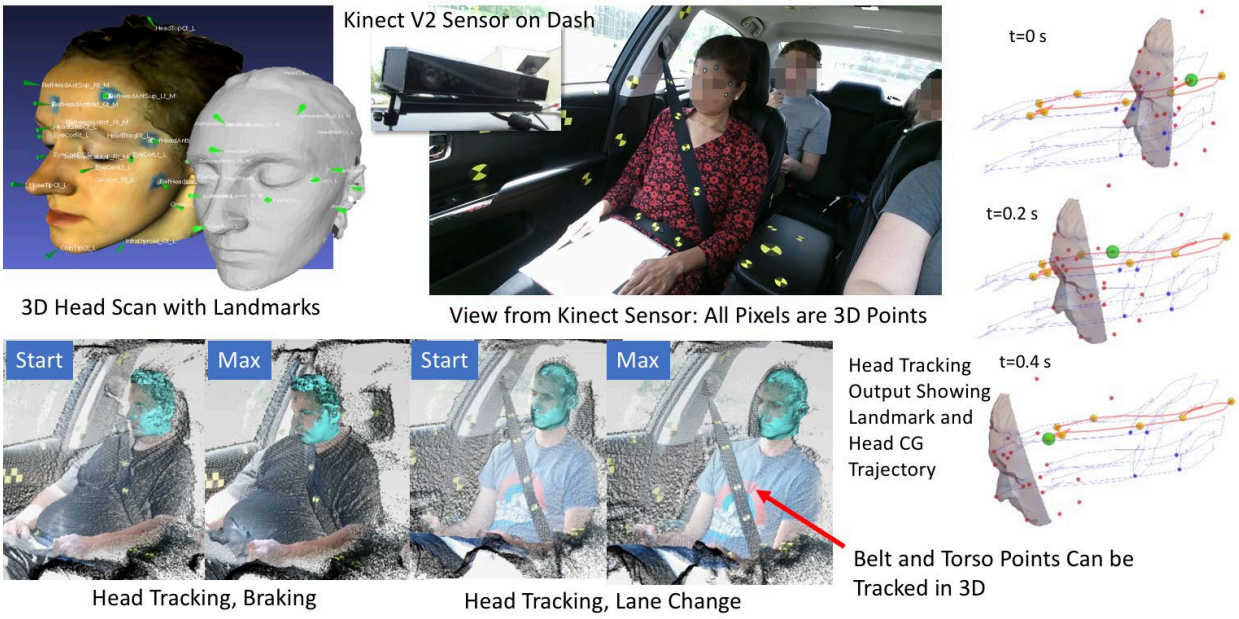

Figure 1. In-vehicle automated posture tracking using UMTRI's Kinect-based system.

Prior to testing, a 3D head scan is obtained using a handheld scanner in about one minute. Landmarks are manually picked on the scan to enable estimation of head CG location. In the vehicle, our software system uses the Kinect sensor to record 3D data and video at 30 Hz. Using an automated method, we fit the head scan to the subject's dynamic data, obtaining an accurate 3D representation of head position and orientation over time. We can also track the 3D coordinates of any point in the scene over time, for example points on the belt or torso, relative to the subject or vehicle.

After several minutes on the course, during which time they answered oral and written questions concerning the vehicle ride and handling, the participants were subjected to a 1-g, maximal braking event from 56 kh/hr (35 mph). The ride continued for about 5 minutes, during which a rapid rightward lane change, a sharp right turn with braking to a stop, and a second linear hard braking event were conducted. Head excursion data from the four abrupt vehicle maneuvers were analyzed.

Consistent with previous studies with smaller samples, the variance in head excursions across subjects was a large percentage of the mean excursions. The mean (SD) of maximal head CG excursions in braking, lane-change, and turn-and-brake events were 160 (50) mm, 118 (40) mm, and 131 (35) mm, respectively. Forward head excursions in the first, "unaware" braking event were significantly larger than in the second, but the difference (18 mm) was small relative to the standard deviation across subjects.

Head excursions were found to be only moderately related to passenger attributes. Forward head excursion in braking was significantly related to age and body mass index ($p<0.01$), but these factors accounted for only about 20 percent of variance. Participant stature was significantly related to lateral excursion in the lane-change and turn-and-brake trials ($p<0.01$) but accounted

for only about 5 percent of the variance. No other participant attributes were important predictors. Men and women did not exhibit different responses after accounting for body size.

The data was analyzed to develop statistical models of the participant kinematics. For example, Figure 2 shows kinematic corridors for forward head excursion in 1-g braking and lateral head excursion in a rightward lane-change. The individual subject curves show the large variability in subject response to vehicle motions that are very similar.

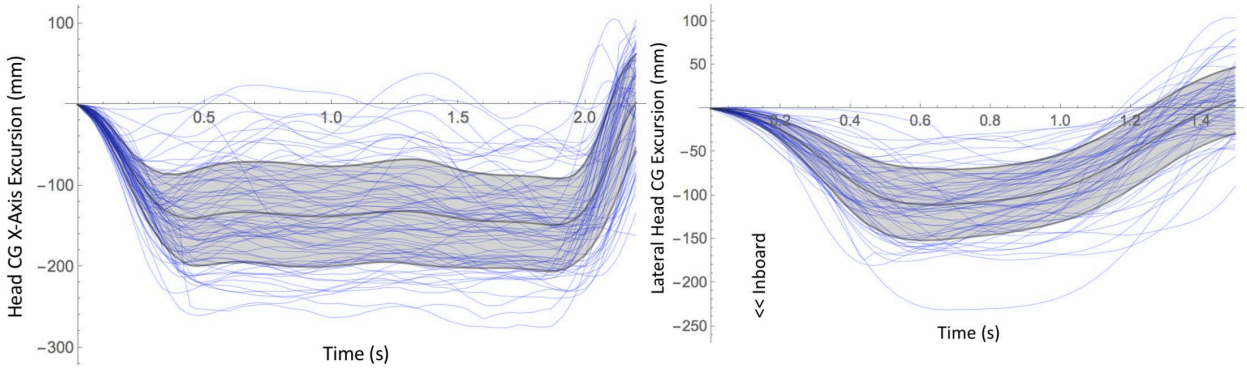

Figure 2. Corridors (mean±sd) for forward head excursion in 1-g braking (left) and inward head excursion in rightward lane change (right). Individual trial data is shown in light lines (Reed et al., 2018).

The conclusions from this UMTRI study included:

1. Head motions in the vehicle maneuvers studied are largely under the control of the passengers

2. Head motion relative to the torso and head angle changes are minimal.

3. The variance in head excursion is large. The range of fore-aft head CG excursions in braking, for example, extended from zero to 280 mm in this study.

4. Kinematic responses in the conditions studied are only modestly related to passenger attributes, such as age and body mass index; instead, passenger behaviors determine the responses.

5. The initial, “unaware” braking trial produced significantly higher excursions, but the difference was less than half of the within-condition population standard deviation.

6. The console adjacent to the passenger provided support during lateral accelerations and probably reduced excursions.

A related study was conducted by Ohio State, Children’s Hospital of Philadelphia, and the University of Virginia. A test track study was conducted with 12 children and the same number of adults. Participants were seated in the rear seat of sedan and subjected to a range of vehicle maneuvers. A marker-based optical motion capture system was used to track head and torso motions, and muscle activity was monitored using surface electromyography. The first results were published in September 2018 at the International Research Council on Biomechanics of

Injury (IRCOBI) conference. Graci et al. (2018) reported kinematics and EMG data for a constant-radius right turn sustained at approximately 0.5 g lateral acceleration for 30 seconds. Data from 9 adults and 5 children 9 to 12 years old were reported. During the initial, transient phase of the maneuver, children had smaller lateral head excursions than adults, even after simple scaling for sitting height. However, head excursions during the steady-state portion of the experiment were not significantly different between subject groups.

Holt et al. (2018) presented preliminary results from a lateral study of volunteer kinematics during exposure to lateral oscillations. Head and torso excursions from 19 adults were recorded using an optical motion capture system during a series of lateral oscillations peaking at approximately 0.7 g. Voluntary bracing and a motorized pre-tensioning seat belt reduced lateral excursions, but deployable seat bolsters did not. The greatest excursions were observed during the first cycle of the test apparatus.

Ghaffari et al. (2018) presented the data from a test track study, focusing on male passenger kinematics in lane-change maneuvers with and without braking. Head and torso excursions were measured for nine men using an optical camera system. Lateral and fore-aft excursions were similar to those observed in previous studies with similar lane-change or braking exposures (e.g., Ólafsdóttir et al., 2013, Reed et al., 2018), and similar standard deviations were observed. As in the previous work, the motorized seat belt reduced excursions significantly.

1.3 Summary of Literature

The previous studies support the following observations and conclusions concerning occupant kinematics during abrupt vehicle maneuvers.

Responses are highly variable: All previous studies have shown that the standard deviation of head excursion in braking or lane change events is at least 50 percent of the mean value.

Responses are volitional: One contributor to the relatively high variability is that the responses are due to posture-maintenance tactics adopted by the person, and these can vary widely. For example, in the UMTRI study, many participants looked up from the questionnaire taped to their thighs when the braking event began and then looked back down. The inertial forces produced by vehicles on road, even during abrupt maneuvers, are relatively small, well within typical activities of daily living. The ~1 g acceleration on the head during abrupt braking, for example, produces a force on the neck similar to the force encountered when a person bends over 90 degrees from the waist.

Pre-tensioning (motorized) seat belts reduce excursions: Several in-vehicle studies and at least one lab study have shown that removing slack and pre-tensioning the seat belt tends to reduce excursions. However, considerable variance in responses remains. This finding is consistent with the observation that most passengers tend to “ride” the locked belt during braking, with the torso substantially engaged by the belt. With less belt slack, the torso and head excursions are reduced.

1.4 Knowledge Gaps and Objectives

Based on the prior state of knowledge in this area, we identified the following gaps as appropriate topics for further research:

Gap 1: Effects of Initial Posture and Position

In our recent testing, and in most other testing of which we are aware, the acceleration events have started with the participants normally seated. Although this is reasonably representative of most vehicle occupant postures, alternative postures may represent disproportionate risks. Consequently, we have identified the following postures of interest: (1) leaning inboard, (2) reaching forward, and (3) reaching obliquely toward the center console.

We also note that several earlier studies have noted the importance of foot placement for torso stability in children (e.g., Bohmann et al., 2011). In our recent study, participants rested their feet on the heels. A posture with the feet flat on the vehicle floor and pulled rearward may reduce postural control and lead to greater excursions.

The fore-aft seat position relative to the belt anchorages is also of interest. The recent UMTRI data showed slightly smaller excursions for individuals whose heads started further forward in the vehicle (all participants used the same seat position). One possibility is that the effectively more-rearward D-ring location these participants experienced increased the efficacy of torso restraint and reduced forward excursion. This can be addressed experimentally by shifting the seat forward relative to the fixed D-ring location.

Reclined postures are also of interest. When passengers recline, the relationship between the torso and a belt mounted on the vehicle body can change dramatically, which may affect forward motions in braking. The greater body weight borne on the seat back could also affect lateral excursions.

Gap 2: Effects of Lateral Support

Our data collection showed that the participants in the front passenger seat contacted the center console and may have gained substantial lateral support from it during lane-change and turning maneuvers. Consequently, quantifying the potential effects of removing this support are important. Also, lateral outboard motions have been examined in several other studies, including the latest Volvo work, but gathering data for left-going lane changes with the current methodology would provide a broader dataset.

Gap 3: Older Children and Smaller Adults in Front Seats

Several previous studies, including the recent OSU/CHOP/UVA study, have examined the kinematics of children with and without booster seats in vehicle second-row seats. We are not aware of any studies that have measured the postures and kinematics of children in front seats. Studying children 13 to 16 years old who are smaller than most adults (below 1,500 mm [59 inches] in stature) is a priority because their small size relative to the seating environment may result in large excursions.

Gap 4: Effects of Vehicle Type

Most testing to date in this domain has been conducted using passenger sedans. The different kinematics of vehicles with higher centers of mass during the maneuvers of interest may result in different occupant kinematics. Seat design and vehicle interior geometry might also affect excursions.

Two studies were conducted to address these gaps. In the *pilot* study, head excursions were compared among three vehicles for 12 participants using a within-subjects design. In the second, *full-scale* study, 90 participants were tested with a wide range of initial conditions that addressed the gaps identified above. Two vehicles were used in some conditions in the full-scale study. The data was analyzed to quantify the effects of passenger characteristics and test conditions on head excursions in lane-change, braking, and turn-and-brake events.

2 METHODS

2.1 Vehicles

In the pilot study, testing was conducted in a 2015 Toyota Avalon passenger car, a 2018 Dodge Caravan minivan, and a 2018 Ford F-150 pickup truck (Figure 1). These vehicles are subsequently referred to as the passenger car, minivan, and truck. The Avalon had leather seats, 4-wheel, antilock braking system, and disc brakes front and rear. The three vehicles were chosen because they had different body styles but are not necessarily representative of any category of vehicle. The Avalon was a different vehicle than the one of the same model used in Reed et al. (2018). All vehicles had conventional emergency locking retractors without motorized pre-pretensioners.

In the full-scale study, testing was conducted in the Avalon used in the pilot study as well as a 2014 Jeep Grand Cherokee Limited, 4-wheel drive, 4-door, SUV, which also had leather seats, a 4-wheel antilock braking system, and disc brakes front and rear.

Figure 3. Test vehicles in pilot study: From left, 2016 Toyota Avalon, 2018 Dodge Caravan, 2018 Ford F-150.

Figure 4. Test vehicles in full-scale study: 2016 Avalon (left) and 2014 Jeep Grand Cherokee (right).

Measurements of the seat and vehicle interior geometry were made using the SAE J826 H-point manikin to establish the seat H-point and seat back angle (SAE A40). In the pilot study, the seat position was set in each vehicle to create similar geometric relationships between the occupant and the upper torso belt anchorage (D-ring) location across vehicles. Specifically, the seat was full rear in the passenger car and moved forward in the minivan and truck to achieve a similar

side-view angle between the D-ring and the seat H-point. The seat back angle was set to 23 degrees in the minivan and truck and 21 degrees in the passenger car.

In the full-scale study, the Avalon seat was set to full-rearward with a 23-degree seat back angle, except where otherwise specified for the particular test condition (see below). The seat in the Grand Cherokee was set to approximately the same H-point-to-D-ring relationship as in the Avalon (see Table 4).

Figure 5. Measuring seat H-point and torso (seat back) angle (left) and seat cushion angle (right) using the SAE J826 manikin and procedures.

2.2 Data Acquisition Equipment

An HD PRo Webcam C920 (PN 960-000764) was mounted to the headliner of the vehicle to monitor foot position, and a MicroStrain 3DM-GX5-10 inertial measurement unit (IMU) was installed near the mass center of the vehicle to quantify the acceleration and rotation rates of the vehicle during events. During testing, linear and rotational accelerations on three axes were recorded from the IMU at 100 Hz and the camera data was recorded at 30 frames per second.

A Microsoft Kinect version 2 sensor was mounted on the dashboard of each vehicle approximately on the centerline, aimed at the right-front (passenger) seat (Figure 6). The Kinect sensor provides 512 × 424-pixel 3D point-cloud data and 1920 × 1080-pixel video data at 30 Hz.

Figure 6. Placement of Kinect sensor in vehicle.

2.3 Head Scanning

Head shape and surface contours were recorded using a hand-held infrared scanner (3D Systems Sense) shown in Figure 7. Prior to scanning, reference points were placed on the participant's forehead and face using non-toxic paint (Table 1 and Figure 8).

Figure 9 shows examples of the head scan data. The location of head landmarks and head tracking targets listed in Table 2 were digitized on the head scans using Meshlab software (http://meshlab.net/).

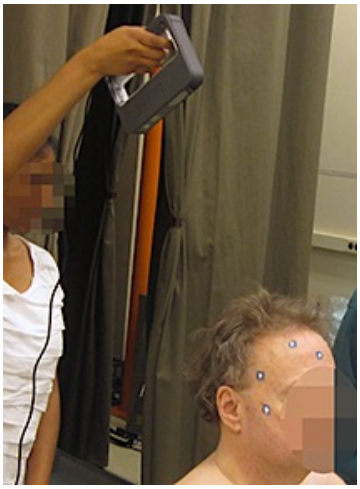

Figure 7. Scanning a participant's head with the hand-held scanner.

Figure 8. Locations of the head targets as seen in a scan of a person's head.

Table 1. Head-Tracking Target Locations

Target	Location
1	Above glabella on the centerline of the face, above where the brow moves with facial expression
2 & 3	On temples, anterior of the hairline (left and right)
4 & 5	Higher on the forehead making a triangle with glabella and temple stamps, placed as superiorly as possible without being covered by hair (left and right)
6 & 7	On the cheekbone, at the tragion height, as far anterior as possible, posterior to skin movement caused by facial expressions (left and right)

Figure 9. Examples of head scans with color texture (left and center) and without (right) to show detail.

Table 2. Landmark and Target Points Digitized in Head Scans

Landmarks	**Head Tracking Targets**
Back of head	Cheekbone, Lt and Rt
Top of head	Temple, Lt and Rt
Gonion, Lt and Rt	Near hairline, Lt and Rt
Tragion, Lt and Rt	Above glabella
Ectoorbitale, Lt and Rt	
Infraorbitale at center of eye Lt and Rt	
Glabella	
Tip of nose	
Tip of chin (mentum)	
Gonion, Lt and Rt)	
Infrathyroid	

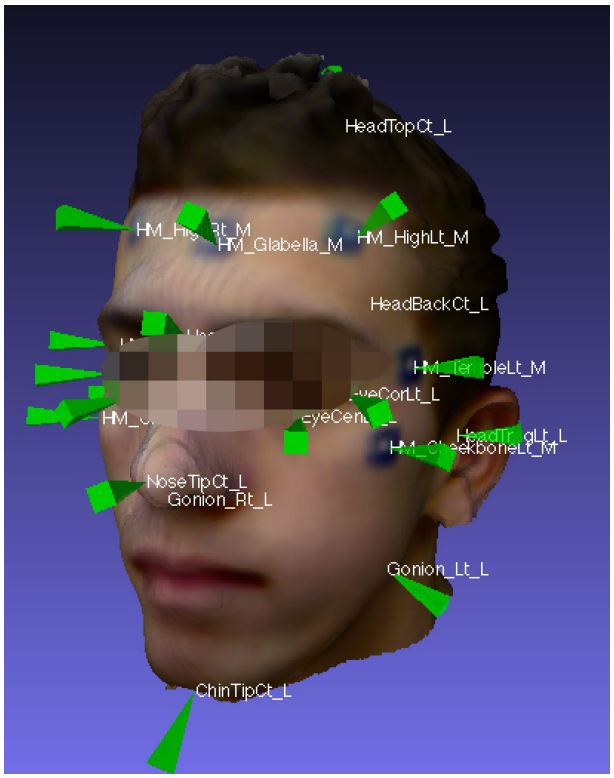

Figure 10. Example of landmarks and head targets digitized in head scans.

2.4 Events with Abrupt Acceleration Exposures

The test driver drove a prescribed route, shown in Figure 11 on a map of the Mcity test facility. During approximately 5 minutes of normal driving, five exposures (abrupt vehicle maneuvers) were presented, always in the same order: braking (B1), turn-and-brake (TB), braking (B2), right-going lane change (L1) and a left-going lane-change (LL). Each braking event (B1 and B2) was conducted using maximum pedal pressure from an initial speed of 56 km/hr (35 mph). In all cases the vehicle antilock brakes engaged. In the pilot study, a second right-going lane-change

maneuver (L2) was conducted instead of the left lane change. L2 differed from L1 in the minivan and truck in that the inboard armrest was raised (made inaccessible). Each lane-change maneuver was conducted at approximately 56 km/hr (35 mph) with recovery to the original travel direction. In the turn-and-brake maneuver, the driver made an abrupt right turn and held the vehicle in the turn while braking aggressively.

Prior to the start of each maneuver, the participants were asked to answer a question read to them aloud or from a questionnaire taped to the lap (in the case of the track position trials) or were asked to reach, lean, or look straight ahead (see test condition definitions). The questions were administered as part of an effort to obfuscate the primary purpose of the study; the results were not analyzed. After each event, the vehicle stopped, and an investigator explained that the maneuver was a simulation of an automated crash avoidance system and asked the participant to compare the severity of maneuver to similar maneuvers they have experienced. Leading into each event the investigator engaged the cruise control to maintain the desired initial speed.

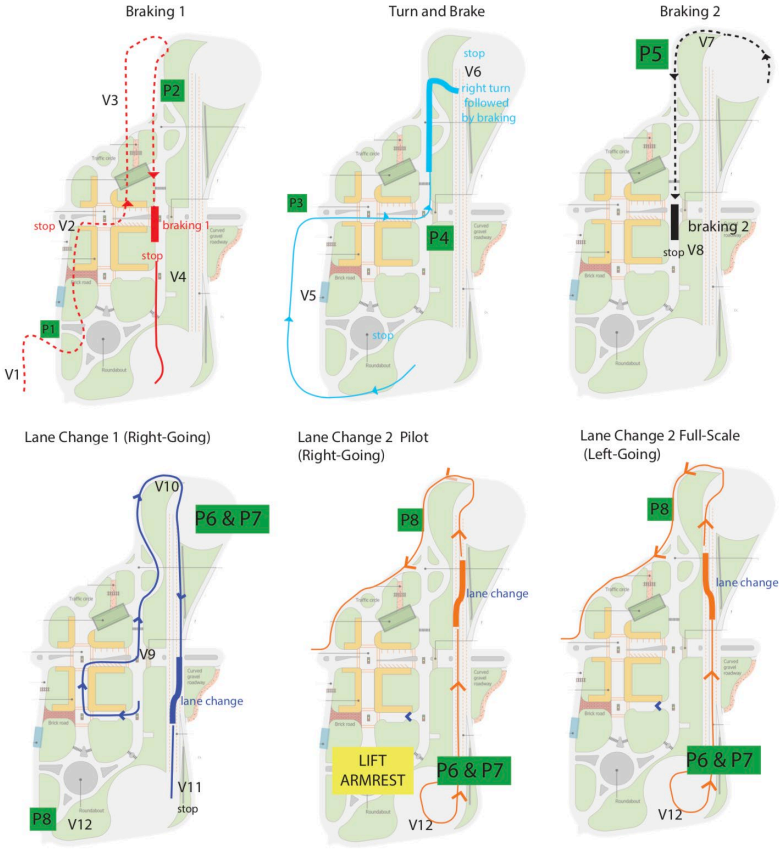

Figure 11. Vehicle route and event positions at Mcity. Events appear from left to right, top to bottom in the order in which they were presented. Braking and lane-change events are conducted on the longest straightaway at an initial speed of 56 km/hr (35 mph). The pilot study used two right lane changes; the full-scale study used a right lane change and a left lane change.

2.5 Head Tracking

Data from the Kinect was used with custom software to track the position and orientation of the occupant's head (see Park et al., 2018, for details of the system development and calibration). The system automatically aligns a 3D scan of the occupant's head to the 3D data obtained at each frame. The head CG location is estimated from landmarks that are manually digitized on the 3D head scan. The mean landmark tracking error over a typical head excursion trajectory is estimated to be 2.4 mm.

Head tracking was accomplished using methods developed in previous studies (Reed et al., 2018; Park et al., 2018). In brief, the Kinect video data was reviewed manually to identify the approximate start and end of each event. The passenger's head location was manually digitized in a 3D frame at the start of the trial to initialize the head tracking algorithm. The head scan data was then automatically aligned to the 3D face data at each frame. The resulting head position and orientation were applied to the head landmark data for each participant.

The head CG location was calculated in a head coordinate frame with the origin at the midpoint between the tragion landmarks, the Y axis to right, and the Z axis perpendicular to the Frankfurt plane. In this coordinate system, the head CG location was estimated on the midsagittal plane and 8.1 mm forward of and 31.5 mm above tragion (Schneider et al., 1983).

Head position could not be tracked successfully in all trials due to issues such as occlusion of the face by the passenger's hand or hair. Forward and inward reaching trials were particularly prone to occlusion. In total, head-CG excursion data was obtained for 1,170 trials. The number of trials available for each condition is presented in the Results section.

The head excursion results are expressed in a right-hand vehicle coordinate system with X positive rearward, Y positive to the occupant's right, and Z positive vertical. The origin is the seat H-point on seat centerline. In some conditions with seat movement, the data was translated to a common seat H-point location to facilitate comparison.

2.6 Test Protocol

The study protocol was approved by an institutional review board for human-subject research at the University of Michigan (HUM00120296). The same experienced test driver performed all maneuvers. Testing was conducted at the University of Michigan's Mcity facility.

Each participant sat in the front passenger position of the test vehicle. The investigator instructed the participants to move all the way back in the seat, and then rock side-to-side a couple of times to "get comfortable," and then slide their feet forward and rest them on their heels (foot position was subsequently changed in some trials). The participants were instructed to rest their palms on their thighs and relax their shoulders. The investigator asked the participants to not use the armrests initially unless the size of the participant required that they had to actively lift their arms to avoid them.

Before placing their arms in the standard posture, the participant put on the seat belt and the investigator adjusted the D-ring height to center the shoulder belt on the participant's clavicle. The investigator then instructed the participant to tighten the seat belt by pulling up on the

shoulder belt near the buckle. If the participant did not tighten the belt or did not place the lap portion of the belt low on the pelvis, the investigator moved the belt and tightened it. The investigator assessed the seat belt fit and, in each case, judged it to be acceptable, based on shoulder belt passing over the approximate center of the shoulder and the overall belt reasonably snug.

Targets were placed on the seat belt webbing where it crossed the sternum, clavicle, and midline of the pelvis (Figure 12). Other targets were placed along the lap and shoulder belt at locations that were visible to the Kinect camera. Participants were asked to keep the head in an "alert position" while the investigator recorded the posture and the location of the seat belt with a FARO Arm.

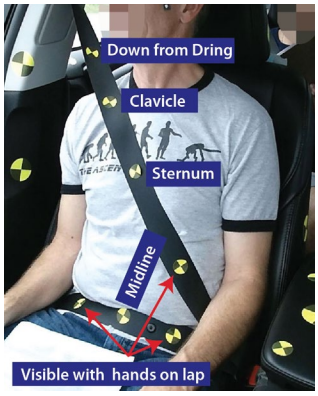

Figure 12. Targets place on belt and vehicle.

2.7 Test Conditions – Pilot Study

In the pilot study, each participant experienced the three vehicles in random sequence. Within each vehicle, the abrupt vehicle maneuvers (exposures) were always conducted in the same sequence noted above.

2.8 Test Conditions – Full-Scale Study

The following sections describe the test conditions for the full-scale study. The test conditions are summarized in Table 3. Each block of test conditions was designed to permit a within-subject assessment of the effects of a particular set of initial conditions across vehicle maneuvers. Each participant was assigned to a particular block of test conditions. The test conditions within each block were presented in random order, except as noted below.

Table 3. Test Conditions

Testing Condition Block	Code	Description	Run Description	Sub Category	Head	D-ring
Seat Position	Aft	Full Aft	Each subject was assigned feet on heels or feet flat	Flat/Heels	Lap	High
Seat Position	Mid	75 mm fwd	--	--	Lap	Mid
Seat Position	For	150 mm fwd	--	--	Lap	Low
Recline	Upp	Upright: 23˚	3 recline angles randomized across rides	None	Alert	High
Recline	Rec	Reclined: 35˚	--	--	HR	High
Recline	Max	More Rec: 47˚	--	--	HR	High
Vehicle	Jp1	Jeep Drive 1	Randomize standard posture and leaning across events	Standard/ Lean Forward	Alert	High
Vehicle	Jp2	Jeep Drive 2	--	--	Alert	High
Vehicle	Av1	Avalon Drive 1	--	--	Alert	High
Vehicle	Av2	Avalon Drive 2	--	--	Alert	High
Retractor	LkM	Locked and 75 mm forward	2 seat track position x 2 retractor conditions	None	Alert	Mid
Retractor	LkF	Locked and 150 mm forward	--	--	Alert	Low
Retractor	OpM	Open and 75 mm forward	--	--	Alert	Mid
Retractor	OpF	Open and 150 mm forward	--	--	Alert	Low
Lean	Dr1	First ride	3 starting postures randomized across events	A/B/Arm	Alert	High
Lean	Dr2	Second ride	--	--	Alert	High
Lean	Dr3	Third Ride	--	--	Alert	High

Notes:

- Category codes: S = standard posture, L = leaning/reaching forward, A= reaching forward, B=reaching forward and inward, Arm = leaning on center-console armrest
- Seat back angle was 23˚ except where noted
- Seat position was full-rear except where noted; seat position in Jeep was adjusted to maximize similarity with Avalon in relationship between D-ring and seat H-point.
- Head positions: Alert=looking forward out windshield; Lap=looking down at questionnaire on lap. The questionnaire was administered orally and answered aloud except for the head=lap conditions.
- D-ring adjustments were made to the extremes available (high and low) to maximize differences in the relationship between the D-ring and shoulder. D-ring adjustments were associated with seat positions, with lower D-ring positions used for more-forward seat positions.

2.8.1 Seat and Foot Position Conditions

The goal of these trials was to evaluate the effects of the relationship between the D-ring and the shoulder on excursions. When the seat is further forward, the belt path from the shoulder to D-ring is angled more rearward, wrapping around the shoulder more, and is also angled more outboard. For thin subjects sitting full rear, the belt often separates from the shoulder near the clavicle, whereas in forward seat positions it wraps over the top of the shoulder. To amplify this effect, the D-ring height was adjusted based on seat position, using the highest D-ring position when the seat was full-rear, middle position for middle seat position, and the lowest D-ring position when the seat was moved forward. The middle seat position was 75 mm forward of full rear and the forward seat position was 150 mm of full rear, except that the seat was moved slightly rearward if the participant's knees were within 25 mm of the knee bolster.

The seat position block was additionally used to evaluate the effects of lower-extremity posture. Each participant was randomly assigned to either have the feet (shoes) resting on the heels, as in previous studies, or with the feet flat on the soles and pulled rearward as much as possible (Figure 13).

Figure 13. Seat track positions rear (left), mid (center), and forward (right) with feet on heels (top) and soles (bottom).

2.8.2 Recline Conditions

The goal of these trials was to evaluate the effects of high levels of recline (Figure 14). Starting with the nominal condition of 23-degree seat back angle (measured as the SAE J826 torso angle), the seat back was reclined an additional 12 degrees (to 35 degrees) and a further 12 degrees (to 47 degrees). Recline conditions were conducted with the seat at the middle position on the seat track. The three recline angles were presented in random sequence, with all maneuvers conducted at each recline angle before moving on to the next recline angle.

Figure 14. Postures in reclined trials: upright (right), mid (center), and reclined (left).

2.8.3 Vehicle Comparison Conditions

Each participant experienced two drives in each vehicle. The participant sat in a neutral posture facing forward and looking out the windshield, except that approximately 5 seconds prior to half of the abrupt events (randomly selected in advance), the participant was asked to reach maximally forward with the left hand (same posture as lean condition A). The conditions were selected so that each participant experienced all five exposures in both vehicles in both initial postures.

The seat position in the Jeep was adjusted to achieve the maximum similarity in D-ring location relative to seat H-point. Table 4 shows the D-ring locations as tested. Figure 15 shows participants in each vehicle.

Table 4. Seatbelt D-ring Location relative to Seat H-point

	X (mm)	Y (mm)	Z (mm)	XZ* Angle (deg)	YZ* Angle (deg)	Cushion Angle (deg)	Seatback Angle (deg)
Jeep	201	282	668	17	23	12.5	23
Avalon	212	244	682	17	20	12.5	23
Difference	-11	38	-14	0	3	0	0

* Angles with respect to vertical of a vector from the D-ring to the seat H-point on seat centerline (XZ=side view, YZ = front view.

Figure 15. Jeep SUV (left) and Avalon sedan (right).

2.8.4 Retractor Conditions

The goal of these trials was to assess the effects of a pre-locked retractor. The belt was locked using the automatic locking (ALR) feature of the seat belt by pulling the belt fully out and then allowing it to retract. Figure 16 shows the process. After the participant was seated in either the middle or forward seat position (Figure 17), the investigator pulled the belt out fully to lock it, then fed it back into the retractor until it was snug over the participant's chest. In unlocked trials, the participant donned the belt as usual. The order of presentation of the two seat positions and locked/unlocked belt were randomized.

Figure 16. Locking the retractor by pulling the belt all the way out switching it from ELR to ALR.

Figure 17. Forward (left) and mid (right) seat track positions.

2.8.5 Leaning/Reaching Conditions

The leaning/reaching conditions were conducted to investigate the effects of non-nominal starting postures. These trials were conducted with the seat track in the middle position and seat back angle at 23 degrees. The participants were coached to assume each of three different postures on a signal. For inboard leaning, the participant was asked to lean maximally inboard

with support from the left forearm or elbow on the center console armrest. For forward leaning, the participant was asked to lean forward as much as possible without upper extremity support. For inward and forward, the participant was asked to reach as far as possible forward toward a tape mark on the center console near the vehicle centerline, touching it if possible. The order of postures was randomized across the five maneuvers, with the drive continuing, and the maneuvers repeated in the same sequence, until each maneuver has been conducted in each posture. The posture was prompted approximately 5 seconds prior to the initiation of the maneuver.

A. Reaching forward

B. Reaching forward near midline of the vehicle

C. Leaning inboard as far as possible while supported on center-console armrest

Figure 18. Lean and reach test conditions from left to right: reaching forward, reaching forward near the midline of the vehicle and leaning as far possible on the armrest without lifting off the seat pan.

2.9 Participant Characteristics

2.9.1 Pilot Study

In the pilot study, data was gathered from 5 men and 7 women 21 to 72 years old. Body mass index (BMI) ranged from 21 to 39 kg/m^2, and stature ranged from 1,522 to 1,784 mm (approximately 8th-percentile-female to 64th-pecentile-male for the U.S. population). Taller participants were excluded to avoid potential knee contact during braking events in the minivan.

2.9.2 Full-Scale Testing

Ninety adults (52 women and 38 men) participated in the study. Table 5 shows the allocation of participants among the test conditions for both the pilot and full-scale studies. Note that the actual number of participants whose data was analyzed for a particular test condition and vehicle maneuver was often smaller than the values in Table 5 due to missing or invalid data. The actual number of participants per test condition for whom data was analyzed is reported in the Results section.

Table 5. Number of Participants in Each Test Condition

Condition	Total	Female	Male	>60 YR	BMI>=30
Pilot (3 Vehicles)	12	7	5	5	4
Full-Scale Study:					
Seat Position (Heels)	13	7	6	6	5
Seat Position (Flat)	12	7	5	3	4
Recline	19	9	10	6	6
Vehicles: Cherokee & Avalon	12	6	6	6	2
Retractor: Locked/Unlocked	17	13	4	7	9
Lean/Reach	17	10	7	5	6
Full-Scale Totals:	90	52	38	33	32
Overall Totals:	102	59	43	38	36

An effort was made to recruit approximately equal numbers of men and women, people older and younger than 60 years, and those above and below a BMI of 30 kg/m^2 within each test-condition block. This effort was not fully successful due to timing and other constraints, but the analysis does not require equal numbers of participants in each cell, only that participant characteristics are broadly distributed. Efforts to recruit participants between 1,450 and 1,500 mm in stature were also largely unsuccessful. These potential participants are mostly 10 to 12 years old and were difficult to reach during summer vacation, when testing was conducted.

Table 6 summarizes the participant age and body measurements. Participants ranged from 14 to 70 years old with a mean of 40 years, and 33 of the participants were 60 or older. Participant age was highly stratified by design, with most participants younger than 30 or older than 60. Participant BMI range was 17 to 49 kg/m^2 with a mean of 26 kg/m^2, and 32 of the participants had BMIs over 30 kg/m^2. Participant stature ranged from 1,512 mm to 1,860 mm. The gender, age, stature, and BMI were approximately balanced across testing conditions. Figure 19, Figure 20, and Figure 21 show stature, weight, gender, and age distributions by test condition block. In testing conditions in which the vehicle seat was moved forward on the seat track only participants with a stature below 1,778 mm (approximately 50th percentile for adult men in the U.S. population) were included to reduce the likelihood of knee bolster contact during testing.

Table 6. Summary of Participant Characteristics

Variable	Mean	SD	Min	5th%ile	50th%ile	95th%ile	Max
Age (yr)	40	21	14	18	27	69	70
Stature (mm)	1,657	105	1,474	1,512	1,632	1,830	1,860
Weight (kg)	74	22	41	46	72	116	145
BMI (kg/m^2)	26	6	17	18	25	39	49
Erect Sitting Height (mm)	876	54	779	801	872	962	1,006

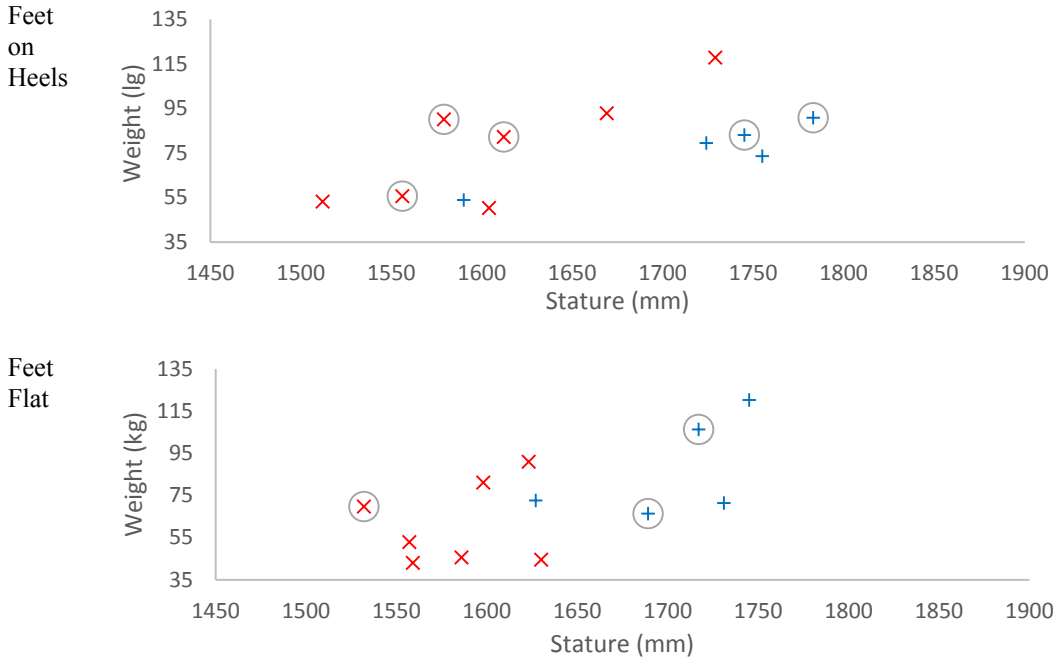

Figure 19. Weight versus stature for track position trials with feet on heels and flat. Data from male and female participants is shown as x and plus symbols, respectively and circled if they were 60 or older.

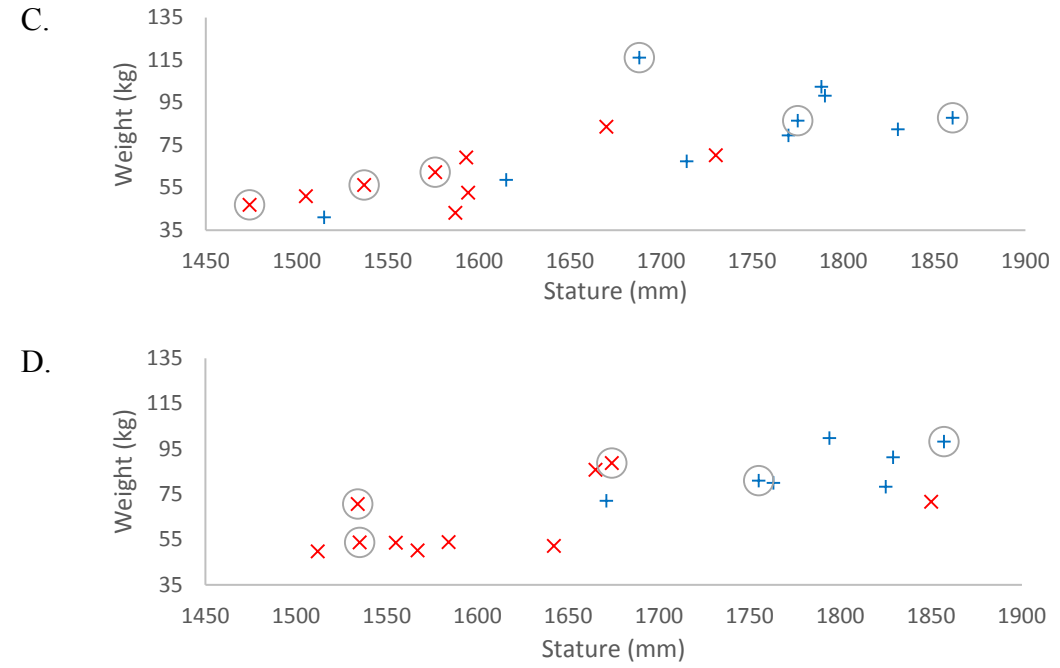

Figure 20. Weight versus stature for trials with different seat back recline angles (C) and different leaning and reaching postures (D). Data from male and female participants is shown as x and plus symbols, respectively and circled if they were 60 or older.

E.

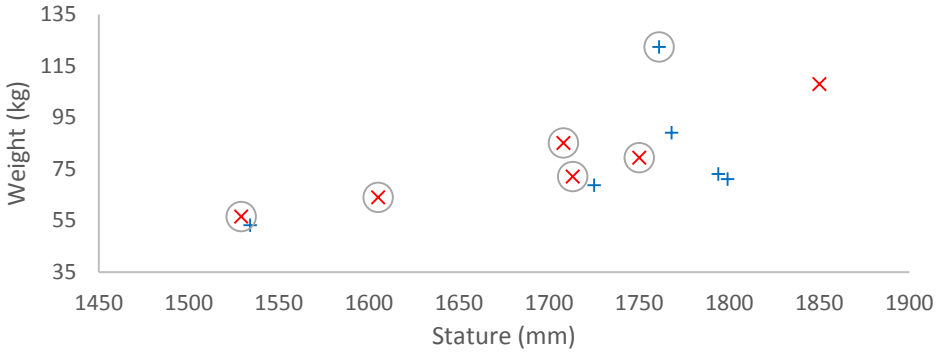

F.

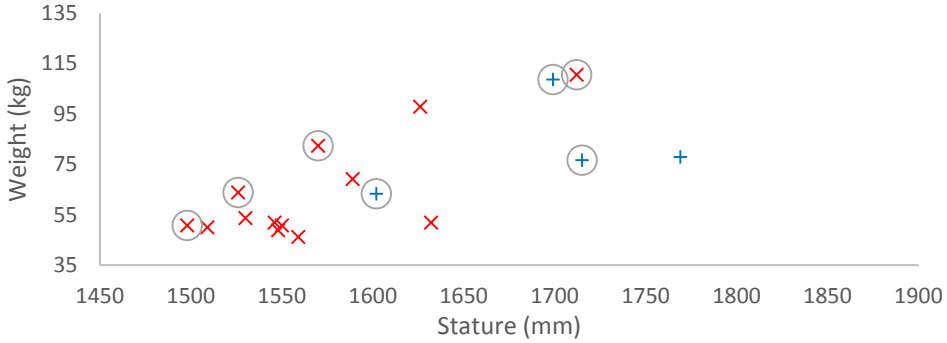

Figure 21. Weight versus stature for sedan-SUV comparison trials (E) and retractor locked/unlocked trails (F). Data from male and female participants is shown as x and plus symbols, respectively and circled if they were 60 or older.

3 RESULTS – PILOT STUDY

3.1 Braking Maneuvers

3.1.1 Vehicle Kinematics

The vehicle accelerations were similar within and across vehicles for the braking maneuvers. Figure 22 shows the longitudinal acceleration for the first braking event in each vehicle. The mean acceleration during the interval from 0.5 to 1.5 seconds into the event (approximately the plateau phase) was -0.89, -0.95, and -0.91 *g* for the minivan, passenger car, and truck. No important differences in acceleration pulse shape were noted across vehicles, although the time to peak was delayed about 200 ms in the passenger car compared to the others.

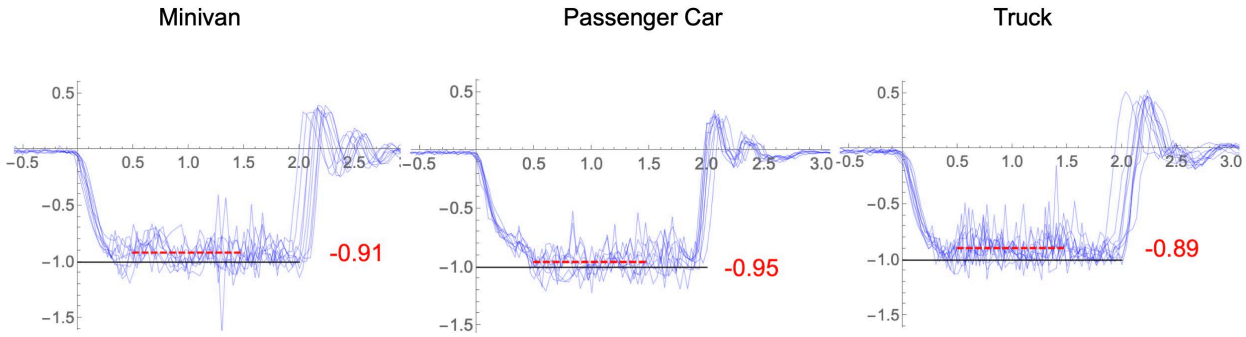

Figure 22. Vehicle longitudinal accelerations (g) during the first braking event. Mean values between 0.5 and 1.5 seconds are shown.

3.1.2 Head Excursions

Figure 23 shows the head CG locations at the start of the first braking event and at the point of maximum forward excursion for each subject across the three vehicles. Table 7 lists the means and standard deviations of head excursions across vehicles. The mean forward excursion in braking was significantly smaller in the passenger car than in the other two vehicles using a paired *t*-test ($p<0.01$). Responses in the minivan and truck were not significantly different. The mean braking excursion in the second event (Figure 24) was consistently smaller than in the first event and significantly smaller when the results were pooled across vehicles ($p<0.01$). The overall mean forward excursion in both the first and second events across vehicles were similar to the results from a single passenger car in the results presented by Reed et al. (2018).

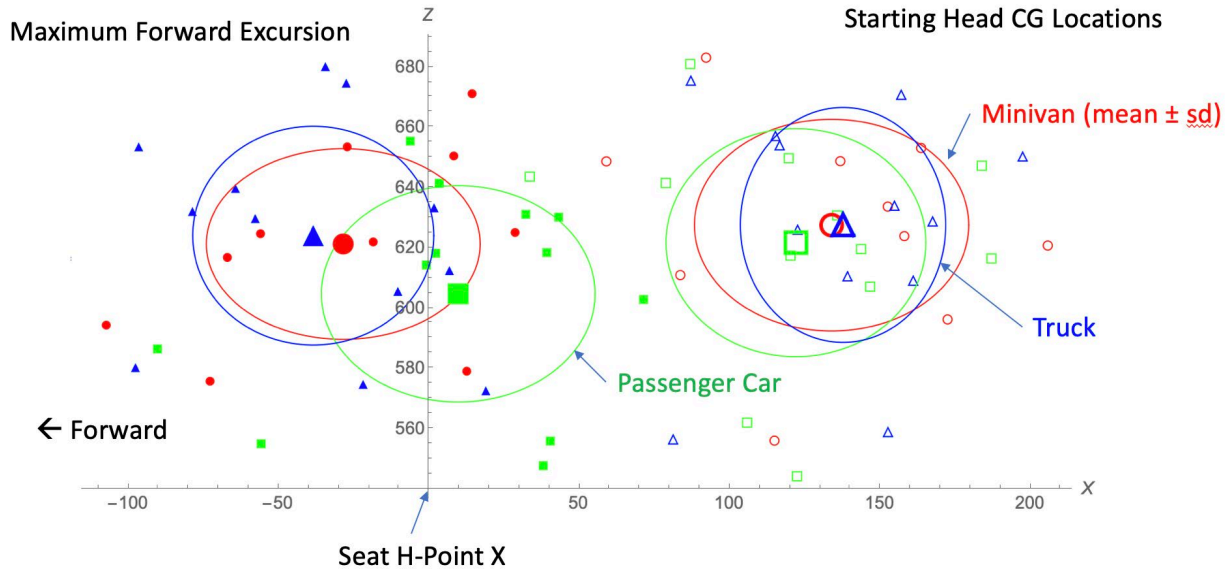

Figure 23. Head CG excursions in the first braking event (B1) in side view (mm). Head CG locations at the start of the event (open symbols) and at the point of maximum forward excursion (filled symbols) are shown for the truck (triangle), minivan (circle), and passenger car (square). The mean for each vehicle is shown with larger symbols. The ellipses for each vehicle have axes with length ± one standard deviation on each axis.

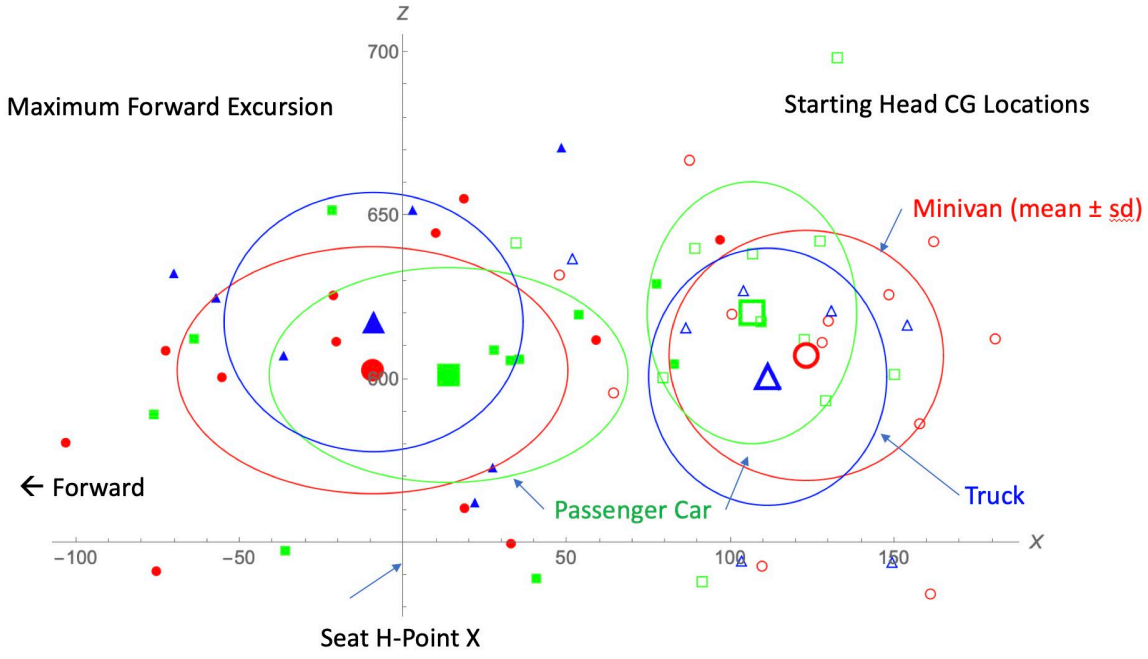

Figure 24. Head CG excursions in the second braking event (B2) in side view (mm). Head CG locations at the start of the event (open symbols) and at the point of maximum forward excursion (filled symbols) are shown for the truck

(triangle), minivan (circle), and passenger car (square). The mean for each vehicle is shown with larger symbols. The ellipses for each vehicle have axes with length ± one standard deviation on each axis.

Table 7. Maximum Head CG Excursions† in Braking and Lane-Change Events by Vehicle: Mean (sd), mm

Vehicle	B1	B2	L1	L2
Minivan	-162 (54)	-133 (54)	-126 (51)	-121 (49)
Passenger Car	-112* (39)	-93* (49)	-110 (49)	-101 (37)
Pickup Truck	-176 (46)	-120 (37)	-140 (68)	-124 (45)
Overall Mean Across Vehicles	-150 (47)	-115^ (47)	-125 (56)	-115 (44)
Reed et al. (2018)	-135 (62)	-115 (51)	-118 (40)	NA

† Negative braking excursions are forward; negative lane-change excursions are inward.

• Significantly smaller than in the other vehicles ($p<0.01$)

^ Significantly smaller than in the first exposure ($p<0.01$)

3.2 Lane-Change Maneuvers

3.2.1 Vehicle Kinematics

Lateral accelerations were similar across vehicles, peaking at about 0.55 g (Figure 25). The total event duration was about 3 seconds.

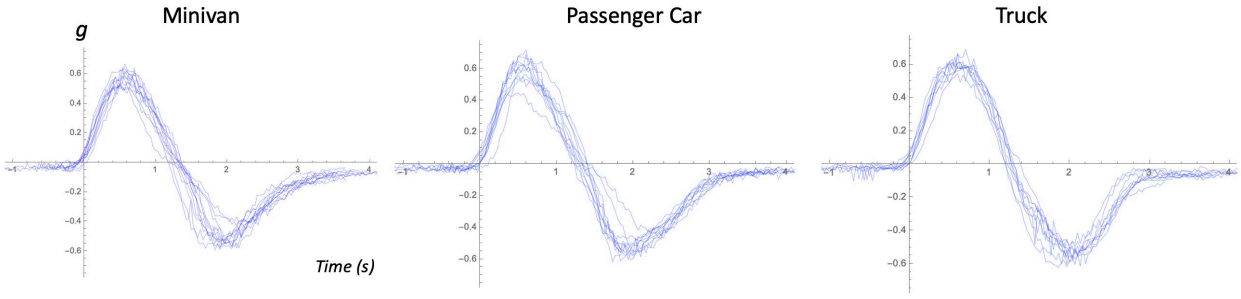

Figure 25. Vehicle lateral accelerations (g) during the first lane-change event.

3.2.2 Head Excursions

Figure 26 shows the starting head CG locations along with the head CG locations at maximum inboard excursion during the first lane-change event. As shown in Table 7, the mean (SD) inboard excursion was 125 (56) mm, similar to the mean value of 118 (40) obtained in the previous study. No significant differences between vehicles were observed using a paired *t*-test. The standard deviations within each vehicle were also similar in magnitude to those observed in the earlier study. Similar results were obtained in the second lane-change event. For every vehicle, the mean response was smaller in the second event, though the difference was not statistically significant.

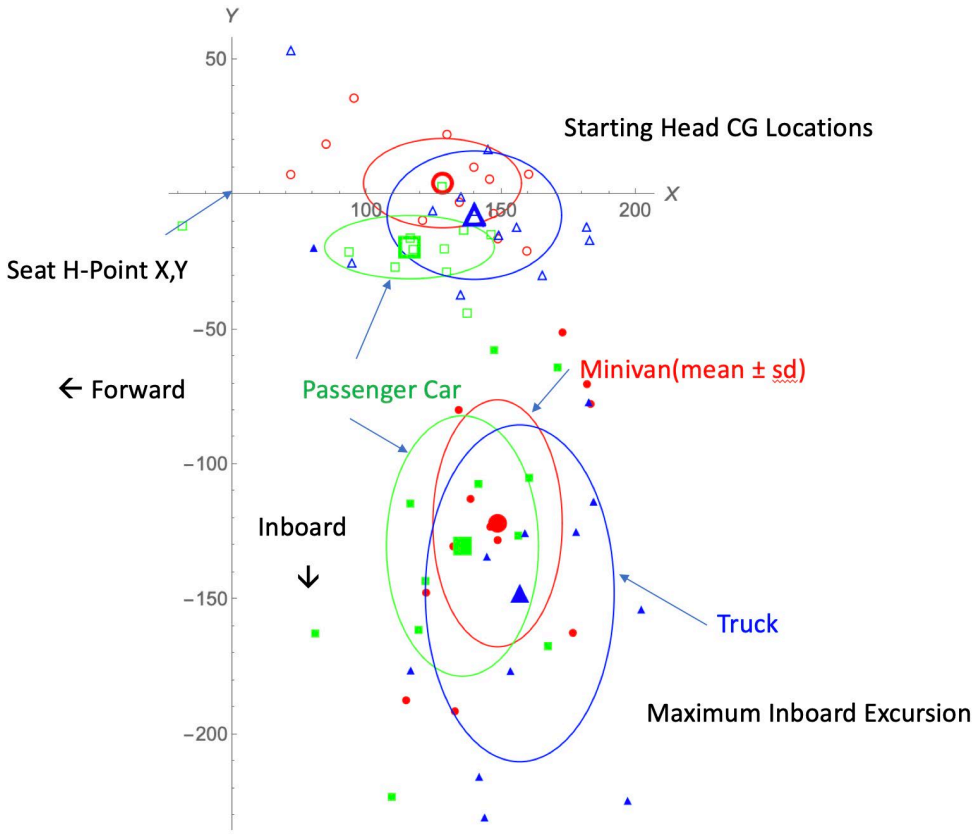

Figure 26. Head CG excursions in the first lane-change event (L1) in top view (mm). Head CG locations at the start of the event and at the point of maximum inboard excursion are shown. The mean for each vehicle is shown as large dots. The ellipses for each vehicle have axes with length ± one standard deviation on each axis.

3.3 Exploration of Excursion Differences in the Passenger Car

A variety of analyses were conducted to determine what may have resulted in the smaller head excursions during braking in the passenger car, but ultimately no definite explanation was established. The seat back angle was 2 degrees more upright in that vehicle, but the angle of the shoulder belt between the D-ring and the participants' shoulders, measured using 3D data digitized from the starting frames in each trial, did not show meaningful differences across vehicles. Vehicle pitch was estimated by integrating the angular acceleration data from the IMU. The mean peak pitch was -2.3, -2.3, and -1.9 degrees for the minivan, passenger car, and truck, respectively, which did not indicate a pattern that could account for the observed difference in occupant kinematics. One possibility is that the belt locked earlier in the passenger car, which would be expected to reduce excursions. Unfortunately, no data on the belt locking times were available. Peak acceleration was reached about 200 ms later in the passenger car than in the other vehicles (see Figure 23), an increase in time-to-peak of about 40 percent. A longer time-to-peak could have provided more time for occupants to control their muscle responses, but the time of peak head excursion during the event varied widely across individuals, indicating a lack of consistency in muscle responses.

The relationship between the IMU and the mean occupant head location was analyzed to assess whether differences in the IMU location across vehicles could contribute meaningfully to the

interpretation of the acceleration experienced by the occupant. On average, the IMU was about 930 mm from the mean head location (inboard and lower). The largest difference across vehicles was that the IMU was about 110 mm higher (closer to the H-point and head) in the passenger car compared with the mean location across vehicles. However, this represents only about 14 percent of the mean value and is unlikely to produce a meaningful difference across vehicles in the relationship between the accelerations measured by the IMU and those experienced by the occupant, which are modulated by the characteristics of the seat as well.

3.4 Discussion of Pilot Results

This was the first study to systematically investigate differences across vehicles in occupant responses to abrupt braking and lane-change events. The within-subject design allowed a sensitive evaluation of differences. The vehicle kinematics were similar across vehicles, except that the mean peak pitch in the truck during braking was lower than in the other vehicles.

No significant differences in lateral head excursion during the lane-change maneuver were noted, and the results were generally consistent with the previous study conducted using the same protocol. Raising the armrest on the minivan seat did not significantly affect inboard head excursion.

In braking, the head excursions measured in the passenger car were significantly smaller than in the other two vehicles, though the standard deviation was similar. Interestingly, the mean peak excursion in the first braking event in the passenger car was similar to the mean value from the second event in the earlier study. In the current study, the "first" braking event was on average the third braking event (and sixth event overall) due to the testing of the vehicles sequentially. The practical meaning of this result is unclear. The excursions in the other two vehicles (average B1 excursion of 169 mm) were on average 34 mm greater than in the previous study (about half of the standard deviation of 62 mm in the previous study). Because the vehicle accelerations were very similar, the differences are likely due to the belts and seats. Ólafsdóttir et al. (2013), who measured kinematics and muscle activity for 11 men and 9 women in the passenger seat of a sedan under maximal braking of about 1.1 *g*, reported peak head excursions of around -180 (50) mm, more similar to the average of the minivan and truck than to the passenger car in the current study.

This pilot study was limited by the relatively small sample size, although the within-subject design allowed for greater statistical power than if separate subject pools were used for each vehicle. The use of repeated exposures in a short period of time reduced the element of surprise. However, Reed et al. (2018) showed only a small mean reduction in head excursion of 15 mm in a second braking exposure.

The sample size in the pilot study was too small to assess the effects of participant characteristics on head excursions. Reed et al. (2018) showed significant effects of age and BMI on forward excursion in braking and of stature on inboard excursion during a right-going lane change. These effects are comparable in size across the occupant population to the vehicle difference documented in the current work. For example, the effect of a difference of age from 20 to 70 years is a reduction in forward excursion in braking of about 30 mm, similar to the difference between vehicles in the current study as well as the standard deviation within vehicle. Overall,

the results of the two studies indicate that a large range of head locations is possible during an abrupt vehicle maneuver regardless of occupant characteristics.

These results suggest that head excursions in braking may differ somewhat across vehicles. Although the differences were small relative to the large between-subject variance, this finding prompted the use of two vehicles in the subsequent full-scale study. The hypothesis that early retractor locking may influence excursion was examined in the full-scale study by pre-locking the retractor.

4 RESULTS — FULL-SCALE STUDY

Figure 27 and Figure 28 show acceleration plots for each of the exposures for both vehicles. Corridors based on the mean ± one standard deviation are shown along with individual acceleration traces. The braking acceleration in Avalon was more variable over time in a fairly consistent pattern, while the acceleration in the Jeep was approximately constant. Both vehicles achieved more than 0.9 g during the plateau phase. Braking to a stop from 56 km/hr (35 mph) required approximately two seconds in the Avalon and about 2.25 seconds in the Jeep, on average.

The lane-change maneuvers produced about 0.7 g for both the initial turn and recovery phases. Right-going and left-going accelerations had approximately the same absolute peak values and timing. Each maneuver was completed in about three seconds. The turn-and-brake maneuver was most variable, with lateral accelerations fluctuating rapidly as the front tires slid on the pavement. The typical lateral peak acceleration was about 0.7 g, similar to the lane change. Longitudinal acceleration varied more widely, but typically ramped up to about 0.7 g near the end of the event.

Overall, the exposures were judged to be consistent with peak accelerations typically within 10 percent and overall durations within about 0.25 second. No notable differences in performance between the Avalon and Jeep were noted. As planned, the vehicle kinematics also matched the events from the 2018 study.

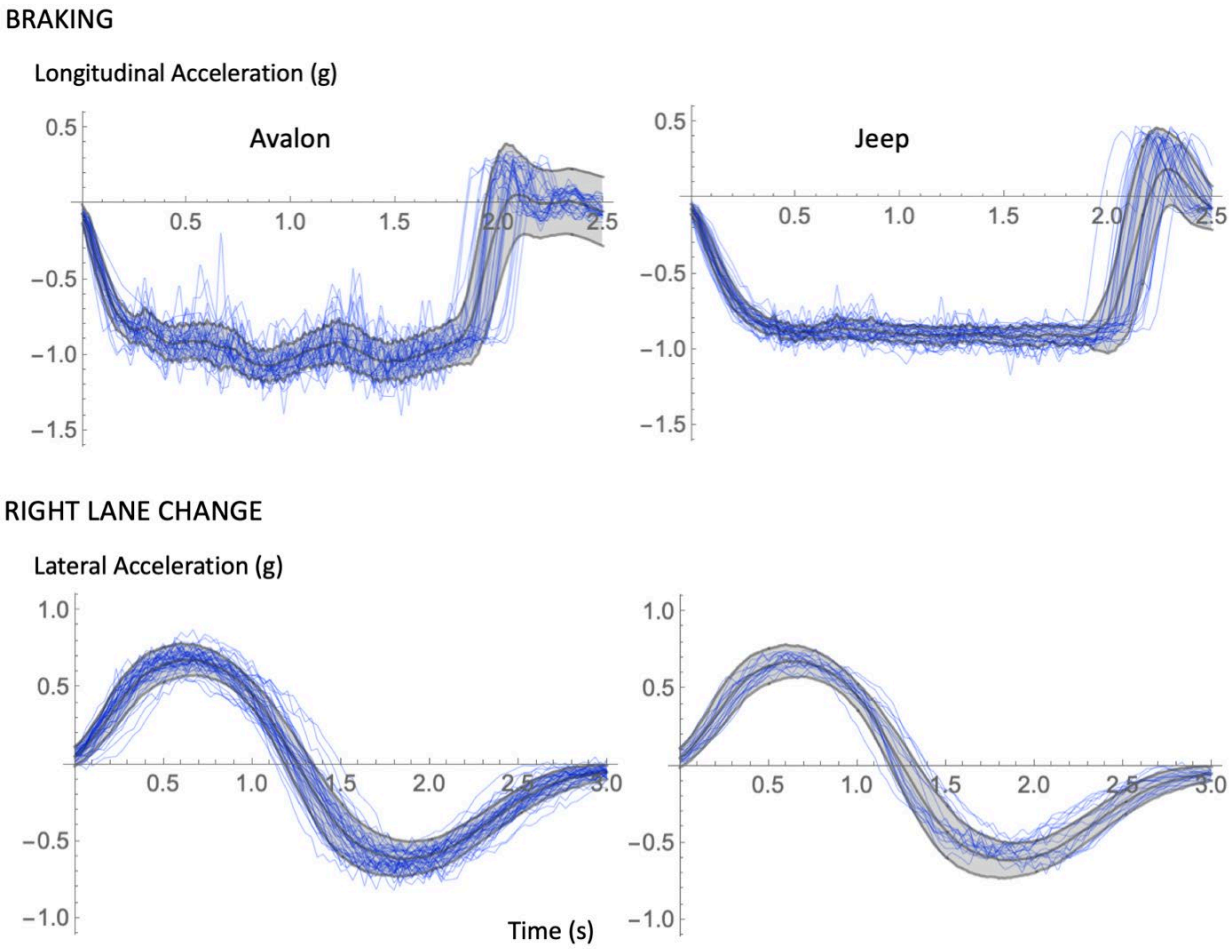

Figure 27. Acceleration corridors for braking and right-lane-change maneuvers. Corridors are mean ± one standard deviation.

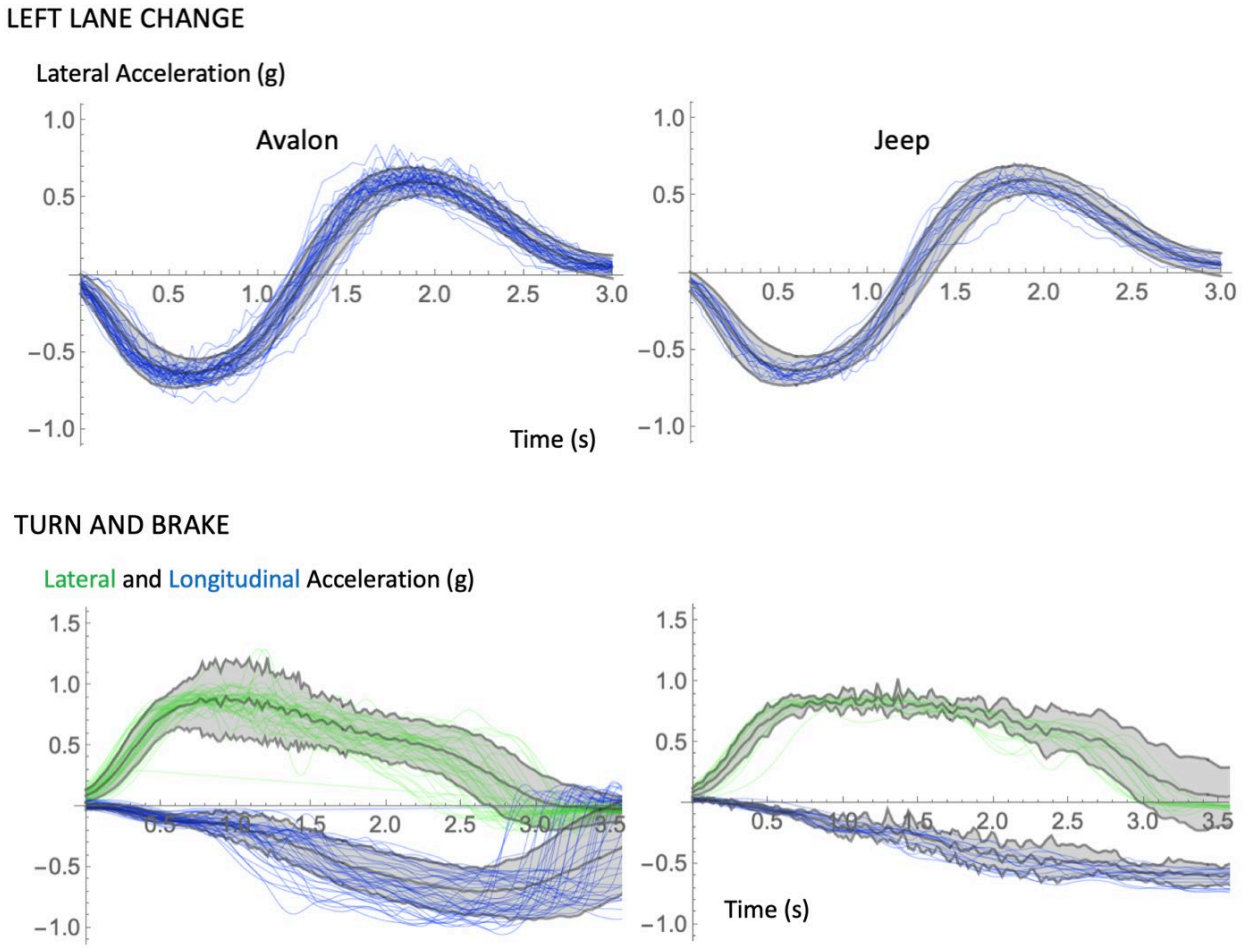

Figure 28. Acceleration corridors for left-lane-change and turn-and-brake maneuvers. Corridors are mean ± one standard deviation.

4.1 Analysis of Maximum Head Excursion

The maximum and minimum coordinate values of head CG location during each trial were computed on all three axes. Figure 27 shows the maximum and minimum values on the X and Y axes for all tracked trials with valid maximum excursion data (8,190 locations). Note that these data are normalized for seat position, i.e., adjusted to have a common seat H-point location (usually full rear). The plot shows that, relative to the seat, a wide range of head locations is produced by the vehicle maneuvers. Leaving out the starting head locations in reclined postures, the head locations span a range of about 500 mm fore-aft and laterally, with a few values extending farther. When reclined trials are included, the fore-aft range of head locations before and during the trials is about 800 mm relative to seat H-point. Note that the use by passengers of different seat positions would tend to increase the fore-aft dispersion. A typical fore-aft seat track adjustment range is 240 mm.

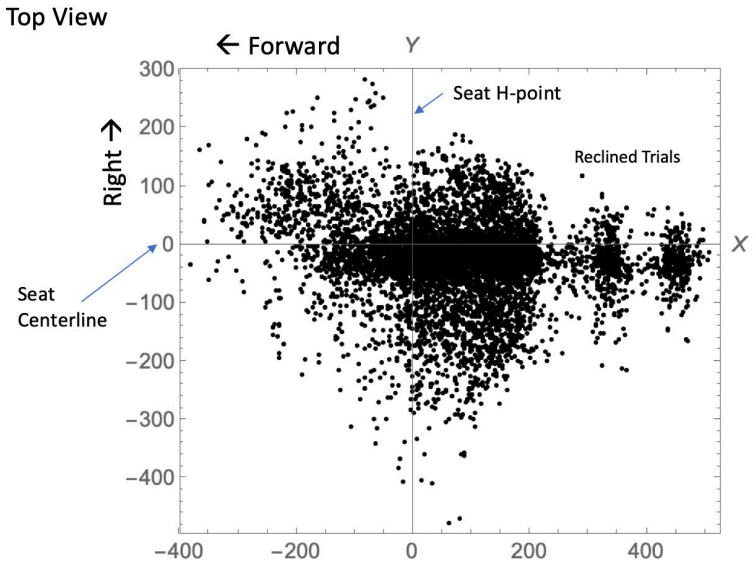

Figure 29. Maximum and minimum X and Y locations for the head CG in every tracked trial (mm) relative to seat H-point on seat centerline.

The maximum excursion values in the primary direction of head motion are presented for each set of initial conditions across the various exposures. Within each set of conditions, statistical tests were performed using linear regression to assess whether the maximum excursions differed based on the initial conditions and/or participant stature, or BMI. All reported condition and covariate effects are statistically significant with $p<0.01$, except where noted. Potential two-way interactions among test conditions and between test conditions and anthropometric variables were also evaluated, though none was found to be significant.

Based on the lack of independent gender effects in the earlier study (Reed et al., 2018), no effort was made to differentiate gender effects from anthropometric effects with the much smaller number of participants per condition available in the current study.

4.2 Maximum Head Excursions — Braking

This section presents head excursion results for braking events. Braking events tended to cause the occupant's head to move forward relative to the seat. The maximum forward excursion of the head CG was analyzed. Note that the forward direction is –X, so more-negative excursions are further forward. All analyses are conducted with respect to seat H-point except where noted.

Each participant experienced two braking events in each test condition (B1 and B2 – see Figure 11). Statistical analyses showed no significant differences in forward head excursion between B1 and B2, so these events were pooled for analysis, resulting in an approximate doubling of the number of available trials for each condition.

4.2.1 Braking — Seat Position Conditions

Figure 28 shows the starting head CG locations along with the locations at the maximum forward point for each braking event in the seat position block of trials. The data have been adjusted to a

common seat H-point location. Table 8 lists the mean and standard deviation of the excursion, obtained by subtracting the initial head location from the location at maximum forward excursion. Note that the –X direction is forward. The regression analysis showed the excursion was reduced when the seat was further forward but placing the feet flat increased excursion. Older participants experienced less excursion. The regression function is given by

X Excursion (Braking) = -242 + 0.332 SeatPosition + 25.0 Heels + 1.22 Age, R^2_{adj} = 0.39, RMSE = 44.7 mm

where SeatPosition is mm forward of full rear, heels is a binary variable equal to one with the feet on the heels and zero with the feet flat, and age is in years. Note positive coefficients indicate that increases in the variable produce less excursion.

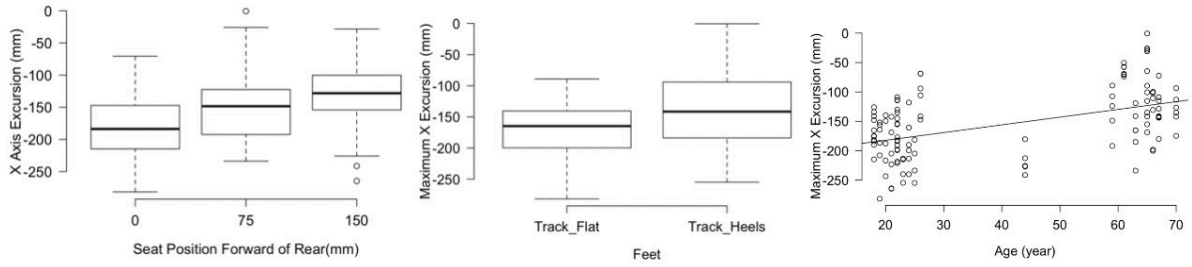

Figure 30

Figure 31 illustrates the significant factor effects.

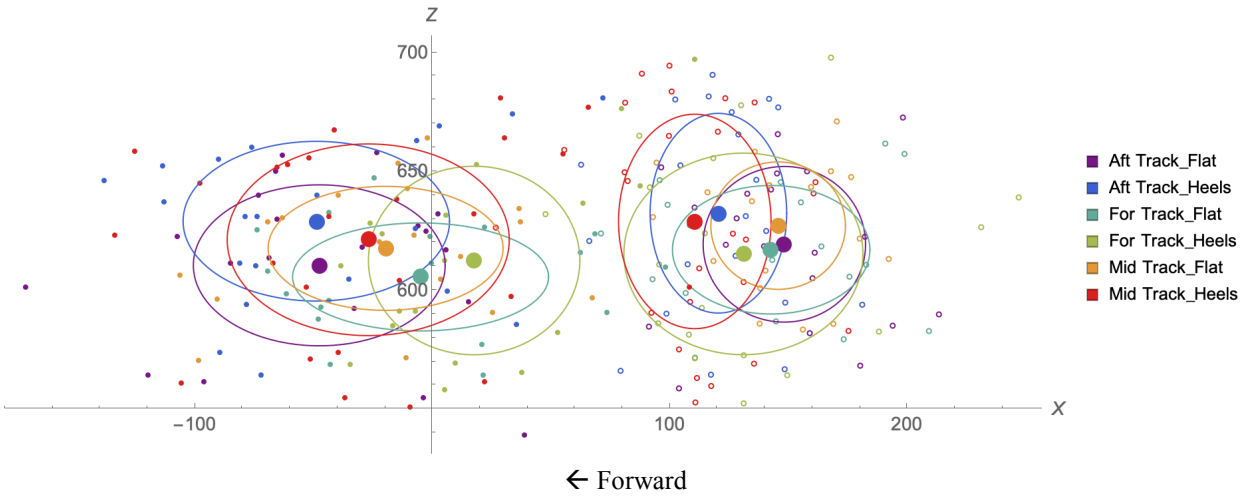

Figure 31. Side view of starting (right side of plot) and ending (left side of plot) head CG locations (mm) relative to seat H-point for braking trials in seat position conditions. Data was adjusted to a common seat H-point location. Large symbols are condition means. Ellipses show ±1SD on each axis.

Table 8. Maximum Forward Head Excursions for Braking Trials in Seat Position Conditions (Mean and Standard Deviation, mm)

Seat Position	Feet	N	Mean X	SD X
Aft	Flat	20	-195.9	43.1
Aft	Heels	21	-169.4	53.9
Mid	Flat	18	-165.3	37.2
Mid	Heels	26	-137.6	63.7
For	Flat	18	-147.7	43.8
For	Heels	18	-113.4	60.3

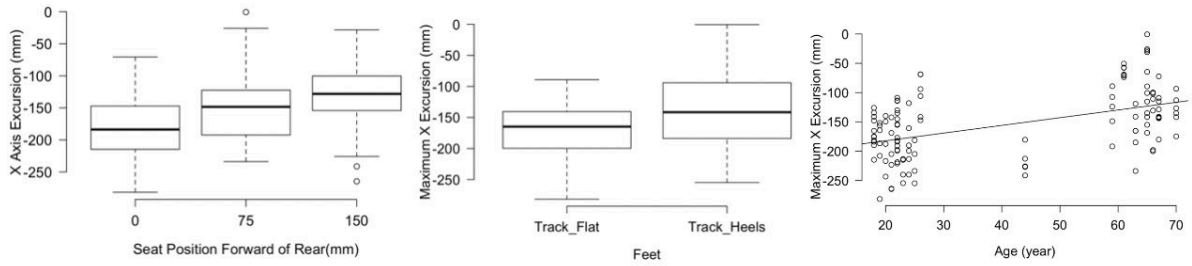

Figure 32. Effects of predictors on maximum forward excursion in braking trials in the seat position block.

4.2.2 Braking — Recline Conditions

Figure 30 shows that increasing recline was associated with larger head excursions in recline, but the effect was greater at the middle recline position than the maximum recline as shown in Figure 31. Table 10 shows that the variance in excursion also increased with increasing recline (see also the increased length of the ellipses in Figure 30). No significant anthropometric effects were observed.

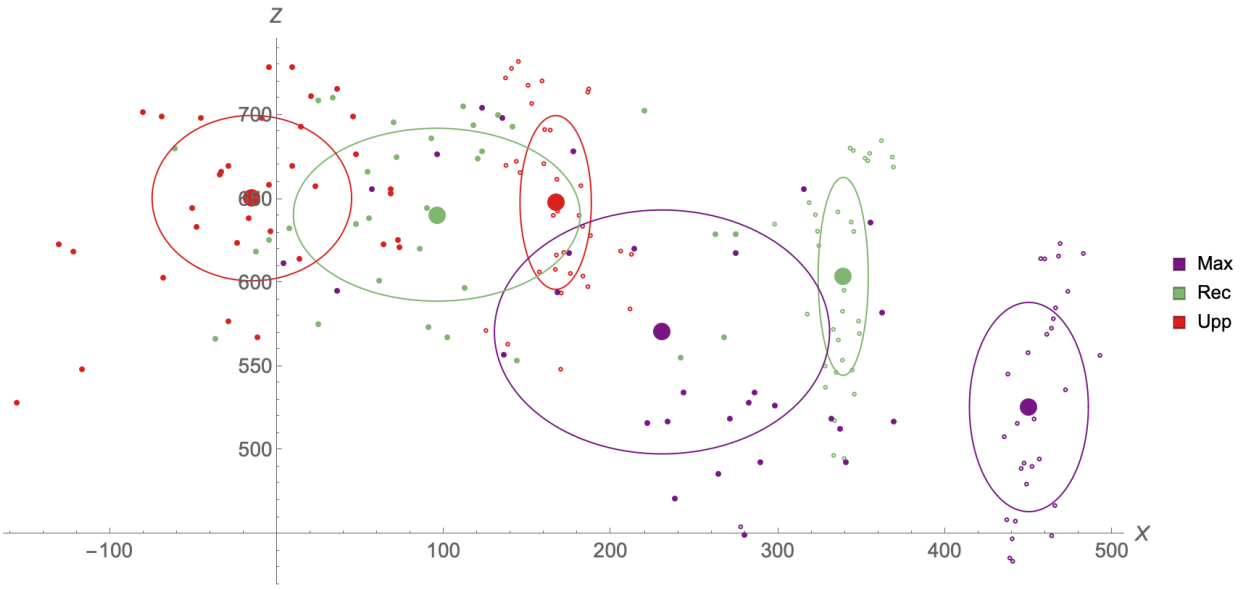

Figure 33. Side view of starting (right side of plot) and ending (left side of plot) head CG locations (mm) relative to seat H-point for braking trials in recline conditions (Upp=normal upright, back angle 23 degrees, Rec=reclined to 35 degrees, Max=reclined to 47 degrees). Large symbols are condition means. Ellipses show ±1SD on each axis.

Table 9. Maximum Forward Head Excursions for Braking Trials in Recline Conditions (Mean and Standard Deviation, mm)

Seat Back Angle	N	Mean X	SD X
23˚	35	-181.9	51.6
35˚	32	-243.3	84.4
47˚	30	-219.6	108.5

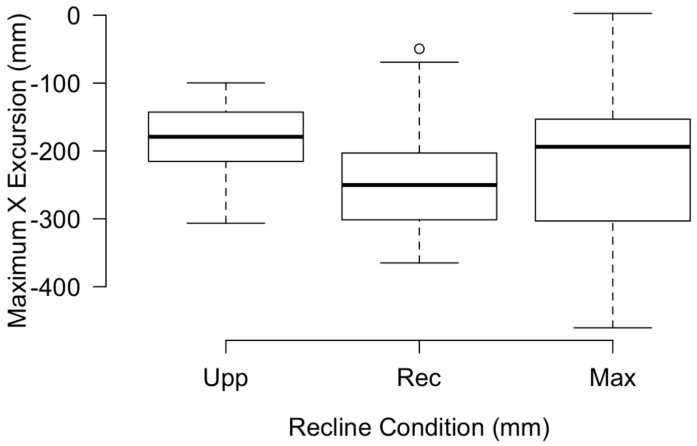

Figure 34. Effects of recline condition on forward head excursion in braking trials (Upp=23 deg, Rec=35 deg, Max=47 degree seat back angle).

4.2.3 Braking — Vehicle Conditions

Figure 32 shows starting and maximum-forward head locations for braking trials in the vehicle block, which included a forward-leaning posture as well as a standard posture. No significant effects were observed, though excursions tended to be smaller in the forward-leaning posture (Table 10). Unlike in the pilot study, no differences were noted across vehicles in forward excursions in the standard starting posture. No significant anthropometric effects were observed.

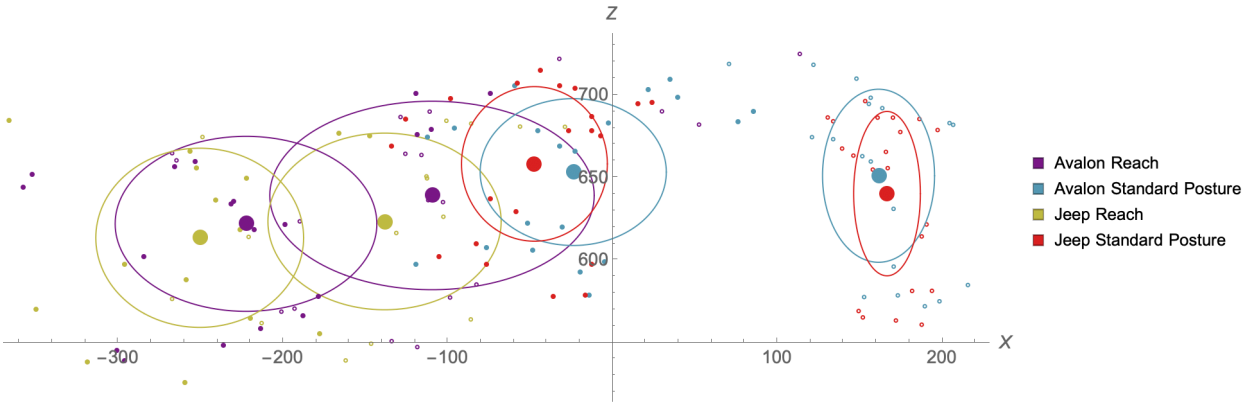

Figure 35. Side view of starting (right side of plot) and ending (left side of plot) head CG locations (mm) relative to seat H-point for braking trials in vehicle conditions. Large symbols are condition means. Ellipses show ±1SD on each axis.

Table 10. Maximum Forward Head Excursions for Braking Trials in Vehicle Conditions (Mean and Standard Deviation, mm)

Vehicle	Condition	N	Mean X	SD X
Avalon	Reach	19	-112.9	29.5
Avalon	Standard Posture	20	-185.3	61.3
Jeep	Reach	15	-112.2	32.8
Jeep	Standard Posture	21	-213.9	50.8

4.2.4 Braking — Retractor

A non-significant trend toward lower head excursions in the forward seat position was noted in the braking trials in the retractor block of conditions, but no effect of the retractor was noted (Figure 33 and Table 11). However, older age was associated with less excursion. The regression function was

$$\text{X Excursion (Braking)} = -179 + 0.757\ \text{Age},\ R^2_{adj} = 0.15,\ \text{RMSE} = 37.0\ \text{mm}$$

Figure 34 illustrates the age effect.

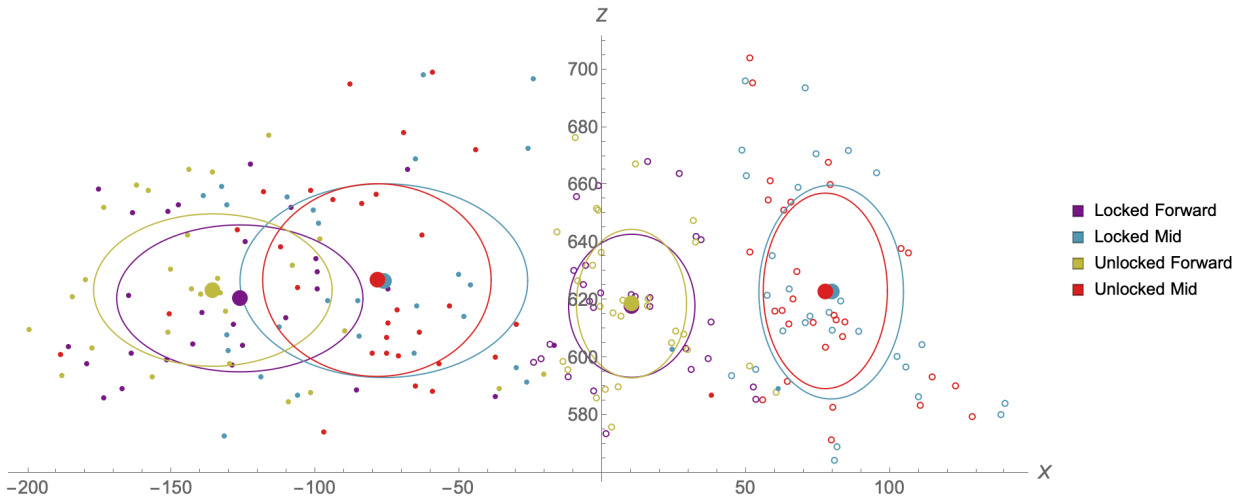

Figure 36. Side view of starting (right side of plot) and ending (left side of plot) head CG locations (mm) relative to seat H-point for braking trials in retractor conditions. Large symbols are condition means. Ellipses show ±1SD on each axis.

Table 11. Maximum Forward Head Excursions for Braking Trials in Retractor Conditions (Mean and Standard Deviation, mm)

Retractor	Seat Position	N	Mean X	SD X
Locked	Forward	28	-136.4	37.5
Locked	Mid	28	-155.7	43.4
Unlocked	Forward	28	-145.7	39.3
Unlocked	Mid	30	-156.1	38.6

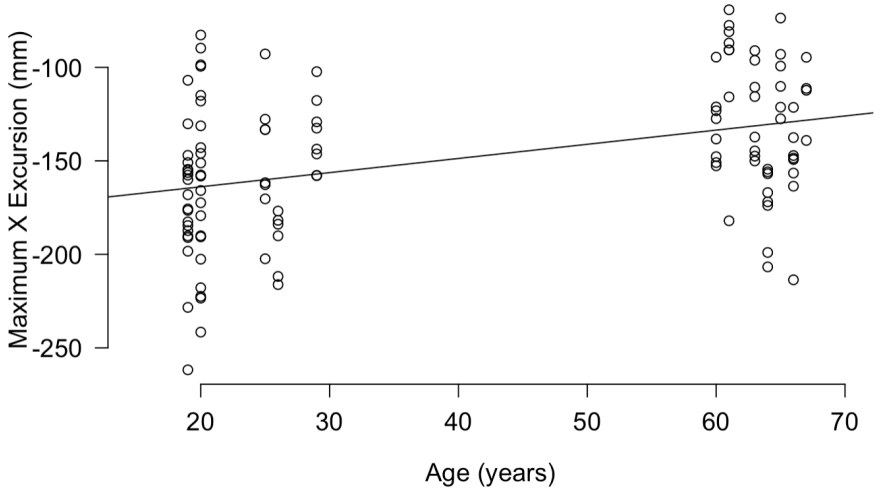

Figure 37. Effect of age on forward excursion in braking trials in the retractor block of conditions.

4.2.5 Braking — Lean/Reach Conditions

Figure 35 and Table 12 illustrate the strong effects of leaning conditions on head excursion. The top-view plot shows the initial head location is well forward of the seat H-point for the forward and forward-inboard conditions, and over 150 mm inboard on average for the Arm trials, in which the participant leaned on the center console. The pattern of head movement was markedly different for the Arm trials, with the head moving forward and toward the seat centerline, whereas the movement was smaller and predominantly forward for the other two conditions. The larger excursion with the Arm condition was the only significant effect in the regression analysis.

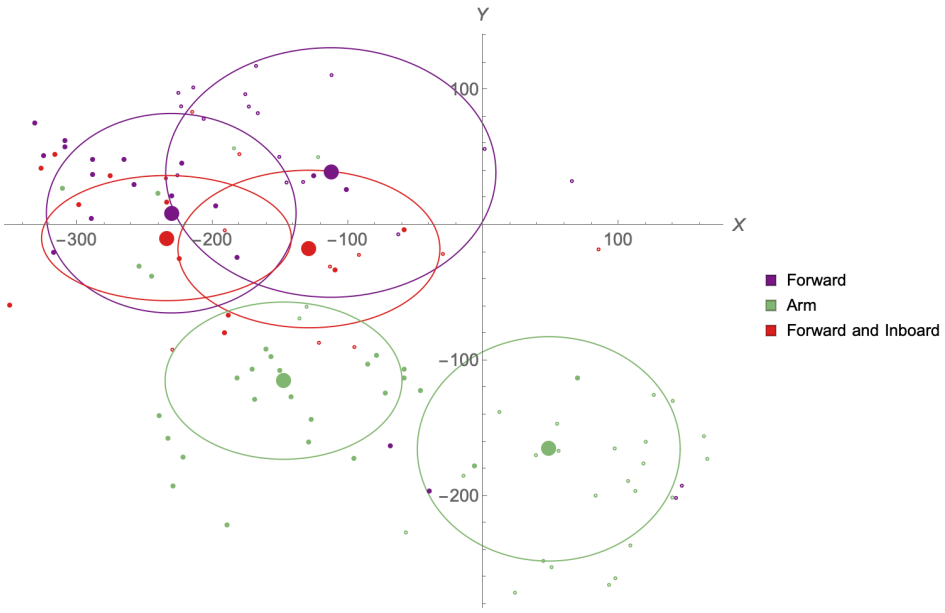

Figure 38. Top view of starting and maximum-excursion (left side of plot) head CG locations (mm) relative to seat H-point for braking trials in lean/reach conditions. Large symbols are condition means. Ellipses show ±1SD on each axis.

Table 12. Maximum Forward Head Excursions for Braking Trials in Lean/Reach Conditions (Mean and Standard Deviation, mm)

Lean/Reach	N	Mean X	SD X
Forward	18	-117.9	41
Arm	27	-195.8	66
Forward and Inboard	11	-105.2	23.2

4.3 Maximum Head Excursions — Right Lane Change

This section presents head excursion results for right-going lane change. This maneuver tended to cause the participant's head to move inboard (to the left) during the initial phase of the trial. The maximum inboard excursion of the head CG was analyzed. Note that the inboard direction is –Y, so more-negative excursions are further inboard. All analyses are conducted with respect to seat H-point and seat centerline except where noted.

4.3.1 Right Lane Change — Seat Position Conditions

Figure 36 plots head CG locations in top view for right lane change trials in the seat track block. No significant differences in mean excursion across conditions were noted (Table 13), although excursions tended to be larger with the feet flat rather than on the heels (p=0.03). Older participants tended to produce less excursion (p=0.03).

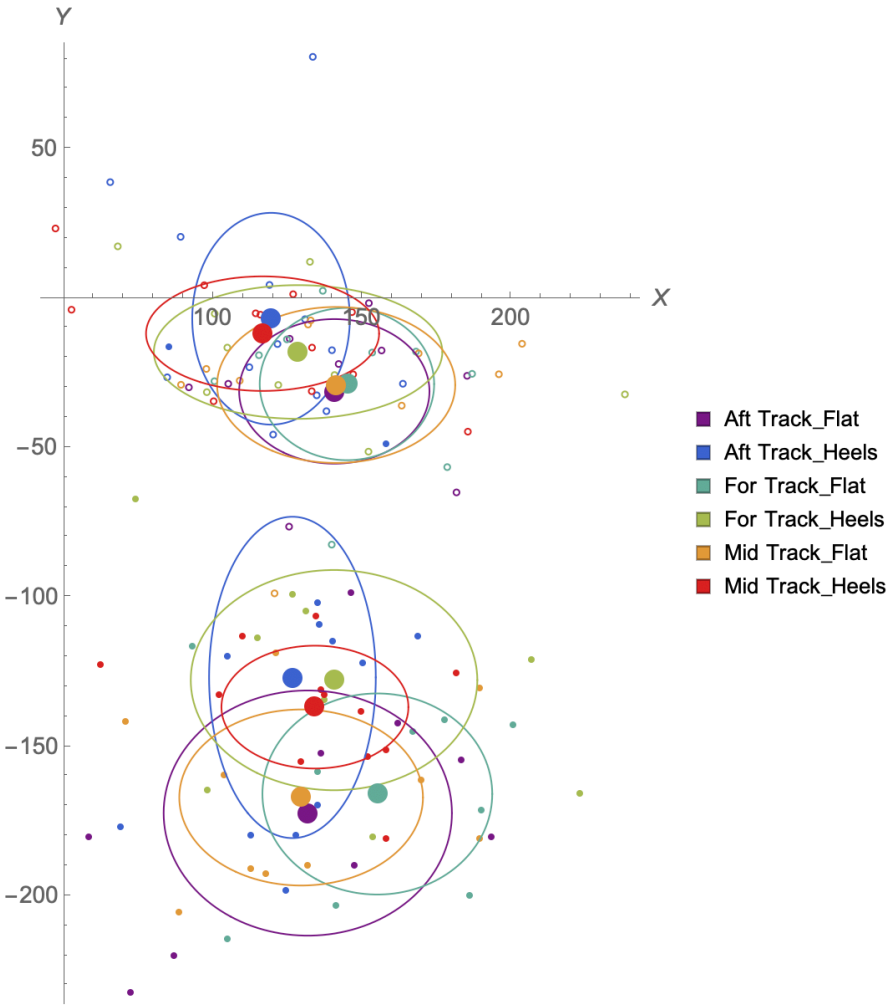

Figure 39. Top view of starting and maximum-excursion (bottom of plot) head CG locations (mm) relative to seat H-point for right lane change trials in seat position conditions. Large symbols are condition means. Ellipses show ±1SD on each axis.

Table 13. Maximum Inboard Head Excursions for Right Lane Change Trials in Seat Position Conditions (Mean and Standard Deviation, mm)

Seat Position	Feet	N	Mean Y	SD Y
Aft	Flat	9	-141.1	37.0
Aft	Heels	13	-120.0	56.1
Mid	Flat	10	-138.0	26.1
Mid	Heels	12	-125.0	21.6
For	Flat	9	-137.2	35.0
For	Heels	9	-109.8	29.9

4.3.2 Right Lane Change — Recline Conditions

Figure 37 shows a strong effect of recline on inboard excursion in right lane change trials, as documented in Table 14 and Figure 38. The regression function was

Y Excursion (Rt Lane Change) = -198 + 3.14 SeatBackAngle, R^2_{adj} = 0.43, RMSE = 35.2 mm

where SeatBackAngle is in degrees from vertical. No anthropometric variables had significant effects.

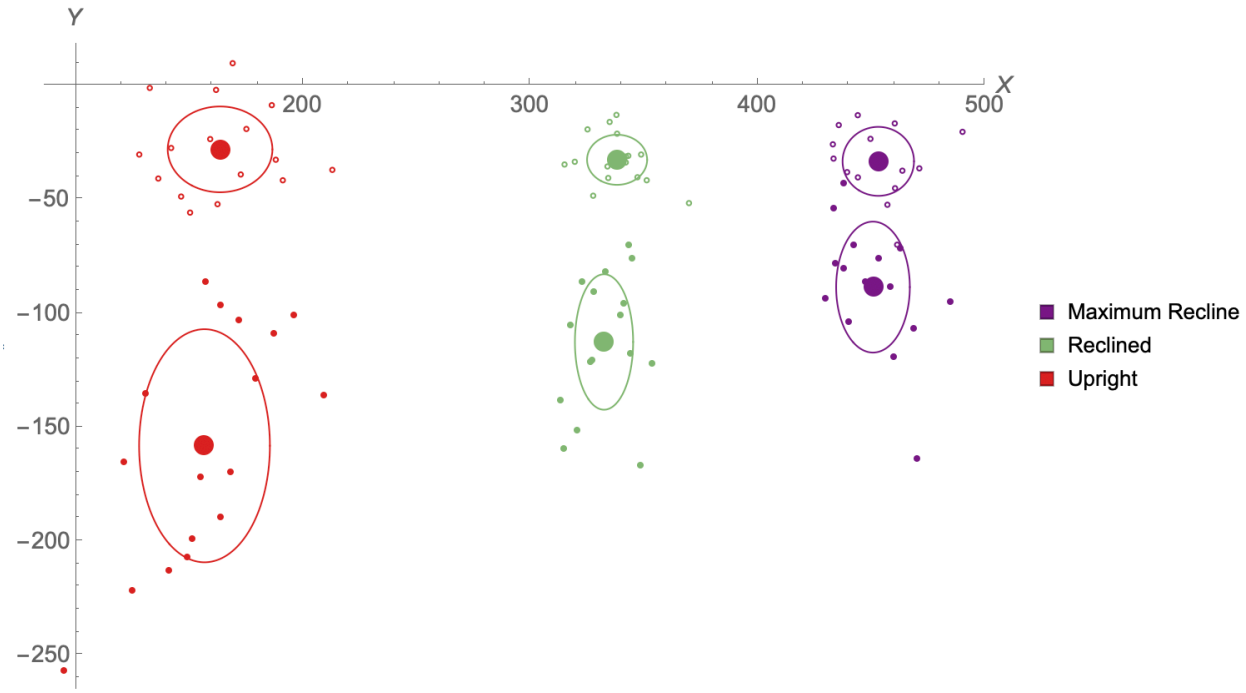

Figure 40. Top view of starting and maximum-excursion (bottom of plot) head CG locations (mm) relative to seat H-point for right lane change trials in recline conditions. Large symbols are condition means. Ellipses show ±1SD on each axis.

Table 14. Maximum Inboard Head Excursions for Right Lane Change Trials in Recline Conditions (Mean and Standard Deviation, mm)

Recline	N	Mean Y	SD Y
Upright: 23˚	17	-130.1	46.9
Reclined: 35˚	16	-80	29.8
Max: 47˚	15	-55.2	21.9

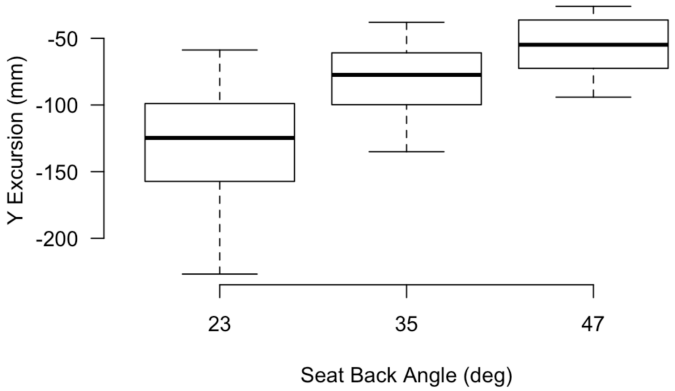

Figure 41. Effect of seat back angle on inboard head excursion in right lane change trials.

4.3.3 Right Lane Change — Vehicle Conditions

No difference in inboard excursion across vehicles was noted in either the reach or standard postures (Figure 39), but the excursion was much larger when the participant was reaching forward prior to the event (Table 15).

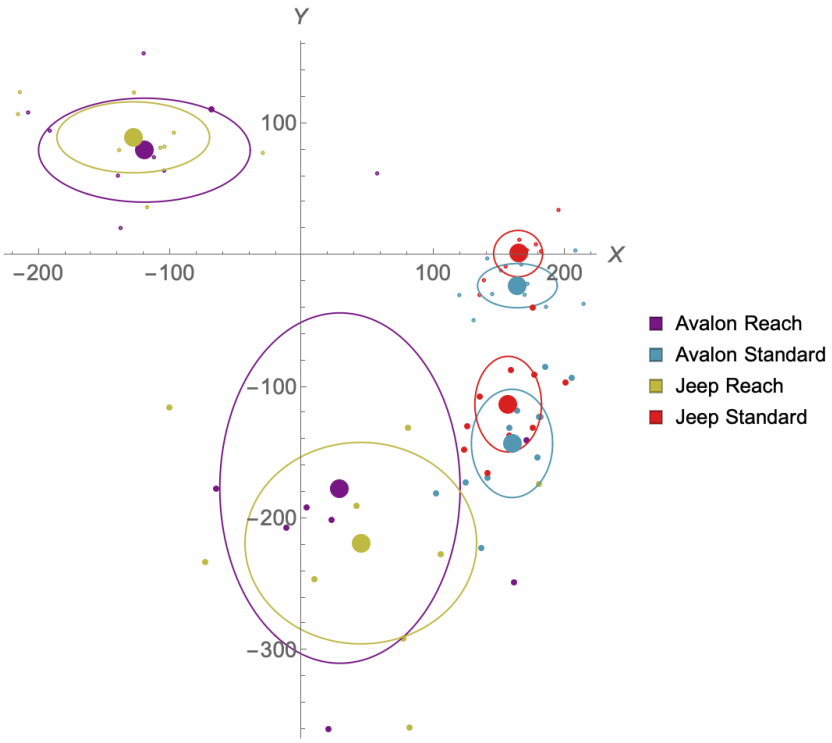

Figure 42. Top view of starting and maximum-excursion (bottom of plot) head CG locations (mm) relative to seat H-point for right lane change trials in vehicle block conditions. Large symbols are condition means. Ellipses show ±1SD on each axis.

Table 15. Maximum Inboard Head Excursions for Right Lane Change Trials in Vehicle Block Conditions (Mean and Standard Deviation, mm)

Vehicle	Posture	N	Mean Y	SD Y
Avalon	Reach	8	-256.5	118.7
Avalon	Standard	11	-119.7	37.6
Jeep	Reach	9	-308	99.1
Jeep	Standard	10	-114.3	33.5

4.3.4 Right Lane Change — Retractor Conditions

In the retractor block of trials, no differences in inboard head excursion were noted due to seat position or retractor condition, but a minor effect of stature was noted, with larger stature associated with greater inboard excursion (Figure 40 and Table 16). The regression equation was

$$\text{Y Excursion (Rt Lane Change)} = 223 - 0.209\ \text{Stature},\ R^2_{adj} = 0.14,\ \text{RMSE} = 36.6\ \text{mm}$$

for Stature in mm.

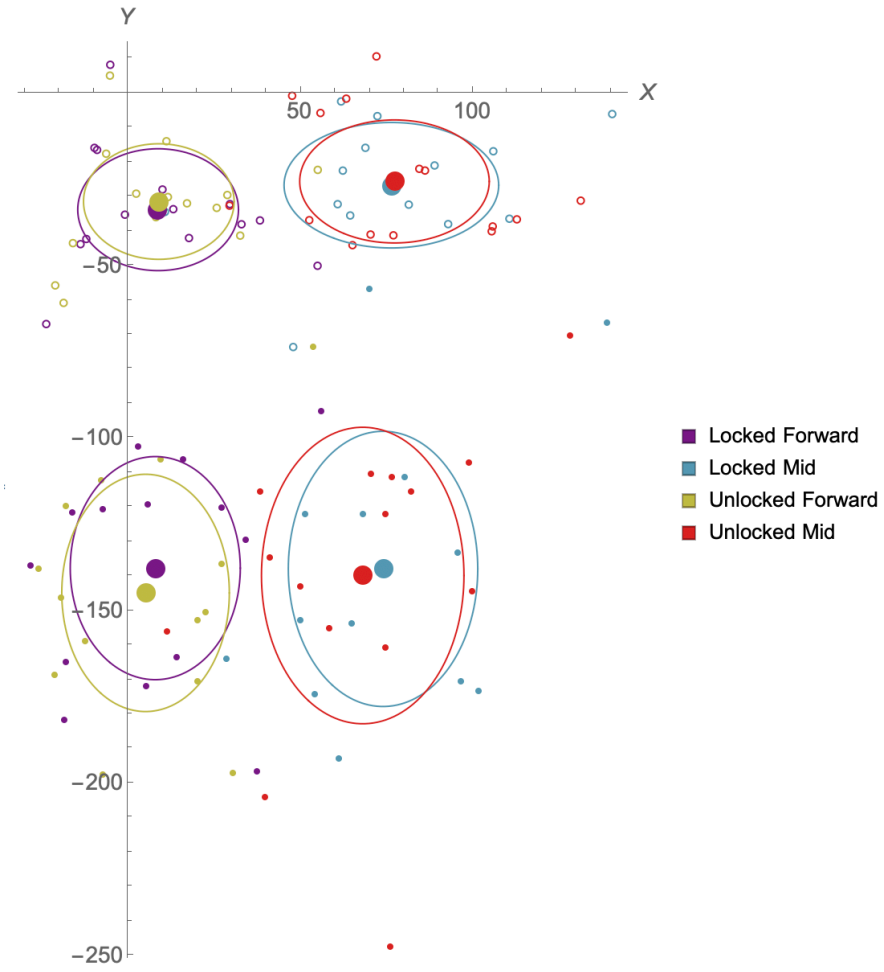

Figure 43. Top view of starting and maximum-excursion (bottom of plot) head CG locations (mm) relative to seat H-point for right lane change trials in retractor block conditions. Large symbols are condition means. Ellipses show ±1SD on each axis.

Table 16. Maximum Inboard Head Excursions for Right Lane Change Trials in Retractor Block Conditions (Mean and Standard Deviation, mm)

Retractor	Seat Position	N	Mean Y	SD Y
Locked	Forward	14	-103.9	39.5
Locked	Mid	14	-111.2	36.9
Unlocked	Forward	14	-113.5	40.0
Unlocked	Mid	15	-114.2	44.0

4.3.5 Lane Change — Reach/Lean Conditions

In the leaning conditions, inboard excursion during the right lane change was markedly lower with the arm lean than in the other two conditions (Figure 41 and Table 17) due to the arm bracing on the console prior to and during the event. No significant effects of anthropometric variables were noted. Excursions appeared lower with forward-and-inboard reach than with the

forward reach, but the small number of successfully tracked trials for the former, and the larger variance in the latter, eliminated the possibility of finding a significant difference.

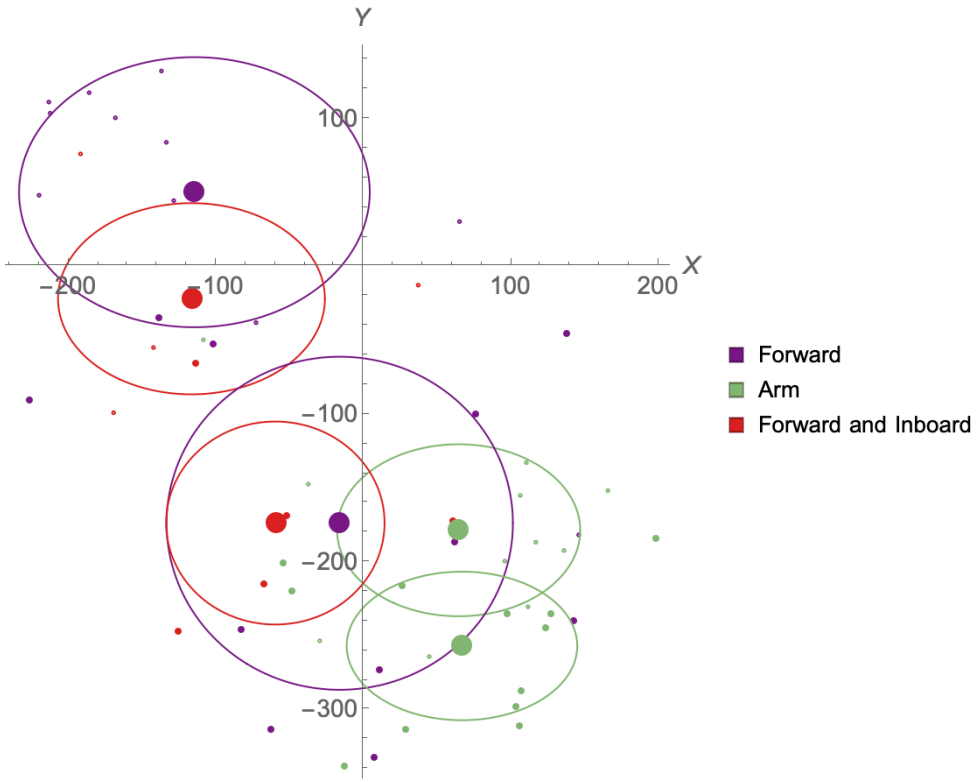

Figure 44. Top view of starting and maximum-excursion (bottom of plot) head CG locations (mm) relative to seat H-point for right lane change trials in lean/reach block conditions. Large symbols are condition means. Ellipses show ±1SD on each axis.

Table 17. Maximum Inboard Head Excursions for Right Lane Change Trials in Lean/Reach Block Conditions (Mean and Standard Deviation, mm)

Lean/Reach	N	Mean Y	SD Y
Forward	11	-224.2	147.0
Arm	12	-78.3	32.8
Forward and Inboard	5	-151.9	87.4

4.4 Maximum Head Excursions — Left Lane Change

This section presents head excursion results for left-going lane change, which tended to move the occupant's head outboard. The maximum outboard excursion of the head CG was analyzed. Note that the outboard direction is +Y, so more-positive excursions are further outboard. All analyses are conducted with respect to seat H-point and seat centerline except where noted.

4.4.1 Left Lane Change — Seat Position Conditions

Seat position did not significantly affect outboard head excursion, but the mean excursion was 22 mm larger with the feet flat than with the feet on the heels (Figure 42 and Table 18). No anthropometric effects were observed.

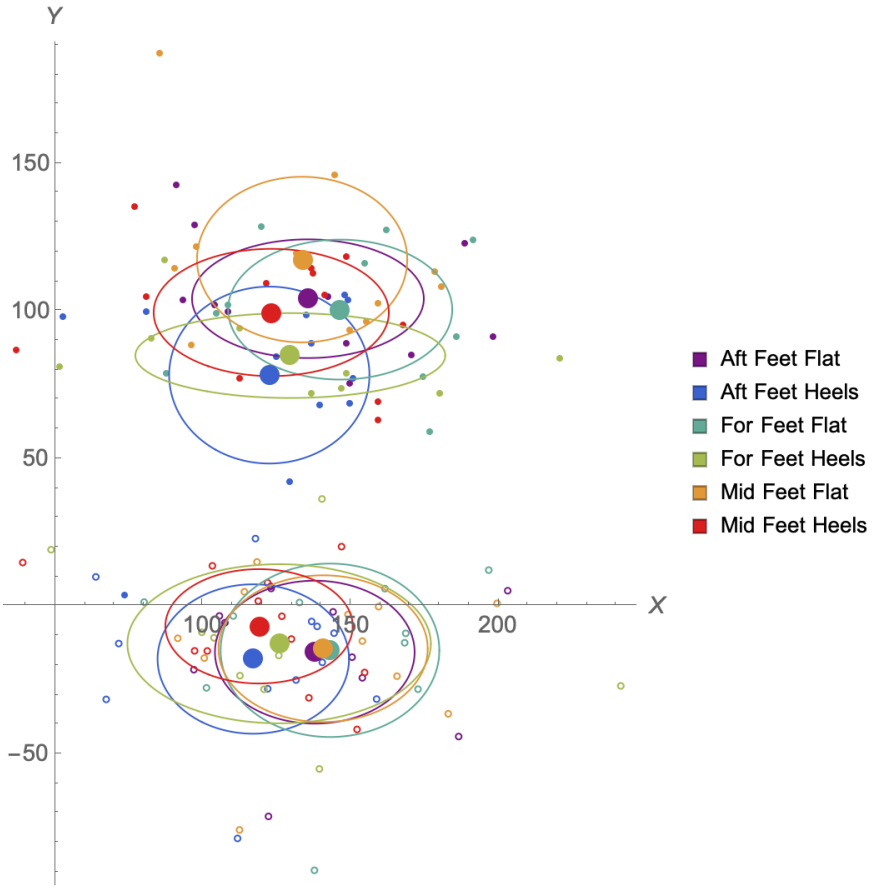

Figure 45. Top view of starting and maximum-excursion (outboard, top of plot) head CG locations (mm) relative to seat H-point for left lane change trials in seat position block conditions. Large symbols are condition means. Ellipses show ±1SD on each axis.

Table 18. Maximum Outboard Head Excursions for Left Lane Change Trials in Seat Position Block Conditions (Mean and Standard Deviation, mm)

Seat Position	Feet	N	Mean Y	SD Y
Aft	Flat	11	119.7	24.5
Aft	Heels	12	96.2	35.9
Mid	Flat	11	131.8	32.5
Mid	Heels	12	106.3	25.5
For	Flat	10	115.4	20.3
For	Heels	9	97.6	30.5

4.4.2 Left Lane Change —Recline Conditions

As with the right-going lane-change trials, increased seat back angle was associated with smaller head excursions (Figure 43 and Table 19). The regression function for seat back angle as a continuous variable was

Y Excursion (Lt Lane Change) = 123 – 1.51 SeatBackAngle, R^2_{adj} = 0.27, RMSE = 23.6 mm

No anthropometric effects were observed.

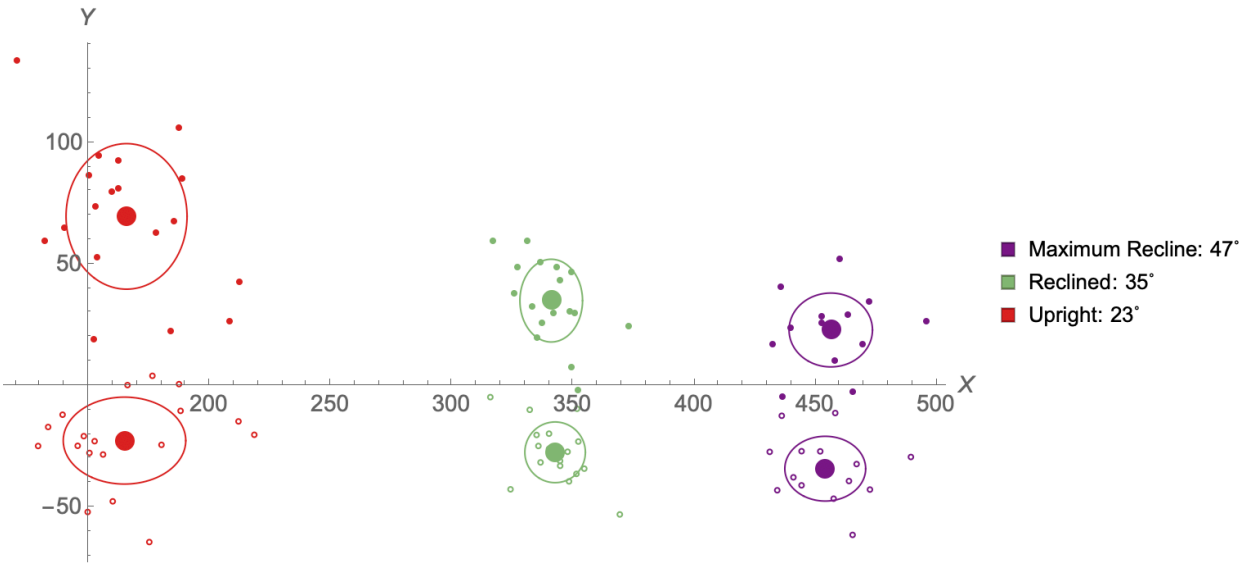

Figure 46. Top view of starting and maximum-excursion (outboard, top of plot) head CG locations (mm) relative to seat H-point for left lane change trials in recline conditions. Large symbols are condition means. Ellipses show ±1SD on each axis.

Table 19. Maximum Outboard Head Excursions for Left Lane Change Trials in Recline Conditions (Mean and Standard Deviation, mm)

Recline	N	Mean Y	SD Y
Upright: 23˚	18	92.3	28.8
Reclined: 35˚	17	62.4	20.9
Max: 47˚	14	57.1	16.5

4.4.3 Left Lane Chane — Vehicle Conditions

In the standard posture, mean outboard head excursion was significantly larger in the Jeep than in the Avalon, possibly due to a larger amount of space available (Figure 44 and Table 20). However, although the excursions were larger in reach trials, no difference between vehicles was noted, possibly due to the large variability across participants. No anthropometric effects were noted.

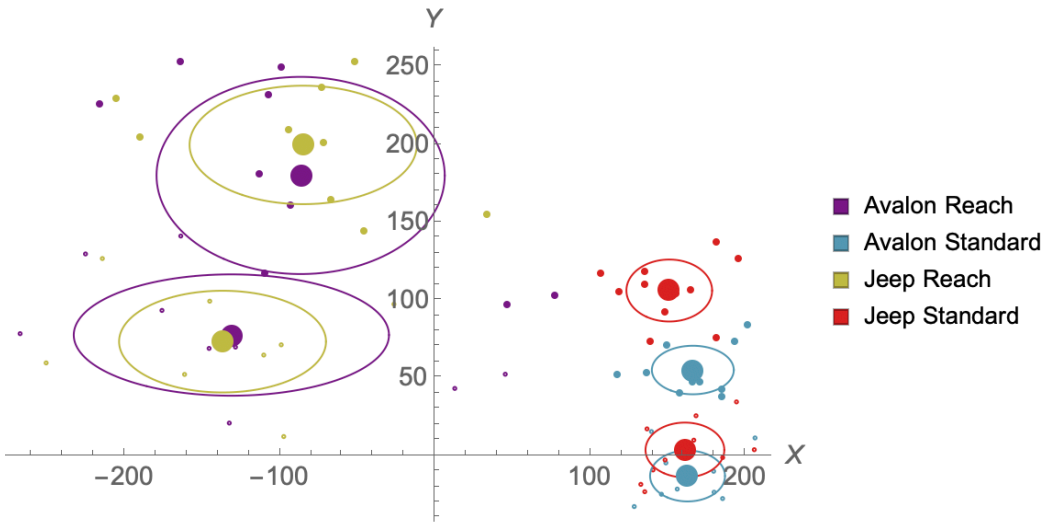

Figure 47. Top view of starting and maximum-excursion (outboard, top of plot) head CG locations (mm) relative to seat H-point for left lane change trials in vehicle block conditions. Large symbols are condition means. Ellipses show ±1SD on each axis.

Table 20. Maximum Outboard Head Excursions for Left Lane Change Trials in Vehicle Block Conditions (Mean and Standard Deviation, mm)

Vehicle	Posture	N	Mean Y	SD Y
Avalon	Reach	9	102.5	43.8
Avalon	Standard	10	68.1	15.3
Jeep	Reach	9	126.4	42.7
Jeep	Standard	11	102.5	23.3

4.4.4 Left Lane Change — Retractor Conditions

No significant differences due to seat position or retractor were observed in the retractor block trials (Figure 45 and Table 21). A minor trend toward greater excursion with greater stature was observed (p=0.02).

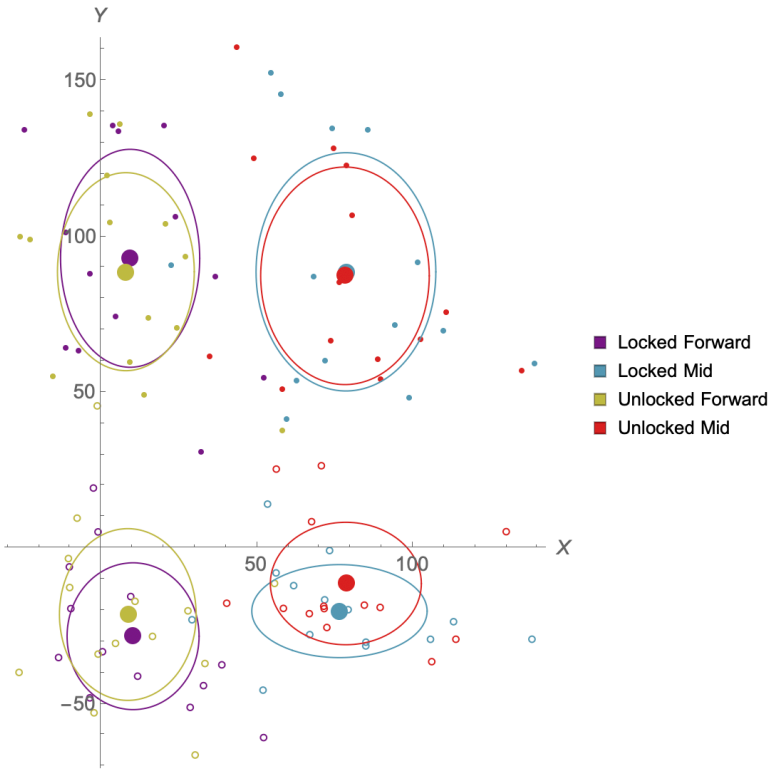

Figure 48. Top view of starting and maximum-excursion (outboard, top of plot) head CG locations (mm) relative to seat H-point for left lane change trials in retractor block conditions. Large symbols are condition means. Ellipses show ±1SD on each axis

Table 21. Maximum Outboard Head Excursions for Left Lane Change Trials in Retractor Block Conditions (Mean and Standard Deviation, mm)

Retractor	Seat Position	N	Mean Y	SD Y
Locked	Forward	13	121.3	28.1
Locked	Mid	14	108.9	37.6
Unlocked	Forward	14	110	31.4
Unlocked	Mid	14	98.8	27.4

4.4.5 Left Lane Chane — Lean/Reach Conditions

Outboard head excursions were significantly larger in Arm (inboard leaning) trials than in the other two reach/lean conditions, with participants' heads returning to the seat centerline, on average (Figure 46 and Table 22). Increased age was associated with reduced outboard excursion in Arm conditions only, with the regression function

$$\text{Y Excursion (Lt Lane Change)} = 250 - 1.81\ \text{Age},\ R^2_{ad} = 0.42,\ \text{RMSE}=38.6\ \text{mm}$$

for age in years.

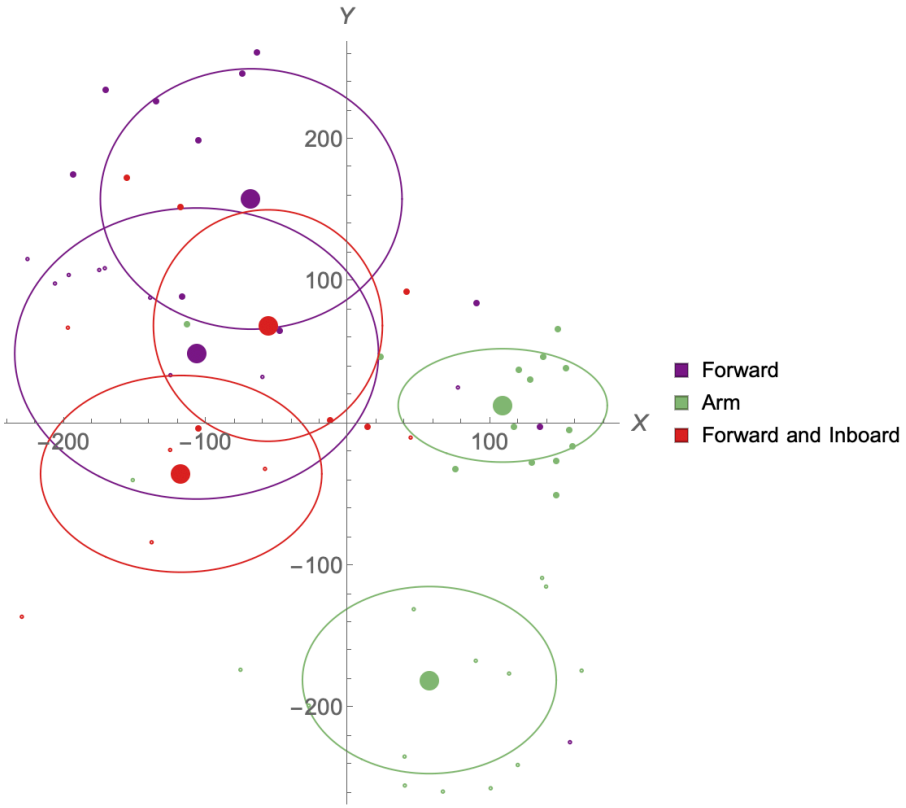

Figure 49. Top view of starting and maximum-excursion (outboard, top of plot) head CG locations (mm) relative to seat H-point for left lane change trials in lean/reach block conditions. Large symbols are condition means. Ellipses show ±1SD on each axis. Starting positions are lowest on plot (most negative Y) for each condition.

Table 22. Maximum Outboard Head Excursions for Left Lane Change Trials in Lean/Reach Block Conditions (Mean and Standard Deviation, mm)

Lean/Reach	N	Mean Y	SD Y
Forward	10	108.7	58
Arm	14	193.2	50.9
Forward and Inboard	6	104.3	47.3

4.5 Maximum Head Excursions — Turn and Brake

This section presents head excursion results for the turn and brake event, in which the driver executed an abrupt right turn accompanied by hard braking. This event tends to move the occupants head inboard and then forward. Both maximum inboard and forward excursions of the head CG were analyzed. Note that the forward direction is –X, so more-negative X excursions are further forward. The inboard direction is –Y, so more-negative Y excursions are further inboard. All analyses are conducted with respect to seat H-point and seat centerline except where noted.

4.5.1 Turn and Brake — Seat Position Conditions

Figure 47 plots the initial head locations (on seat centerline rearward of seat H-point, i.e., to the right in the figure) as well as the most inboard (lower in the figure) and most forward (to the left in the figure). Table 23 shows means and standard deviations for each condition. No significant effects of conditions or anthropometric variables were noted for either X or Y excursion.

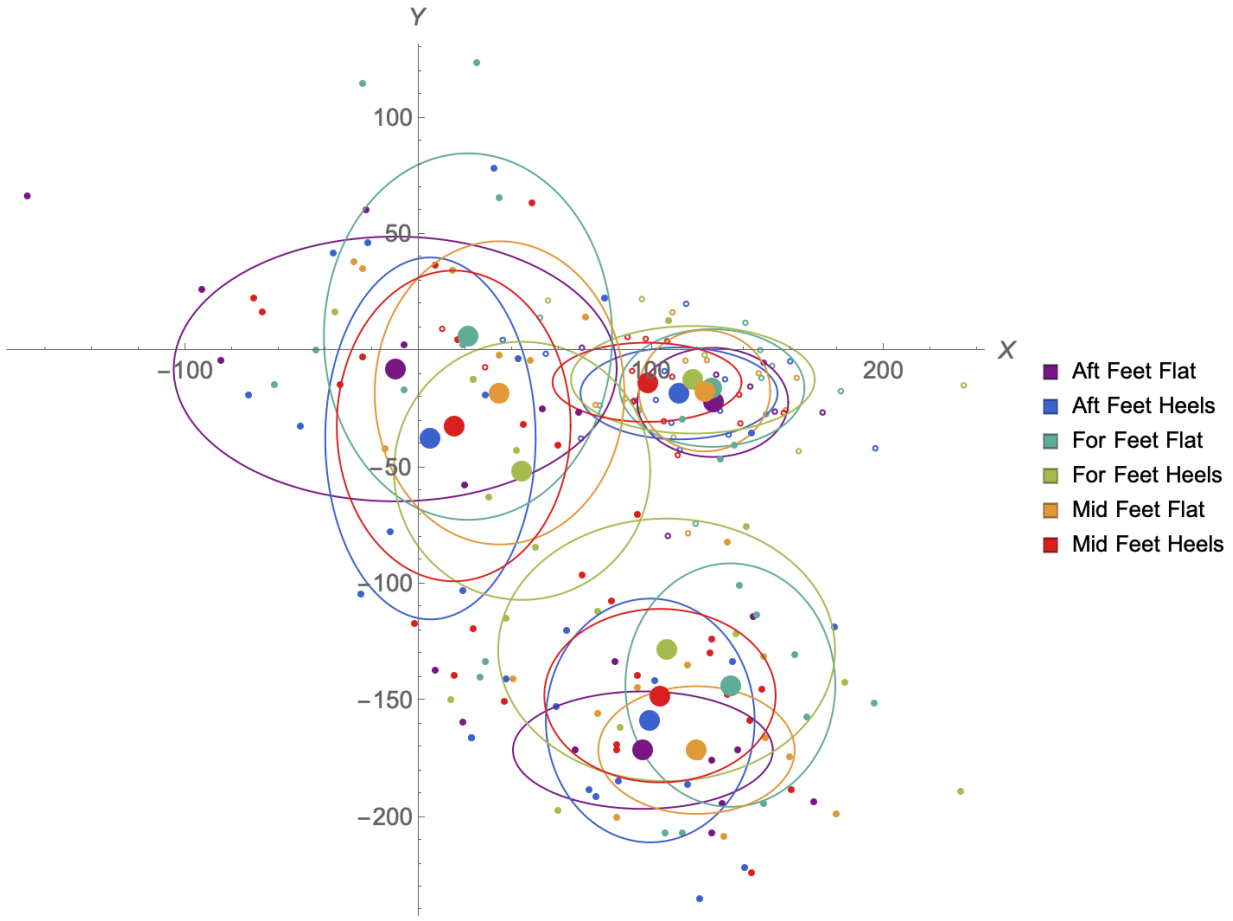

Figure 50. Top view of head CG locations (mm) in the starting location and at the maximum X-axis (forward) excursion (left side of plot) and maximum Y-axis excursion (bottom of plot) relative to seat H-point for turn-and-brake trials in seat position block conditions. Large symbols are condition means. Ellipses show ±1SD on each axis.

Table 23. Maximum Forward (X) and Inboard (Y) Head Excursions for Turn and Brake Trials in Seat Position Conditions
(Mean and Standard Deviation, mm)

Seat Position	Feet	N	Mean X	SD X	Mean Y	SD Y
Aft	Flat	9	-136.5	78.8	-149.2	21.6
Aft	Heels	13	-106.8	46.6	-140.3	45.4
Mid	Flat	9	-88.1	44.6	-127.5	47.3
Mid	Heels	13	-83.1	46.6	-115.9	43.0
For	Flat	10	-104.9	66.9	-154.1	20.8
For	Heels	9	-73.4	36.3	-134.5	24.4

4.5.2 Turn and Brake — Recline Conditions

Figure 48 shows starting head locations along with the points of maximum inboard (Y) and forward (X) excursions. The figure and Table 24 show reduced inboard excursion with increased recline angle, consistent with the findings from the lane-change trials. The regression function was

$$\text{Y Excursion (TB)} = -180 + 2.44\ \text{SeatBackAngle},\ R^2_{adj} = 0.22,\ \text{RMSE}=42.3$$

Increased stature was associated with reduced fore-aft excursion:

$$\text{X Excursion (TB)} = -626 + 0.300\ \text{Stature},\ R^2_{adj} = 0.25,\ \text{RMSE}=58.7\ \text{mm}$$

for stature in mm.

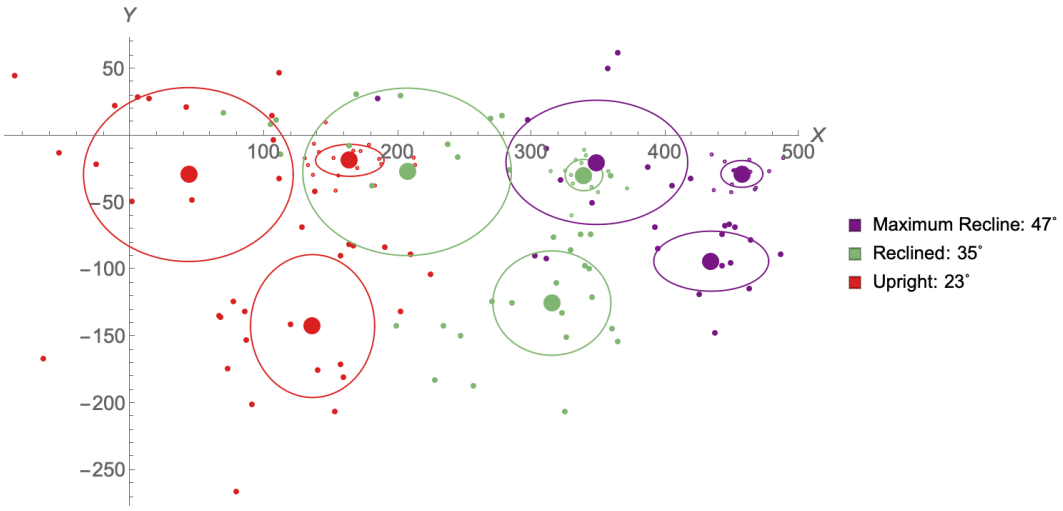

Figure 51. Top view of head CG locations (mm) in the starting location and at the maximum X-axis (forward) excursion (left side of plot) and maximum Y-axis excursion (bottom of plot) relative to seat H-point for turn-and-brake trials in recline conditions. Large symbols are condition means. Ellipses show ±1SD on each axis.

Table 24. Maximum Forward (X) and Inboard (Y) Head Excursions for Turn and Brake Trials in Recline Conditions (Mean and Standard Deviation, mm)

Seat Position	N	Mean X	SD X	Mean Y	SD Y
Upright: 23˚	18	-120.7	66.2	-123.9	54.3
Reclined: 35˚	17	-132.3	74.2	-95.7	40.8
Max: 47˚	13	-108.4	63.7	-65.2	23.9

4.5.3 Turn and Brake — Vehicle Conditions

In the vehicle-block conditions, the analyses were conducted separately for each axis and for the standard and reach trials. Fore-aft (X) excursion in the standard posture (Figure 49 and Table 25) was significantly associated with both stature and age

$$\text{X Excursion (TB, Standard Posture)} = -1220 + 0.58\ \text{Stature} + 2.14\ \text{Age},\ R^2_{adj} = 0.60,\ \text{RMSE} = 49.6\ \text{mm}$$

Both increased stature and increased age were associated with reduced excursion. In the reach trials, forward excursion was greater in the Jeep than in the Avalon and greater for participants with higher BMI:

$$\text{X Excursion (TB, Lean Posture)} = 187 - 67.6\ \text{Jeep} - 8.7\ \text{BMI},\ R^2_{adj} = 0.62,\ \text{RMSE} = 30.5\ \text{mm}$$

where Jeep has value 1 for trials in the Jeep and 0 in the Avalon and BMI is in kg/m^2. For Y excursion, no significant differences were found due to test conditions or anthropometric variables.

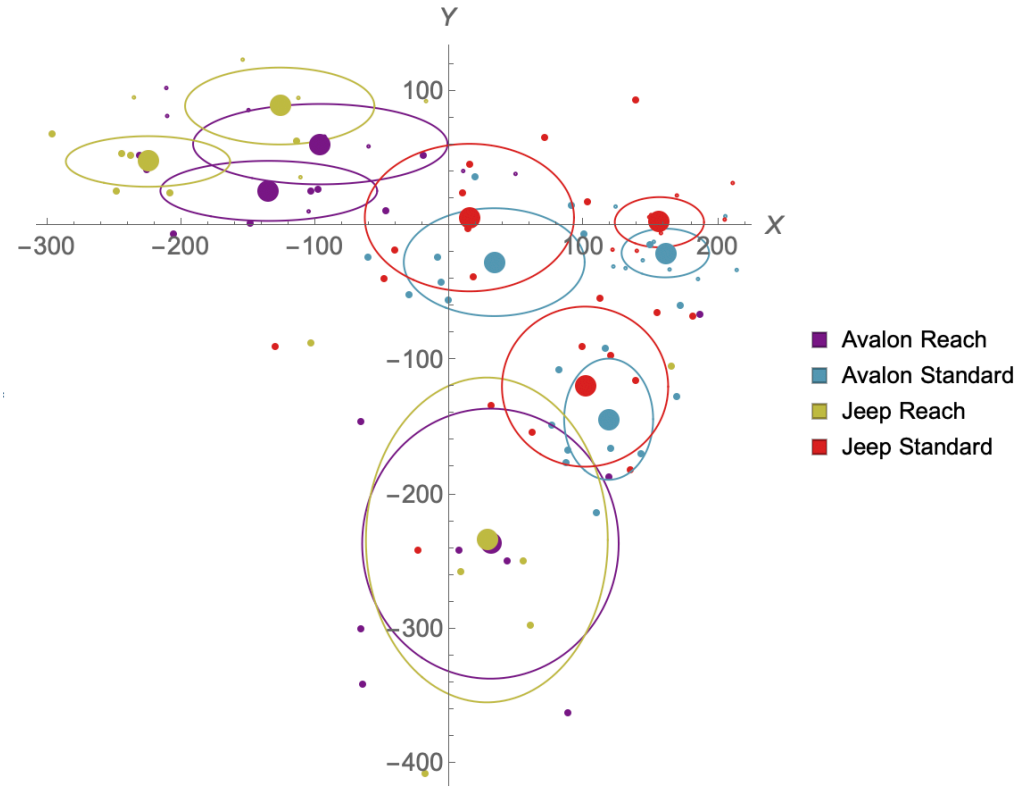

Figure 52. Top view of head CG locations (mm) in the starting location and at the maximum X-axis (forward) excursion (left side of plot) and maximum Y-axis excursion (bottom of plot) relative to seat H-point for turn-and-brake trials in vehicle block conditions. Large symbols are condition means. Ellipses show ±1SD on each axis

Table 25. Maximum Forward (X) and Inboard (Y) Head Excursions for Turn and Brake Trials in Vehicle Conditions (Mean and Standard Deviation, mm)

Vehicle	Posture	N	Mean X	SD X	Mean Y	SD Y
Avalon	Reach	8	-38.4	28	-297.3	123.2
Avalon	Standard	10	-127.5	67.8	-123.7	40.2
Jeep	Reach	6	-98.2	53.8	-322.9	140.5
Jeep	Standard	10	-141.6	91.1	-122.4	58.8

4.5.4 Turn and Brake — Retractor Conditions

In the retractor block conditions (Figure 50 and Table 26), no effects of the retractor or seat position were noted, but X excursion was reduced for older participants:

$$\text{X Excursion (TB)} = -137 + 1.1\ \text{Age},\ R^2_{adj} = 0.25,\ \text{RMSE}=37.6$$

On the Y axis, higher BMI was associated with increased excursion:

$$\text{Y Excursion (TB)} = -45.3 - 2.22\ \text{BMI},\ R^2_{adj} = 0.13,\ \text{RMSE}=32.8\ \text{mm}$$

A trend toward reduced excursion with increased age was noted (p=0.02).

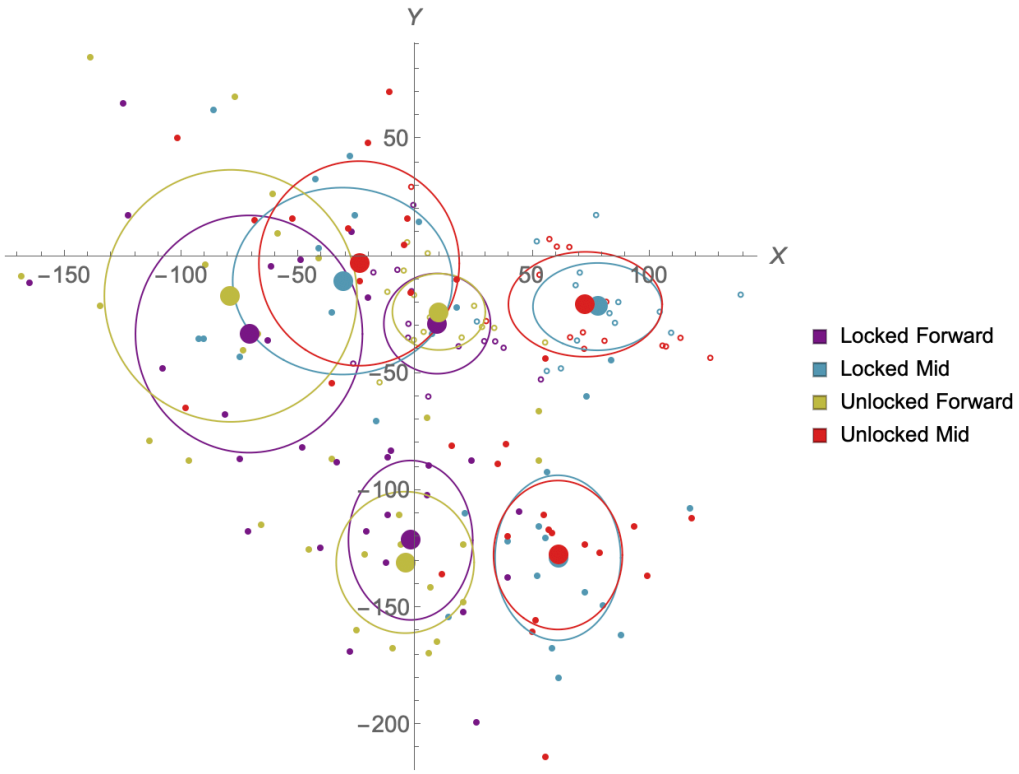

Figure 53. Top view of head CG locations (mm) in the starting location and at the maximum X-axis (forward) excursion (left side of plot) and maximum Y-axis excursion (bottom of plot) relative to seat H-point for turn-and-brake trials in retractor block conditions. Large symbols are condition means. Ellipses show ±1SD on each axis.

Table 26. Maximum Forward (X) and Inboard (Y) Head Excursions for Turn and Brake Trials in Retractor Conditions
(Mean and Standard Deviation, mm)

Retractor	Seat	N	Mean X	SD X	Mean Y	SD Y
Locked	Forward	14	-80.5	39.4	-92.5	33.5
Locked	Mid	14	-109.0	36.4	-107.2	36.0
Unlocked	Forward	14	-89.0	47.6	-106.9	38.5
Unlocked	Mid	15	-96.7	49.5	-107.0	34.6

4.5.5 Turn and Brake — Lean/Reach Conditions

Figure 51 and Table 27 show the maximum forward and inboard excursions for turn and brake in the reach/lean conditions. The X excursion was significantly larger in the Arm condition than in the others, but no anthropometric effects were observed. Y excursions tended to be smaller in the

Arm condition (p=0.03), but N was small as noted earlier. No anthropometric effects were noted for Y excursion in any condition.

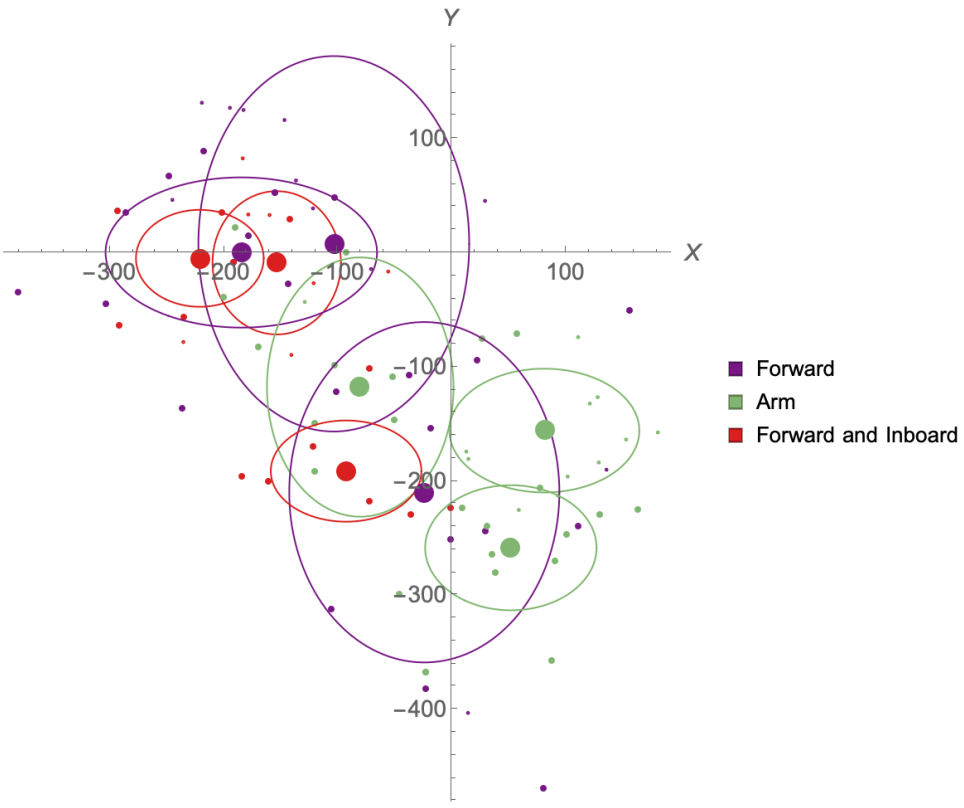

Figure 54. Top view of head CG locations (mm) in the starting location and at the maximum X-axis (forward) excursion (left side of plot) and maximum Y-axis excursion (bottom of plot) relative to seat H-point for turn-and-brake trials in reach/lean block conditions. Large symbols are condition means. Ellipses show ±1SD on each axis.

Table 27. Maximum Forward (X) and Inboard (Y) Head Excursions for Turn and Brake Trials in Lean/Reach Conditions
(Mean and Standard Deviation, mm)

Lean/Reach	N	Mean X	SD X	Mean Y	SD Y
Forward	11	-81.1	50.6	-217.6	159.6
Arm	12	-161.5	70.6	-102.6	71.1
Forward and Inboard	7	-67.5	35.6	-182.4	98.2

4.6 Summary of Significant Effects on Maximum Head Excursion on Primary Axes

Table 28 summarizes the significant effects of initial conditions and anthropometric variables on forward and lateral excursion across the vehicle maneuvers. Table 29 shows conditions under which subject covariates had significant effects. Although sample sizes are relatively small in individual conditions, a lack of significant effect generally means that the effect is small enough

to be neglected. For more robust tests of covariate effects in a small number of conditions, see Reed et al. (2018).

Table 28. Summary of Effects on Maximum Head Excursions

Variable	Effect on Forward Excursion	Effect on Lateral Excursion
Seat Position	Greater excursion when seat is more rearward	No significant effect
Foot Placement	Larger excursion when feet are flat on soles and smaller when feet are on heels	Larger excursion when feet are flat than when feet are on heels.
Recline	Greater excursion with greater recline	Greater excursion more upright
Vehicle	No significant effect	Greater excursion in Jeep only for outboard motion in left lane change in standard posture
Retractor	No significant effect	No significant effect
Lean/Reach	Greater excursion with arm lean than with forward or forward+inboard lean; Reduced excursion with forward lean than in standard posture	Greater excursion with forward or forward+inboard lean than in standard posture; Reduced inboard excursion with arm lean in right lane change but increased outboard excursion with arm lean in left lane change

Table 29. Conditions in Which Anthropometric Variables Were Associated With More (+) or Less (–) Excursion

Condition	Exposure	Stature	Age	BMI
Braking	Seat Position		–	
	Retractor		–	
Right Lane Change	Seat Position		–	
	Retractor	+		
Left Lane Change	Seat Position			
	Retractor	+		
	Lean/Reach		–	
Turn and Brake (lateral)	Retractor			+
Turn and Brake (fore-aft)	Recline	–		
	Vehicle	–	–	
	Retractor		–	

4.7 Statistical Analysis of Head CG Trajectories

The prior section showed significant differences in maximum head excursion across exposures and test conditions, with some small effects of anthropometric variables. The distribution of maximum excursions provides guidance on the range of possible head locations in crashes due to pre-crash maneuvers. However, a time-history of head location is valuable for other applications, particularly for tuning and validating computational simulations of occupants experiencing abrupt vehicle maneuvers.

To address this need, this section presents a statistical analysis of the time-history of head excursions in the primary directions of motion. The method employs functional regression, which models the entire time-history of the signal rather than just a scalar value such as the peak excursion presented in the previous section. This approach allows visualization of the effects of the test conditions and subject covariates on the excursion trajectory and provides a way to generate corridors that are appropriately adjusted for these factors.

The functional analysis proceeded through the following steps.

1. Each trajectory was first time-zeroed based on an algorithm that identified the first point at which the acceleration on the principal axis (X axis for braking, Y for lane change maneuvers and turn-and-brake) exceed 0.2 g, then projecting the gradient at that point backward to find the axis crossing.
2. Assemble the time-series data to be modeled (head-CG locations on the primary axes versus time).
3. Fit cubic splines to the data to provide smoothing and to reduce the dimension of the data (see Appendix A).
4. Conduct a principal component analysis to visualize the primary modes of variation in the data.
5. Conduct a regression analysis predicting principal component scores from the test conditions and subject covariates (stature, age, etc.).
6. Use the regression analysis to illustrate the effects of test conditions and subject covariates (stature, age, etc.).

Potential predictors in the regression analysis were the following.

- seat position (continuous: mm forward of full rear)
- foot placement (heels or flat)
- lean/reach (forward or no lean)
- seat back angle (continuous: 23, 35, or 47 degrees)
- stature (mm)
- age (year)
- BMI (kg/m^2)

Only main effects were modeled, because the analysis of maximum excursion values suggested that the few significant interactions had small effects and would not contribute meaningfully to the models.

Corridors were developed for a particular combination of predictors using a simulation process:

1. Using the regression functions, predict the mean expected score on each principal component (PC) for the selected vector of predictors.
2. Obtain a large sample (1,000 was used in this section) from a normal distribution with standard deviation equal to the root-mean-square error (residual) from the regression for each principal component; add to the predicted mean score to obtain 1,000 simulated PC score vectors
3. Generate curves using each of these simulated PC vectors (the vector of PC scores is multiplied by the PC matrix to obtain a vector of spline coefficients, which is then used to construct the predicted displacement versus time curve).
4. Compute a corridor as mean ± 1 standard deviation (SD) at each time point.

Note that the choice of 2 SD for the corridor width is arbitrary but follows the typical convention in crash injury biomechanics. Corridors were generated for a few combinations of variables, including those found to be significant predictors of PC scores. The values needed to generate corridors are provided in Appendix B and C. The analyses are presented for each exposure in the same sequence used for the maximum excursion analysis.

4.7.1 Head CG Trajectories — Braking

Head CG excursions versus time on the X axis were aggregated across all braking trials except for the arm-lean conditions (N=427 trials). The arm-lean conditions were excluded due to the differences in responses that resulted from the additional contact point with the interior.

Figure 52 shows a subset of time-zeroed X excursions for braking trials. Note the large amount of variability in both the magnitude and shape of the curves.

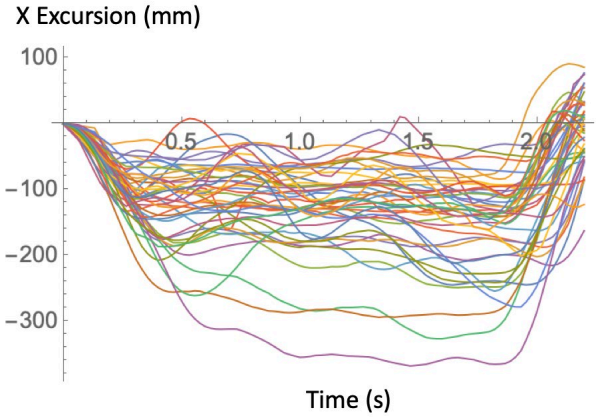

Figure 55. Subset of 50 time-zeroed head-CG excursions on the X axis (-X = forward).

Each trajectory was fit with a cubic basis spline having 12 evenly spaced knots. (The spline calculations are described in detail in Appendix A.) Figure 53 shows typical trajectory fits. The spline fit was generally excellent. The median and 95th-percentile root-mean-square error across curves were 4.1 and 7.5 mm, respectively.

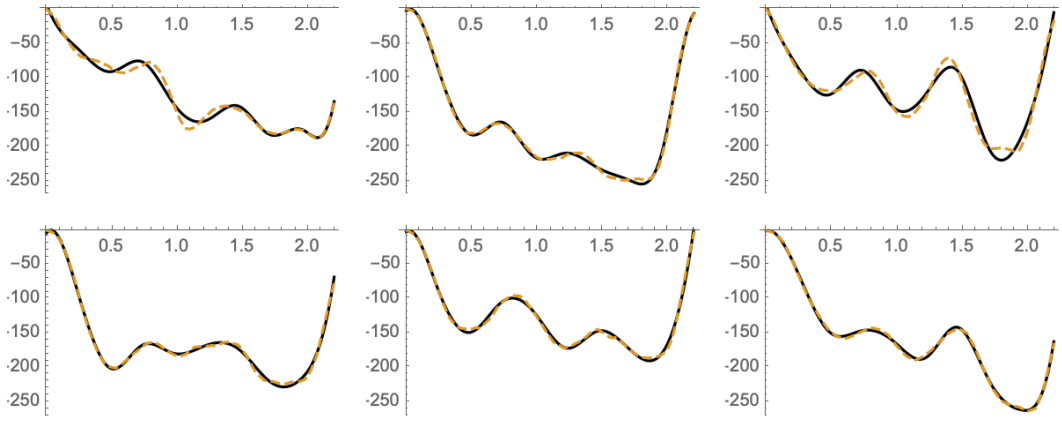

Figure 56. Examples of fitting trajectory data (dashed lines) with cubic basis splines (solid lines).

Following spline fitting, each trajectory curve was represented by a vector of 12 values, representing the coefficients (or weights) for each basis spline curve. Subsequent analysis focused on statistical modeling of these twelve values.

A principal component analysis was conducted to examine the primary modes of variation across the dataset. The first three principal components (PCs) were found to account for 95 percent of the variance in the spline coefficients. Figure 54 illustrates the first three PCs. The first relates primarily to magnitude, while the second and third relate to the shape of the curve.

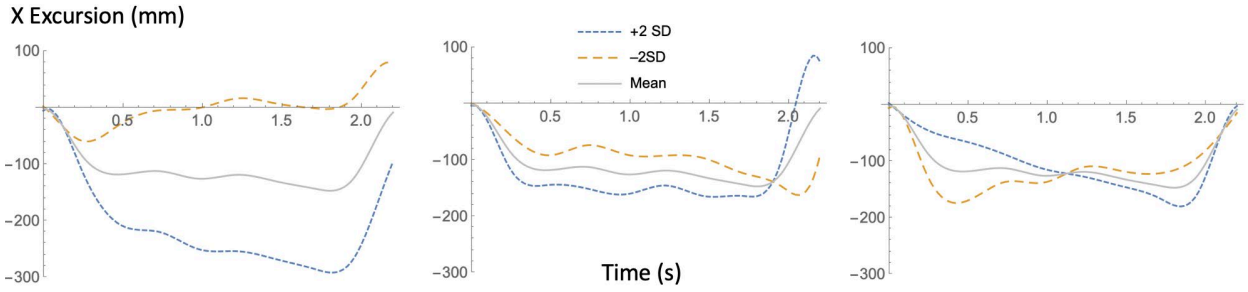

Figure 57. Illustration of first three principal components (PCs) in braking X-axis excursion data.

An exploratory regression analysis was conducted to determine the relationships between the potential predictors listed above and the scores on each of the first three PCs. Significant effects ($p<0.05$) were found for the variables listed in Table 30. The first PC was significantly affected by all predictors except for stature, with an adjusted R^2 value of 0.17. The second PC was not substantially affected by any predictor, meaning that this PC captures effects of subject differences that are not associated with the potential predictors. PC3, which relates to the excursion increasing or decreasing during the exposure (see Figure 54) was significantly affected by all predictors except for forward lean and age. Figure 55-Figure 60 show the effects of each predictor on the excursion trajectory.

Table 30. Effects of Predictors on Principal Component Scores: Braking

Predictor	PC1	PC2	PC3
Seat Position	***		***
Feet Flat	*		***
Forward Lean	***		
Recline	***		***
Age	***		
BMI			
Stature		*	***
R^2_{adj}	0.17	0.01	0.22

* p<0.05, ** p<0.01, *** p<0.001

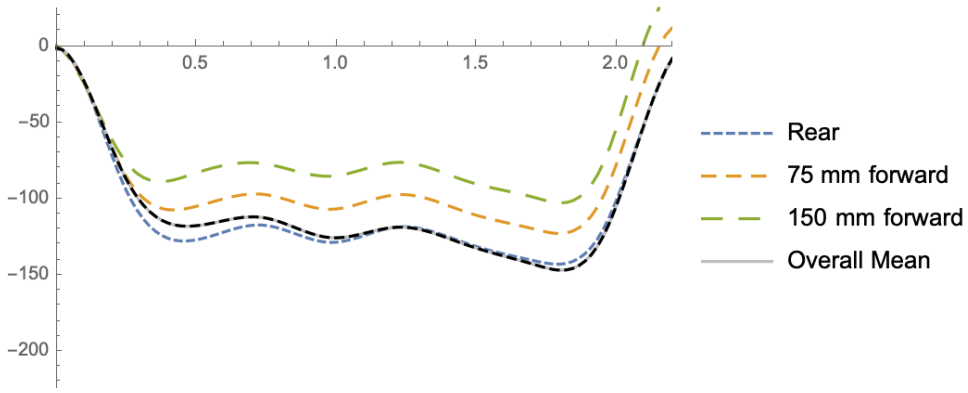

Figure 58. Effects of seat position on x-axis head excursion (mm) versus time (s) in braking.

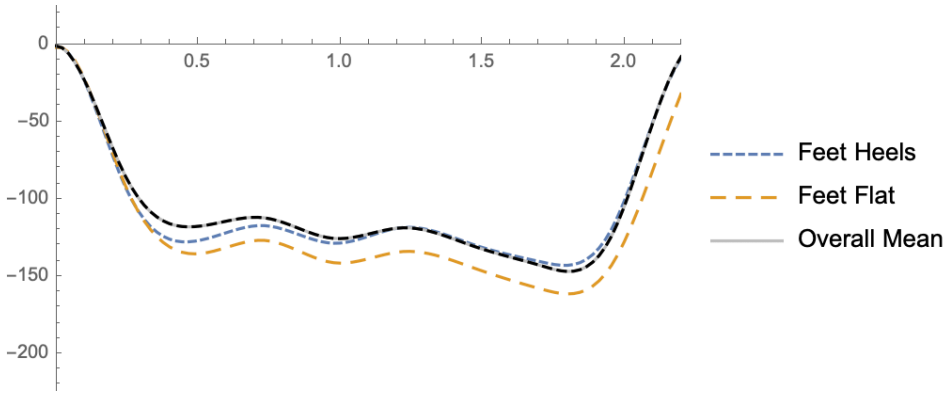

Figure 59. Effects of foot posture on x-axis head excursion (mm) versus time (s) in braking.

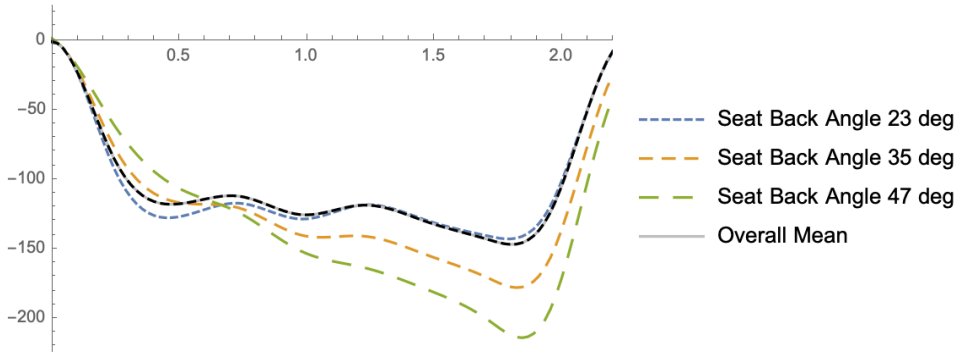

Figure 60. Effects of recline on x-axis head excursion (mm) versus time (s) in braking.

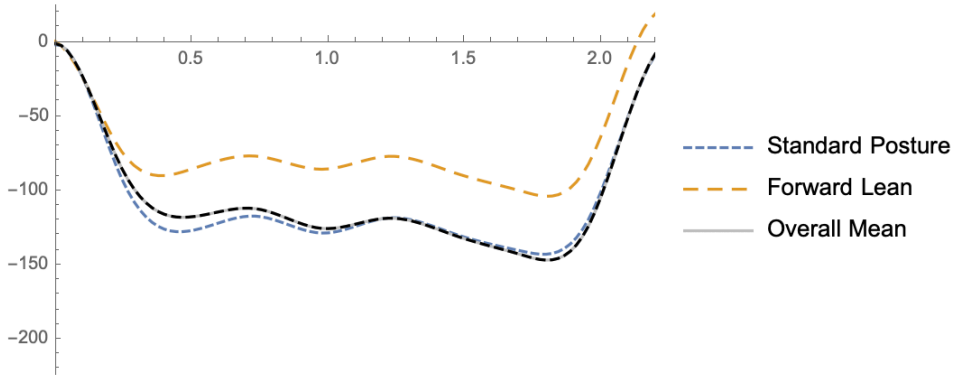

Figure 61. Effects of forward lean on x-axis head excursion (mm) versus time (s) in braking.

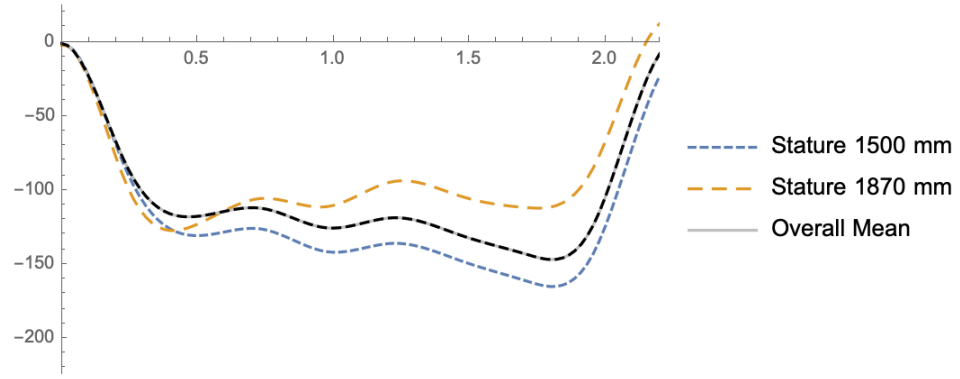

Figure 62. Effects of stature on x-axis head excursion (mm) versus time (s) in braking.

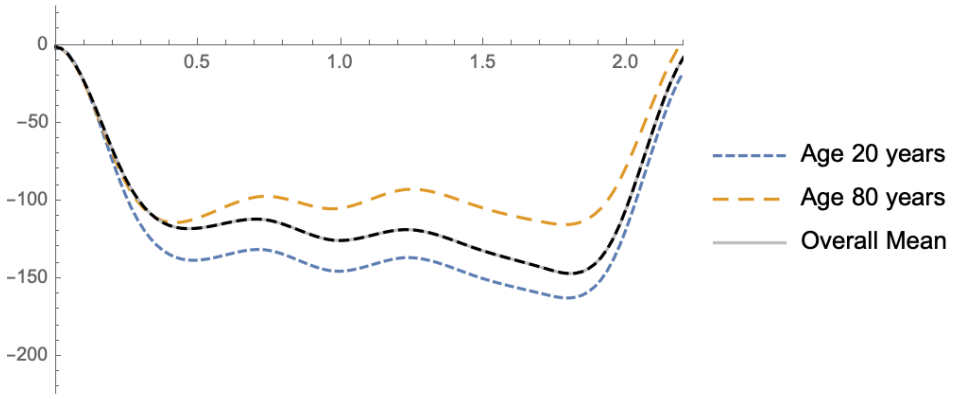

Figure 63. Effects of age on x-axis head excursion (mm) versus time (s) in braking.

Figure 61 shows a corridor (mean±1SD) for x-axis head excursion in braking (tabulated values are in Appendix D). Due to the structure of the model, the corridor width is the same regardless of the predictor values. Reviewing Figure 61 along with the preceding figures indicates that the factor effects are small compared with the residual variance that is not accounted for by any predictor, consistent with the relatively small R^2 values in Table 30. Due to the continuous nature of the model, an infinite number of corridors can be generated based on different combinations of the predictors. Figure 62 shows some examples chosen to demonstrate relatively large differences. Note that a few combinations were not tested and are not meaningful, such as highly reclined with forward lean. Figure 63 shows that combinations of the significant anthropometric effects (stature and age) can result in combined differences approximately equal to one standard deviation (i.e., half the corridor width).

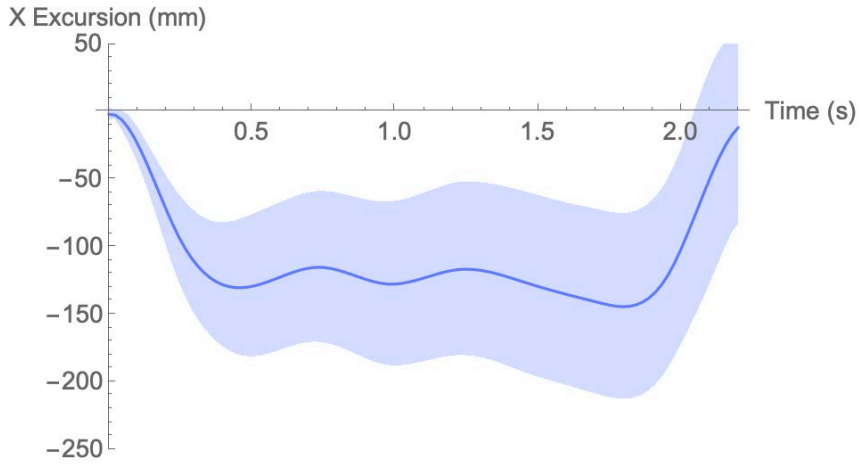

Figure 64. Mean±1SD corridor for head CG x-axis excursion in braking, for seat full rear, feet on heels, seat back angle 23 deg, no forward lean, stature = 1,650 mm, age = 45 years.

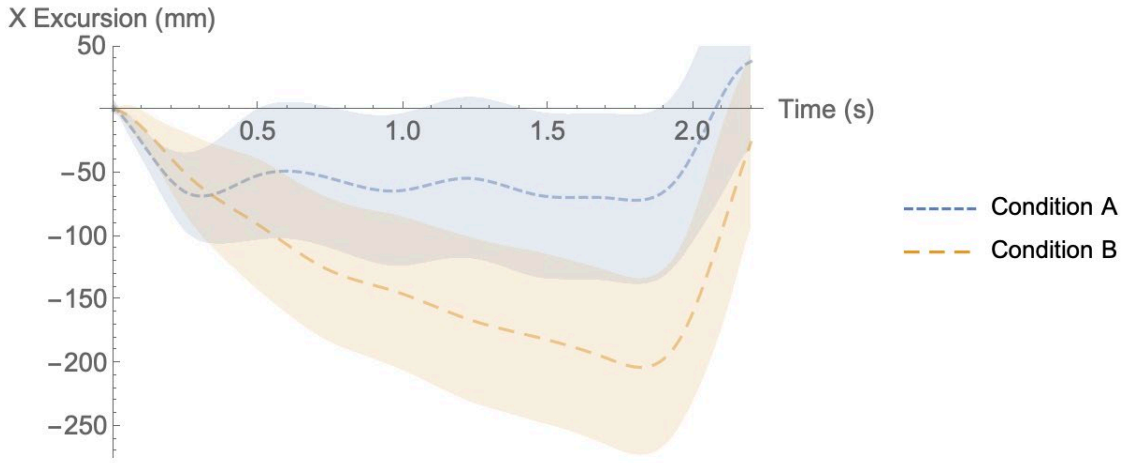

Figure 65. Mean±1SD corridor for head CG x-axis excursion in braking. Condition A (all factors levels chosen to minimize excursion): seat 150 mm forward, feet on heels, seat back angle 23 deg, forward lean, stature = 1,510 mm, age = 80 years; Condition B (all factors levels chosen to maximize excursion): seat full rear, feet flat, seat back angle 47 deg, no forward lean, stature = 1,870 mm, age = 20 years.

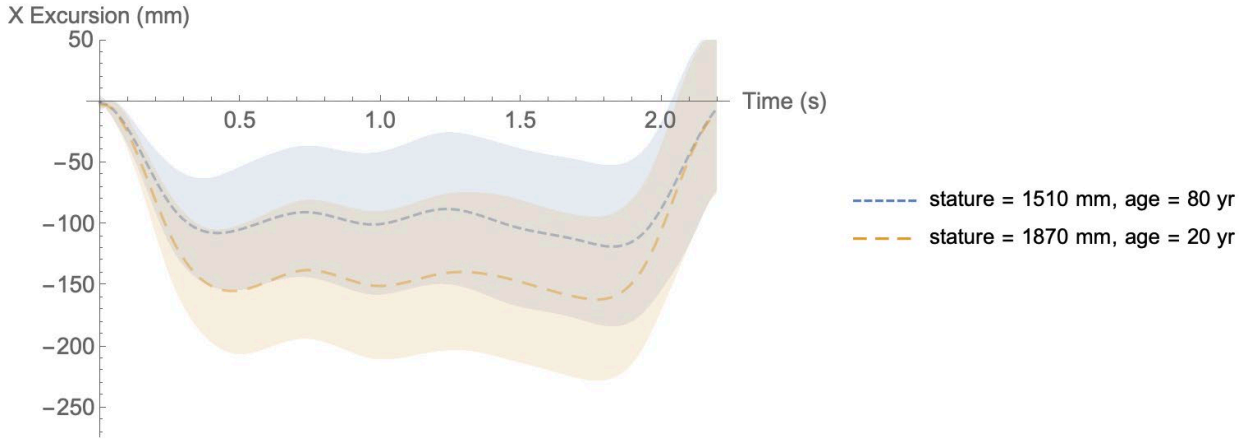

Figure 66. Mean±1SD corridor for head CG x-axis excursion in braking for two stature and age levels. Factors held constant: seat full rear, feet on heels, seat back angle 23 deg, no forward lean.

4.7.2 Head CG Trajectories — Right Lane Change

The inboard (–Y) excursion for the right-going lane change was analyzed using the same techniques. A total of 218 trials were available for analysis. Figure 64 shows a subset of excursion data, demonstrating substantial variability, as expected based on the maximum excursion analysis. The median and 95th-percentile root-mean-square error across curves were 3.3 and 7.6 mm, respectively. The first three PCs accounted for 86 percent of the variance and four PCs accounted for 95 percent. Figure 65 illustrates the first three PCs. The first PC is related to inboard versus outboard (rebound) excursion. The second PC is related to the overall scaling of the motion, and the third primarily captures timing differences.

Table 31 shows that forward lean and recline had the most significant effects on the PC scores, consistent with the maximum excursion analyses above. Figure 66-Figure 71 illustrate the effects of the predictors, showing the large increase in inboard excursion with forward lean compared to a standard posture and a reduction in excursion with increasing recline. The anthropometric effects were comparatively small. Figure 72 illustrates the corridor for a typical combination of variables. Figure 73 shows the range that can be obtained depending on the combination of predictors; Figure 74 illustrates the maximum effect obtained by combinations of anthropometric variables alone.

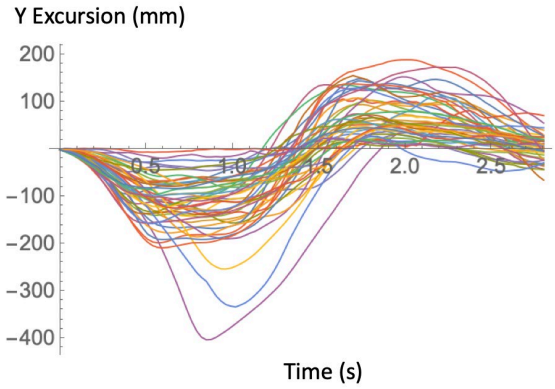

Figure 67. Subset of 50 time-zeroed head-CG excursions on the Y axis (-Y = inboard) in right lane change.

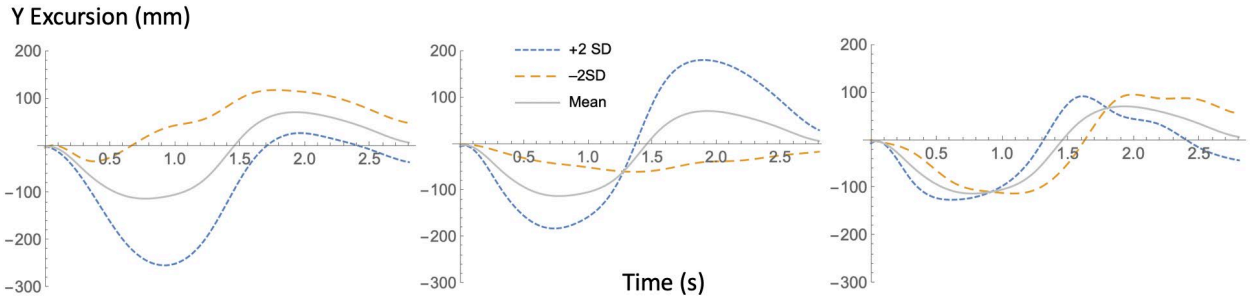

Figure 68. Illustration of first three PCs in Y-axis (inboard) excursion data from right lane change trials.

Table 31. Effects of Predictors on Principal Component Scores: Right Lane Change

Predictor	PC1	PC2	PC3
Seat Position			*
Feet Flat		*	
Forward Lean	***		**
Recline	*	***	
Age		*	
BMI			**
Stature			
R^2_{adj}	0.29	0.11	0.13

* p<0.05, ** p<0.01, *** p<0.001

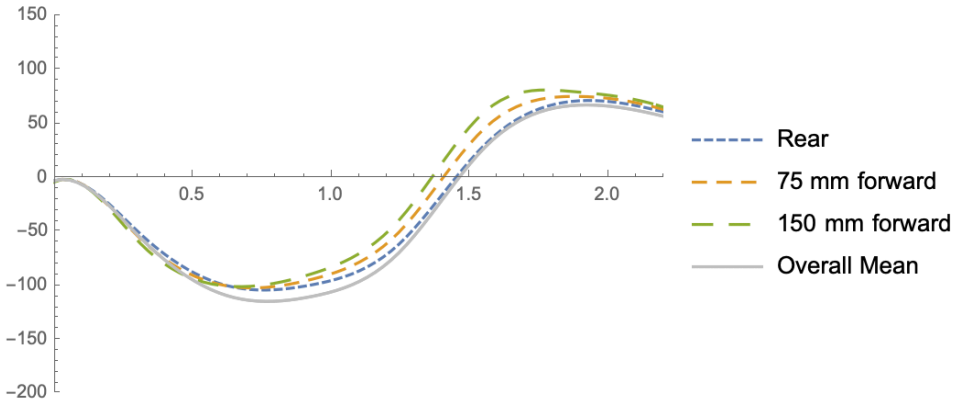

Figure 69. Effects of seat position on y-axis head excursion (mm) versus time (s) in right lane change.

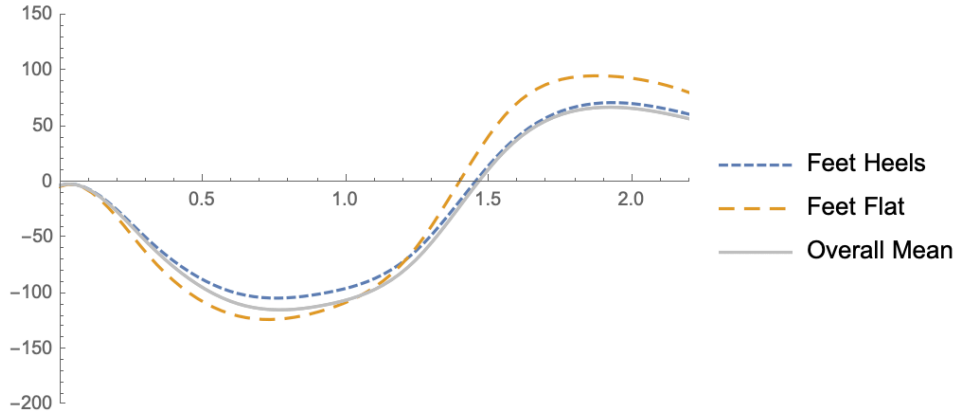

Figure 70. Effects of foot posture on y-axis head excursion (mm) versus time (s) in right lane change.

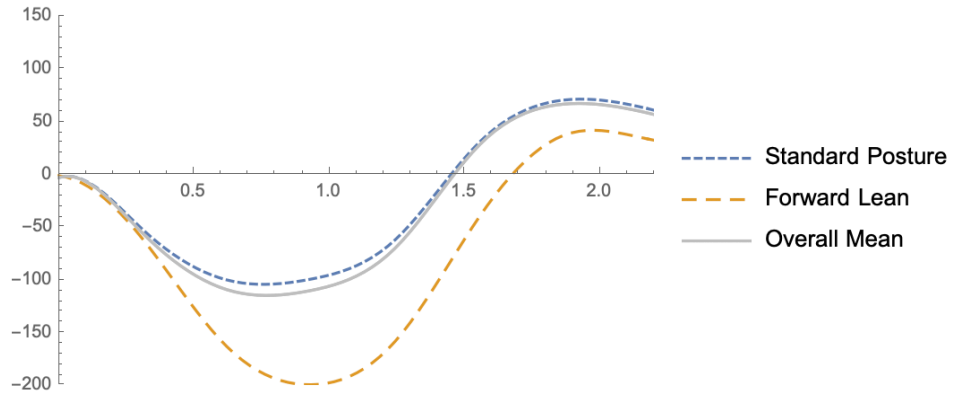

Figure 71. Effects of forward lean on y-axis head excursion (mm) versus time (s) in right lane change.

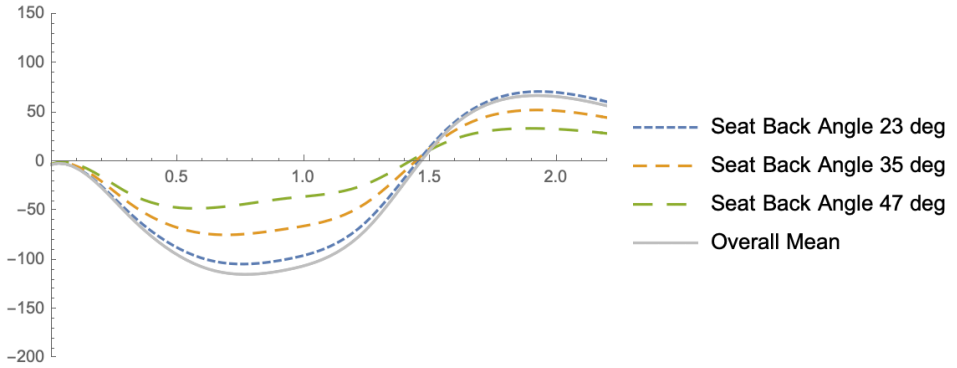

Figure 72. Effects of recline on y-axis head excursion (mm) versus time (s) in right lane change.

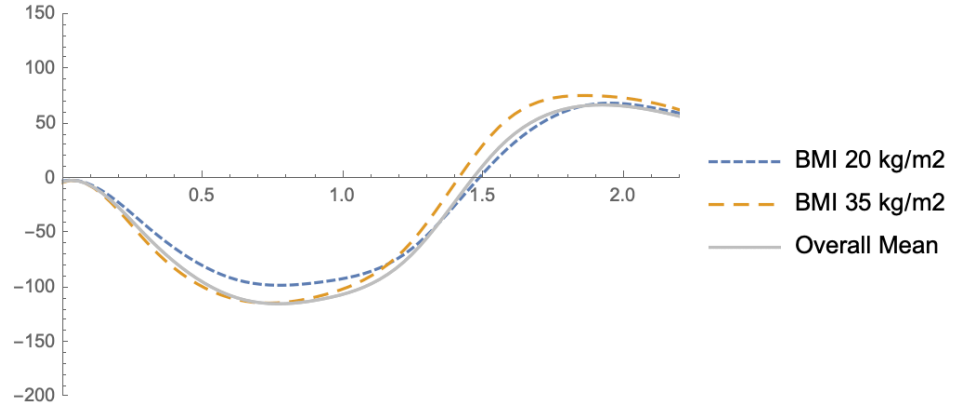

Figure 73. Effects of BMI on y-axis head excursion (mm) versus time (s) in right lane change.

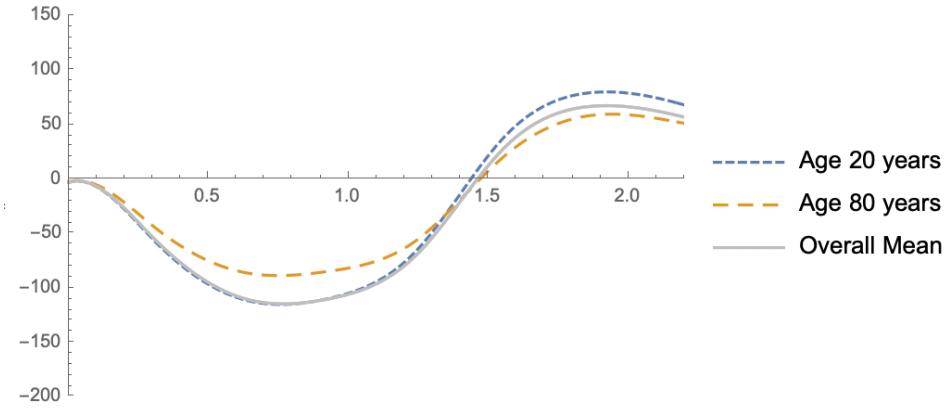

Figure 74. Effects of age on y-axis head excursion (mm) versus time (s) in right lane change.

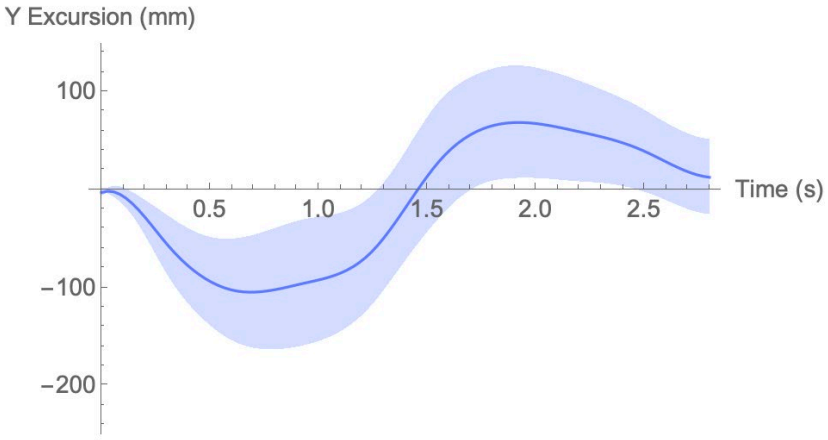

Figure 75. Mean±1SD corridor for head CG y-axis excursion in right lane change, for seat full rear, feet on heels, seat back angle 23 deg, no forward lean, BMI=26 kg/m2, age = 45 years.

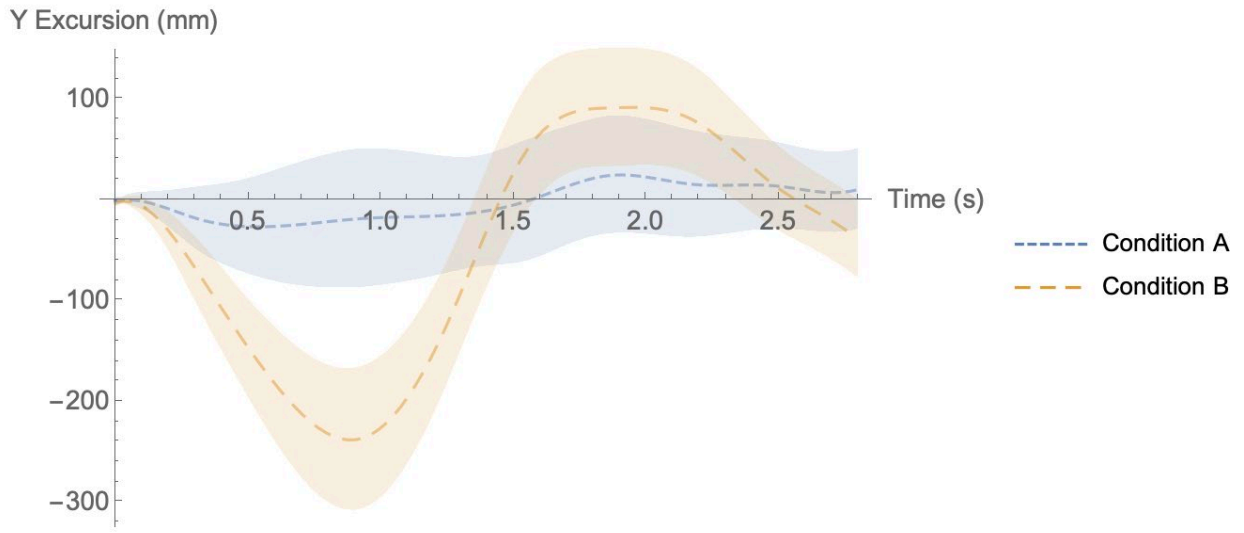

Figure 76. Mean±1SD corridor for head CG y-axis excursion in right lane change for two extreme conditions. Condition A (all factors levels chosen to minimize excursion): seat full forward, feet on heels, seat back angle 47 deg, no forward lean, BMI = 20 kg/m2, age = 80 years; Condition B (all factors levels chosen to maximize excursion): seat 150 mm forward, feet flat, seat back angle 23 deg, leaning forward, BMI=35 kg/m2, age = 20 years.

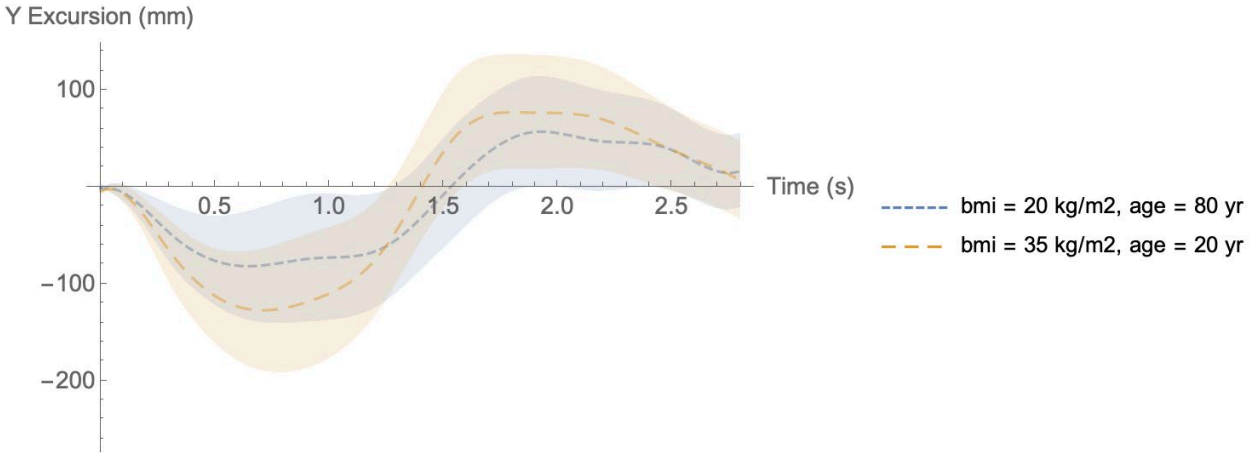

Figure 77. Mean±1SD corridor for head CG y-axis excursion in right lane change for two combinations of anthropometric variables. Factors held constant: seat full rear, feet on heels, seat back angle 23 deg, no forward lean.

4.7.3 Head CG Trajectories — Left Lane Change

The outboard (–Y) excursion for the left-going lane change was analyzed using the same techniques. A total of 239 trials were available for analysis. Figure 75 shows a subset of excursion data, demonstrating substantial variability, as expected based on the maximum excursion analysis. The median and 95th-percentile root-mean-square error across curves were 3.0 and 5.9 mm, respectively. The first three PCs accounted for 86 percent of the variance and four PCs accounted for 95 percent.

Figure 76 illustrates the first three PCs. The first PC is primarily related to inboard (i.e., rebound) excursion. That is, the most prominent way in which the curves differ is in the magnitude of the rebound phase. The second PC is related to the time lag, while the third shows the effects of the outboard excursion magnitude in the initial phase.

Table 32 shows that the predictors had minimal effects on the PC scores. No anthropometric variables had significant effects. The most significant effect was the relationship between recline and PC3, which is primarily related to the magnitude of the outboard excursion. Figure 77-Figure 79 illustrate the effects of the significant predictors.

Figure 80 illustrates the corridor for a typical combination of variables. Figure 81 shows the range that can be obtained depending on the combination of predictors. The effect of the predictors on the rebound phase is larger than on the primary (outboard) phase; with certain combinations of variable, the rebound phase (inboard) motion is comparable in magnitude to that observed in the right-going lane change.

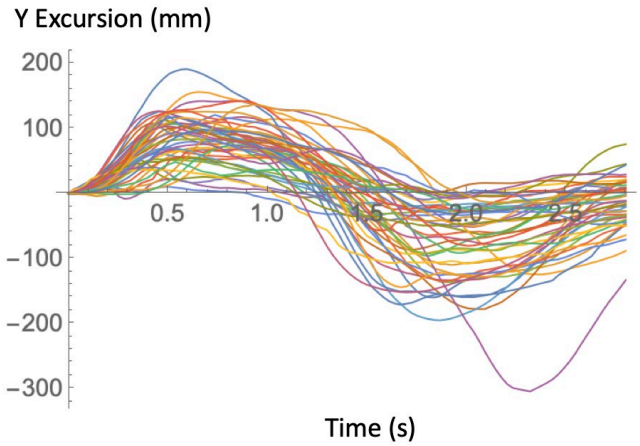

Figure 78. Subset of 50 time-zeroed head-CG excursions on the Y axis (+Y = outboard) in left lane change.

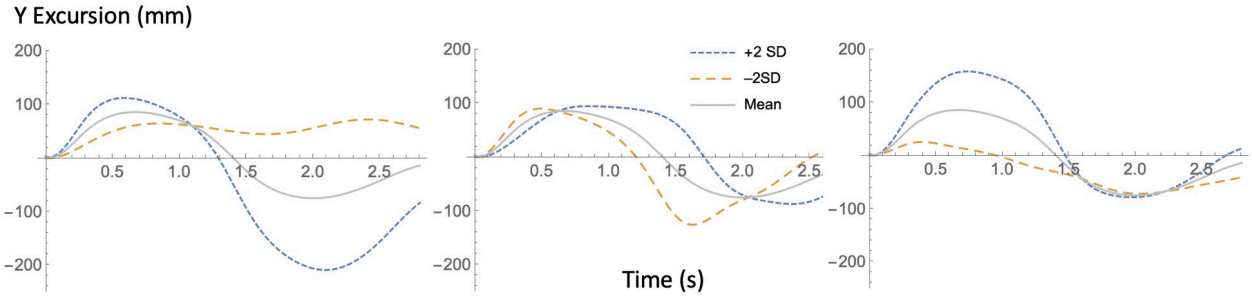

Figure 79. Illustration of first three PCs in Y-axis (outboard) excursion data from left lane change trials.

Table 32. Effects of Predictors on Principal Component Scores: Left Lane Change

Predictor	PC1	PC2	PC3
Seat Position			
Feet Flat	*		
Forward Lean		*	
Recline	*		***
Age			
BMI			
Stature			
R^2_{adj}	0.09	0.07	0.09

* p<0.05, ** p<0.01, *** p<0.001

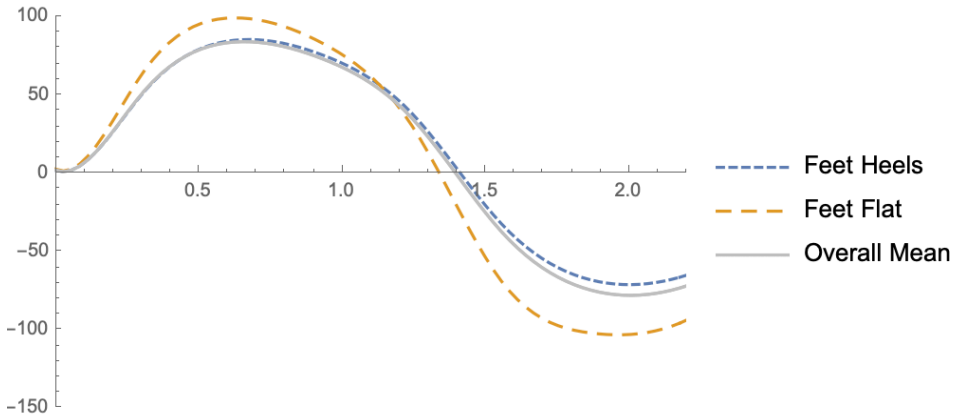

Figure 80. Effects of foot posture on y-axis head excursion (mm) versus time (s) in left lane change.

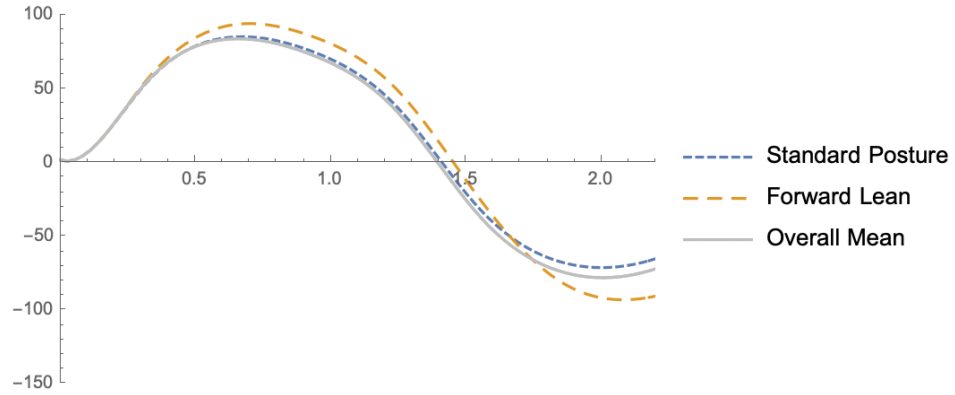

Figure 81. Effects of forward lean on y-axis head excursion (mm) versus time (s) in left lane change.

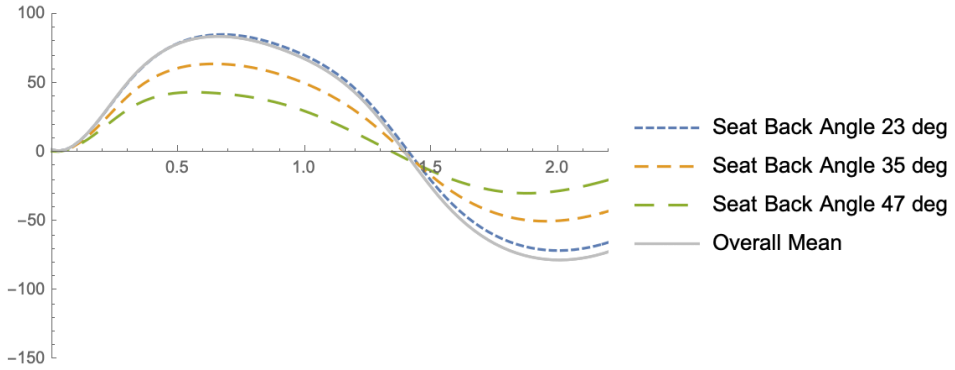

Figure 82. Effects of recline on y-axis head excursion (mm) versus time (s) in left lane change.

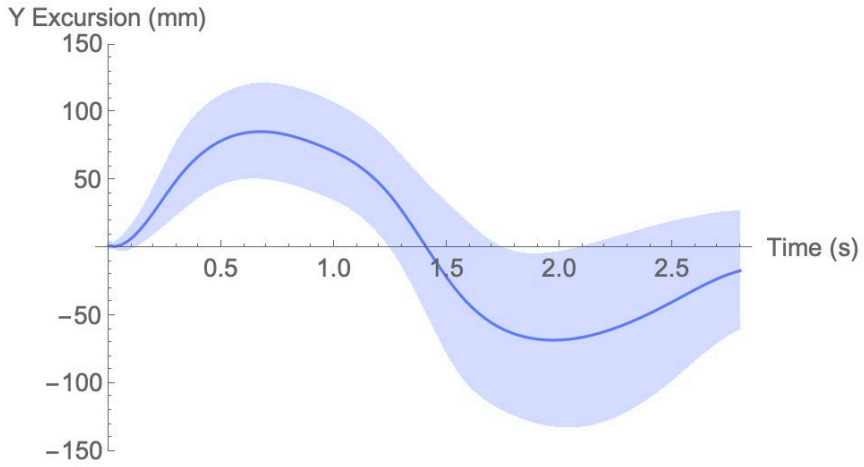

Figure 83. Mean±1SD corridor for head CG y-axis excursion in left lane change, for seat full rear, feet on heels, seat back angle 23 deg, no forward lean, BMI=26 kg/m^2, age = 45 years.

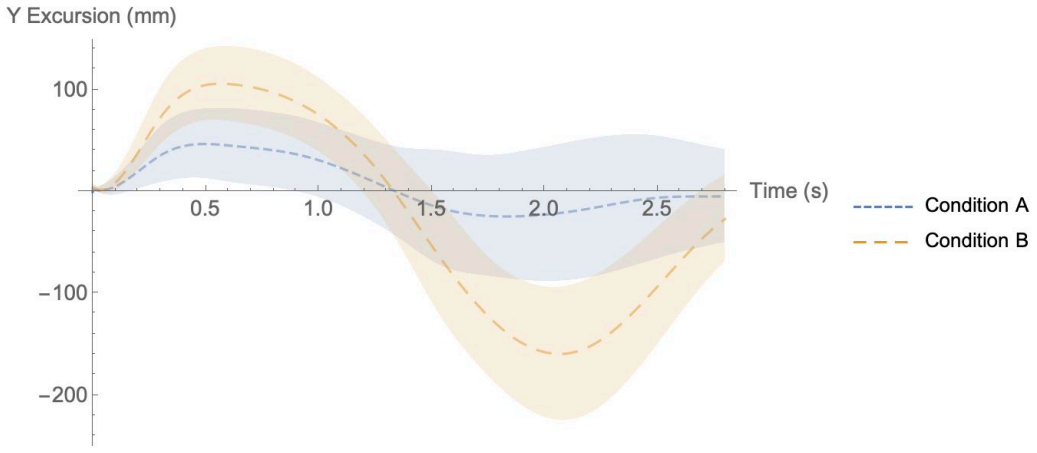

Figure 84. Mean±1SD corridor for head CG y-axis excursion in left lane change for two extreme conditions. Condition A (all factors levels chosen to minimize excursion): seat full rearward, feet on heels, seat back angle 47 deg, no forward lean, BMI = 26 kg/m2, age = 45 years; Condition B (all factors levels chosen to maximize excursion): seat full rearward, feet flat, seat back angle 23 deg, leaning forward, BMI=26 kg/m2, age = 45 years.

4.7.4 Head CG Trajectories — Turn and Brake — X Excursions

The fore-aft head excursions in the 227 turn-and-brake trials available for analysis were highly variable. For some participants, the head moved rearward from the starting point, rather than forward as would be expected based on the braking acceleration. Figure 82 shows a subset of head-CG excursion trajectories on the X axis. The analysis was conducted in the same manner as above. Figure 83 shows the PC plots. The first PC is associated with forward vs. backward movement of the head, while PCs 2 and 3 relate to the shape and duration of the primary phase of motion.

Table 33 and Figure 84 to Figure 87 show that forward lean was by far the most consequential predictor, with a large *rearward* excursion observed in the first part of the exposure. The rapid rise of the lateral acceleration tended to swing the participant's head inboard and rearward prior to the onset of large longitudinal accelerations (see the next section for the analysis lateral movement).

Figure 88 shows a corridor calculated for nominal conditions without forward lean. The corridor includes zero excursion except for a brief interval around 2.5 seconds into the event. Figure 89 shows a corridor with variable values selected maximize differences. As expected from the earlier plots, the primary effect is due to forward lean. Anthropometric factors are not important.

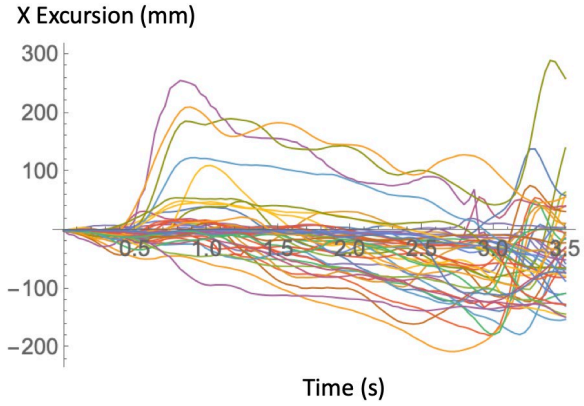

Figure 85. Subset of 50 time-zeroed head-CG excursions on the X axis (-X = forward) in turn-and-brake exposure.

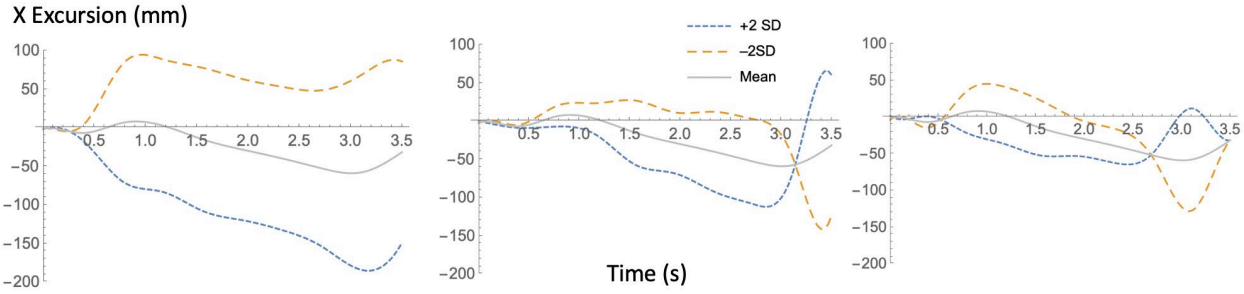

Figure 86. Illustration of first three PCs in X-axis (forward) excursion data from turn-and-brake trials.

Table 33. Effects of Predictors on Principal Component Scores: Turn and Brake X Excursion

Predictor	PC1	PC2	PC3
Seat Position	**		*
Feet Flat			*
Forward Lean	***	**	***
Recline			
Age	*		*
BMI			
Stature			
R^2_{adj}	0.27	0.04	0.23

* p<0.05, ** p<0.01, *** p<0.001

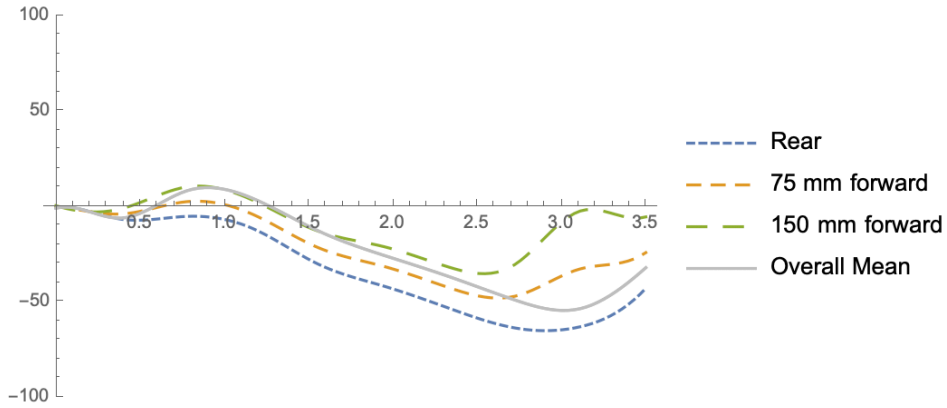

Figure 87. Effects of seat position on x-axis head excursion (mm) versus time (s) in turn-and-brake trials.

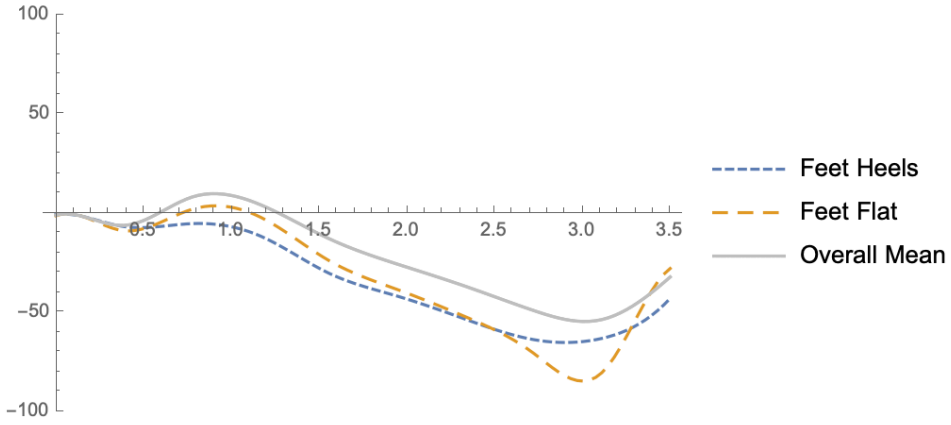

Figure 88. Effects of foot posture on x-axis head excursion (mm) versus time (s) in turn-and-brake trials.

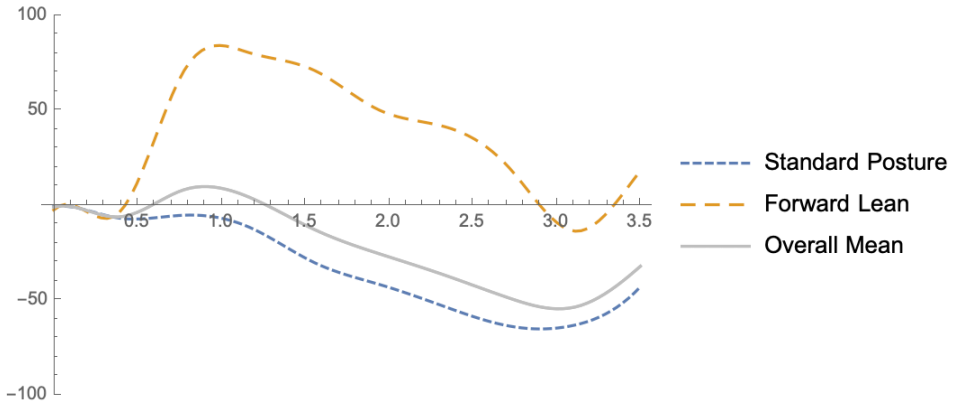

Figure 89. Effects of forward lean on x-axis head excursion (mm) versus time (s) in turn-and-brake trials.

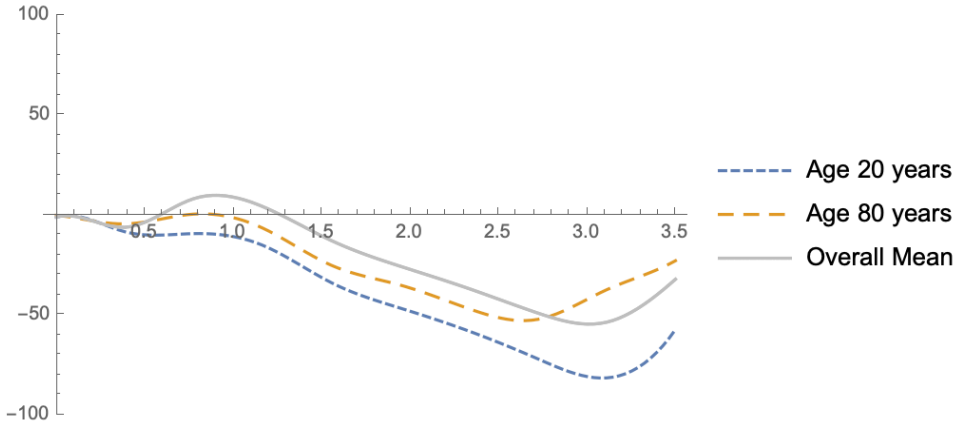

Figure 90. Effects of age on x-axis head excursion (mm) versus time (s) in turn-and-brake trials.

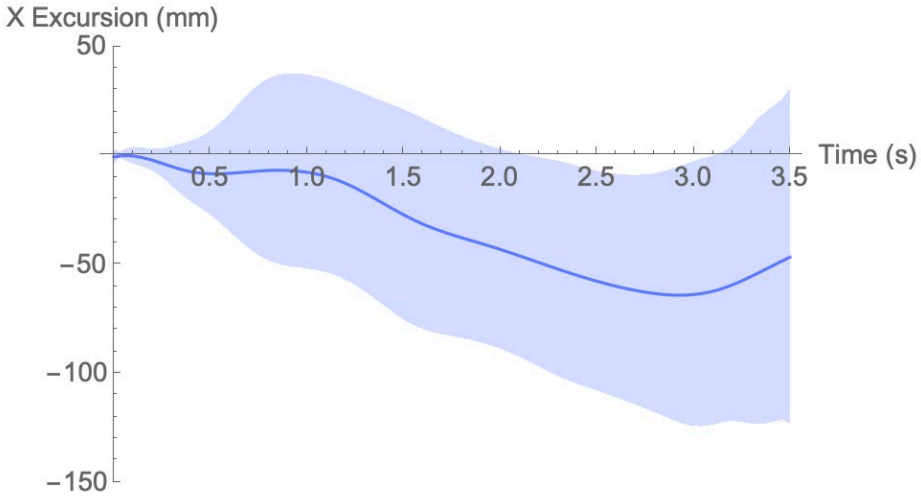

Figure 91. Mean±1SD corridor for head CG x-axis excursion in turn-and-brake trials, for seat full rear, feet on heels, seat back angle 23 deg, no forward lean, BMI=26 kg/m2, age = 45 years.

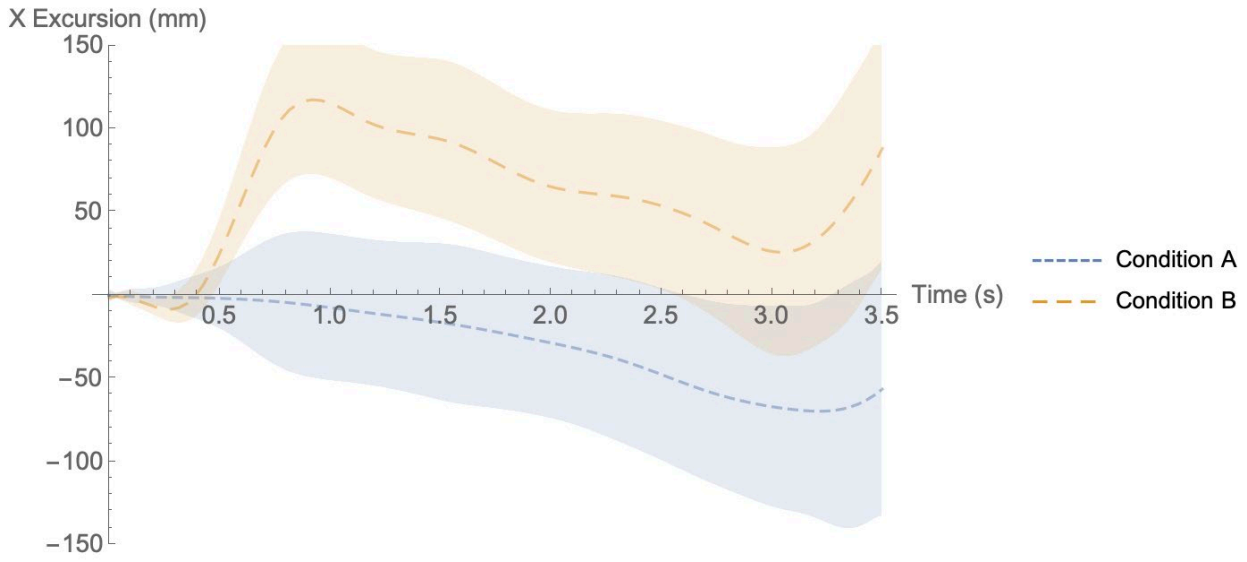

Figure 92. Mean±1SD corridor for head CG x-axis excursion in turn-and-brake trials for two extreme conditions. Condition A (all factors levels chosen to minimize excursion): seat full rearward, feet on heels, seat back angle 23 deg, no forward lean, BMI = 26 kg/m2, age = 45 years; Condition B (all factors levels chosen to maximize excursion): seat 150 mm forward, feet flat, seat back angle 23 deg, leaning forward, BMI=26 kg/m2, age = 45 years.

4.7.5 Head CG Trajectories — Turn and Brake — Y Excursions

The lateral excursions in the turn-and-brake trials were also highly variable, but the typical pattern was increasing inward excursion during the first part of the event, peaking before one second, followed by a return to near the seat centerline. As shown in Figure 90, peak inboard excursions varied widely across participants and conditions, from less than 50 mm inboard to more than 500 mm.

The median and 95th-percentile root-mean-square error for spline fits across curves were 5.2 and 10.7 mm, respectively. The first three PCs accounted for 89 percent of the variance and four PCs accounted for 95 percent. Figure 91 shows that the first PC is related to the overall magnitude of the excursion, the second relates primarily to the duration of the event, and the third is associated with the magnitude of the rebound phase.

Among the potential predictors, only forward lean had a substantial effect (Table 34), with minor differences in trajectory across recline angles and age (Figure 92-Figure 94). Excursion was smaller at larger recline angles. Taller statures were associated with slight smaller inboard excursions. Figure 95 shows an excursion corridor for a typical set of variable values, and Figure 96 shows corridors for extremes. At peak excursion, the standard deviation (half corridor width) is about 80 percent of the peak value, indicating a large amount of residual variance that is not accounted for by the potential predictors.

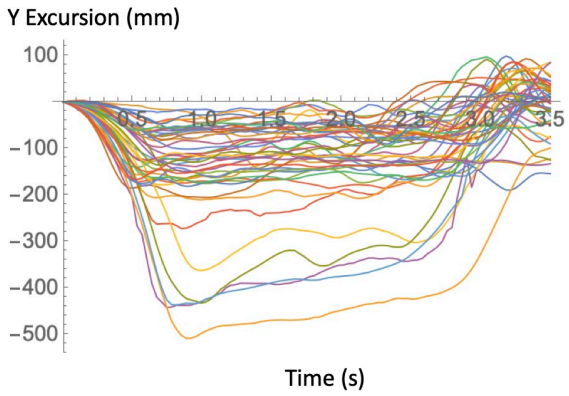

Figure 93. Subset of 50 time-zeroed head-CG excursions on the Y axis (-Y = inboard) in turn-and-brake exposure.

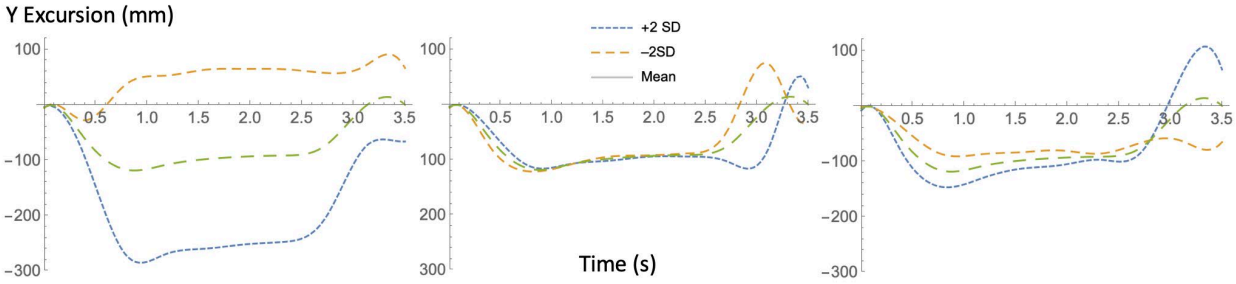

Figure 94. Illustration of first three PCs in Y-axis (lateral) excursion data from turn-and-brake trials.

Table 34. Effects of Predictors on Principal Component Scores: Turn and Brake Y Excursion

Predictor	PC1	PC2	PC3
Seat Position			
Feet Flat			
Forward Lean	***		
Recline	*		
Age			
BMI			
Stature			*
R^2_{adj}	0.26	0.00	0.04

* p<0.05, ** p<0.01, *** p<0.001

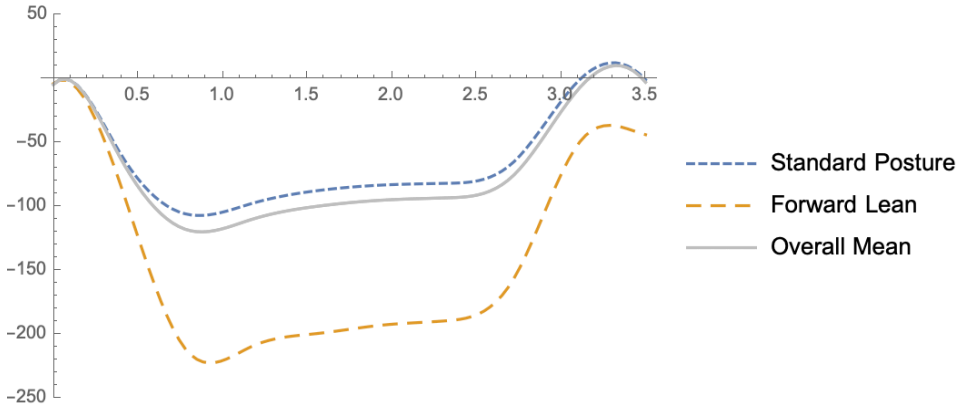

Figure 95. Effects of forward lean on y-axis head excursion (mm) versus time (s) in turn-and-brake trials.

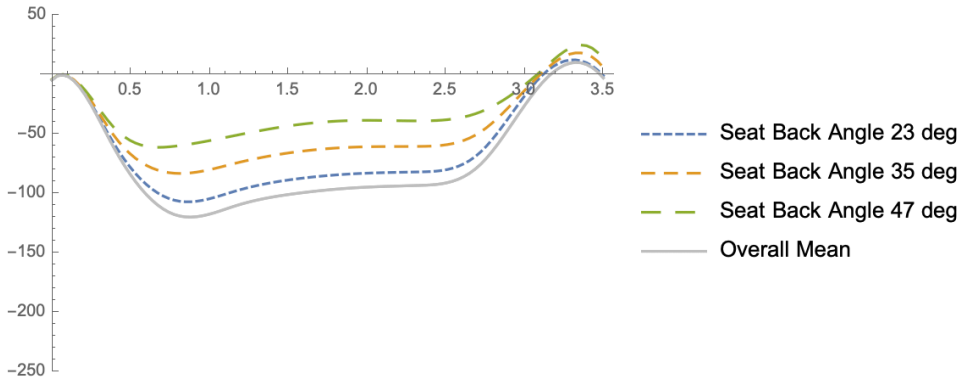

Figure 96. Effects of recline on y-axis head excursion (mm) versus time (s) in turn-and-brake trials.

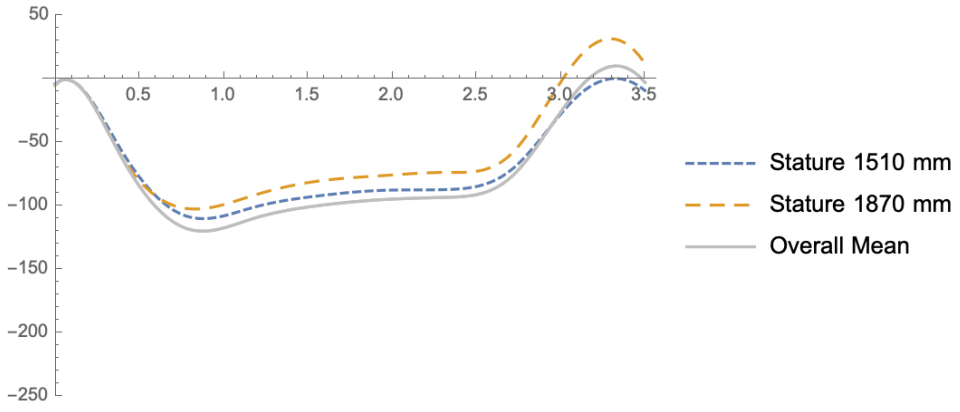

Figure 97. Effects of stature on y-axis head excursion (mm) versus time (s) in turn-and-brake trials.

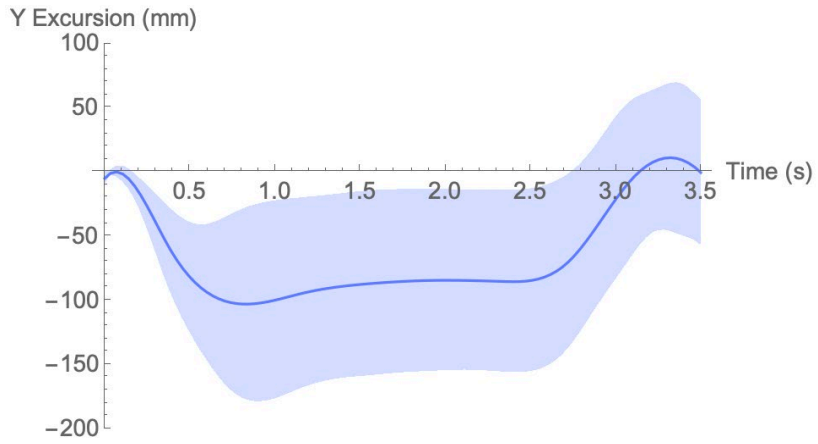

Figure 98. Mean±1SD corridor for head CG x-axis excursion in turn-and-brake trials, for seat full rear, feet on heels, seat back angle 23 deg, no forward lean, BMI=26 kg/m2, age = 45 years, stature 1,650 mm.

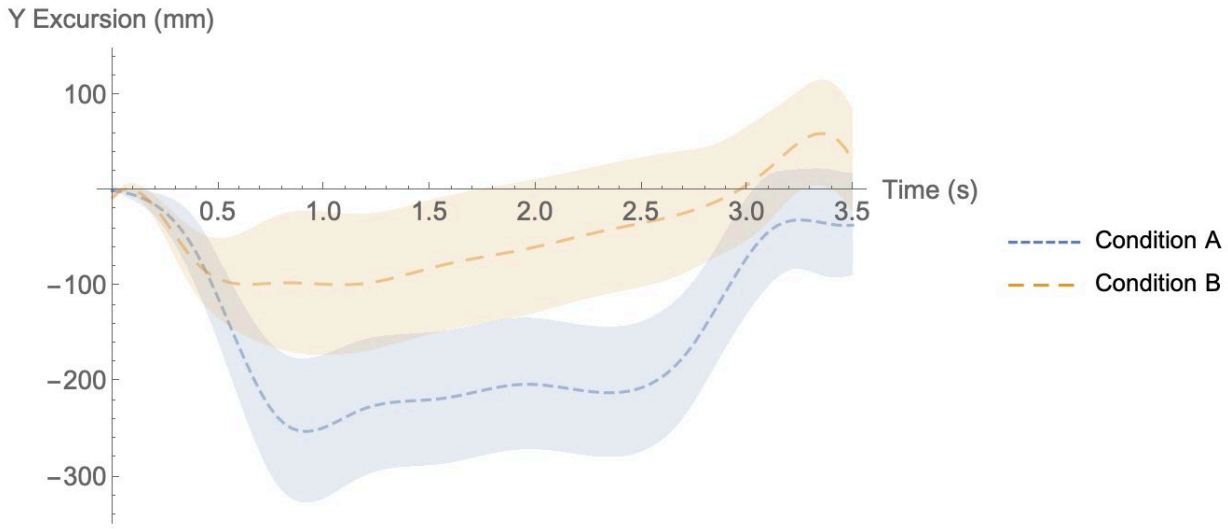

Figure 99. Mean±1SD corridor for head CG y-axis excursion in turn-and-brake trials in two extreme conditions. Condition A (all factors levels chosen to maximize excursion): seat full rearward, feet flat, seat back angle 23 deg, forward lean, BMI = 26 kg/m2, age = 45 years, stature =1510 mm; Condition B (all factors levels chosen to minimize excursion): seat 150 mm forward, feet on heels, seat back angle 47 deg, no lean, BMI=26 kg/m2, age = 45 years, stature=1,870 mm

5 DISCUSSION

5.1 Summary of Findings and Contributions

This study expanded the previous work in this area, notably the 2018 UMTRI study, by greatly expanding the range of initial passenger postures and positions. The choice of conditions was guided by a thorough literature review that identified some important gaps in knowledge. The primary goal of the 2018 study was to rigorously assess the effects of occupant characteristics on excursions, using a large subject pool (90 men and women). Because that study showed that the effects of gender and body dimensions were small, the current study was able to allocate participants to smaller groups to assess the effects of initial posture and positions.

The mean excursions observed in nominal postures were largely consistent with prior work. The mean maximum forward head excursion in braking across a range of conditions was -140 mm (SD 59), which is similar to the values of -135 (62) mm from Reed et al. (2018). In right lane change, the mean maximum inboard head excursion in comparable conditions was -118 (46) mm, almost identical to the corresponding values from the prior study of -118 (40) mm. The resulting excursion corridors are also very similar (compare Figure 61 and Figure 66 with Figure 2). Values were also similar for comparable events in the pilot and full-scale studies.

A primary finding that confirms the results of all previous studies in this domain is that the variance between passengers is large, with the standard deviation typically 50 percent or more of the mean response. Participant characteristics rarely account for more than 25 percent of the variance. However, some of the initial conditions investigated in this study had sizable effects.

Seat Position — Fore-aft seat position was hypothesized to affect head excursion by changing the relationship between the belt and the passenger's shoulder. In particular, the belt tends to wrap around the shoulder more, which may restrict torso motion to a greater extent. The study confirmed that forward head excursions in braking were smaller in more-forward seat positions. Although this finding is consistent with the hypothesis, it is also possible that being further forward in the vehicle caused participants to restrict their movements to a greater extent.

Foot Placement — Prior studies with child passengers found that having secure foot contact with the floor reduced excursion during vehicle maneuvers. The current study examined whether having the feet resting on the heels would produce different excursions than having the feet pulled rearward and resting on the soles (feet flat). A small trend was found toward greater excursions with the feet flat, particularly in lateral maneuvers.

Recline – Recline moves belt away from the torso, which was hypothesized to increase excursions, but also places more of the body weight on the seat back, which was hypothesized to reduce excursion. In braking, excursions were generally larger with greater recline, consistent with the first hypothesis. However, in lateral maneuvers, recline reduced excursions, consistent with the second hypothesis.

Vehicle — The pilot study found small but statistically significant differences in forward head excursion in braking between vehicles. However, the full-scale study did not find a similar difference when comparing between a passenger car and an SUV. However, the outboard head

excursion in left lane change was greater in the larger vehicle, consistent with the hypothesis that passengers will restrict their head movements to avoid contact based on the available space.

Locked Retractor — One potential explanation for the differences between vehicles in the pilot study was differences in the belt system. To assess one aspect of retractor performance, tests were conducted with and without the retractor pre-locked. No effect was found, indicating that the retractor was normally locking very early in the event in this test vehicle.

Leaning/Reaching — By far the largest effects on excursion were noted in the leaning/reaching trials. Participants who were leaning inboard on the armrest reduced their inboard excursions in right lane change but experienced increased excursions (approximately back to the seat centerline) in left lane change. When reaching/leaning forward or forward and inboard, forward excursions in braking were reduced, compared to the neutral posture, but lateral excursions in the lane-change and turn-and-brake events were greatly increased. The large excursion magnitudes and high variability suggested that participants had considerable difficulty controlling their lateral motions when leaning forward.

The previous study found that anthropometric effects were fairly small, so the lack of strong findings in the current study with much smaller number of participants per condition was not a surprise. Gender was not investigated in the current study because the small number of participants did not allow gender to be meaningfully distinguished from stature. However, a few trends with body size were noted.

Stature — Somewhat counter-intuitively, slightly smaller excursions were noted for taller individuals in a few conditions. This may have more to do with these larger participants having greater contact with the seat and vehicle trim than with their longer torsos.

Age — Consistent with the prior study, greater age was associated with reduced head excursion in a range of conditions. This trend could be due to greater biomechanical "stiffness" but is more likely produced primarily by a behavioral difference, with older individuals being more risk-averse and restricting their motions to a greater extent.

BMI — In the prior study, smaller forward head excursions in braking were noted for individuals with higher BMI. This trend was not apparent in the current study, which found only a minor association of higher BMI with greater lateral excursion in some conditions.

Overall, the most important finding of the study is that abrupt vehicle maneuvers associated with attempted crash avoidance can greatly increase the volume of the vehicle compartment within which the front-seat passenger's head could lie. These effects can be substantially magnified if the passenger is leaning forward at the time of the maneuver.

This study also makes a substantial contribution in the use of functional regression to produce parametric response corridors. Typically, kinematic response corridors are generated by simple averaging of a set of curves from individuals who are thought to be similar in size to the target. Often anthropometric differences are addressed by linear scaling based on body dimensions, even in the absence of evidence that such relationships exist. The approach in the current work was developed to model human motion data in ergonomics studies (see Faraway & Reed 2007, Faraway et al., 2007) and has previously been applied to kinematics data from low-speed sled

tests (Samuels et al., 2015). In addition to providing a rigorous way to assess the influence of potential predictors on trajectories, the method enables generation of response corridors for a wide range of conditions and occupant characteristics. The analysis in this report focused on excursion on a single axis versus time for each event (X and Y excursions were modeled separately for turn-and-brake events). The same approach can be used to model trajectories in two or three Cartesian dimensions, as well as simultaneous modeling of other variables, such as segment orientations. However, the presentations of corridors in multiple dimensions is more challenging and such corridors are less useful for the validation of computational models of occupants.

5.2 Implications

The primary implication of this study is that pre-crash maneuvers can produce a wide range of postures. Head excursion is one of the most important aspects of the passenger response to maneuvers, both because the head moves farther than other body parts and because protecting the head is a high priority in occupant protection.

The large amount of variability in the responses has important implications for simulations studies. Conventionally, simulations aim to obtain responses that are within a narrow corridor of a mean value for similar-size occupants. However, these data indicate that, under the conditions studied, occupant characteristics have small effects compared to between-subject variability that is not attributable to anything that can be known about the occupant. Consequently, stochastic simulation that spans the range of possible outcomes is needed.

These findings highlight the need for more research on the robustness of occupant protection systems to non-nominal postures. The lateral excursions are of particular concern because of the potential to change the interactions between the passenger's head and the air bags in both front and side impact. Belt engagement with the shoulder was usually maintained during this testing, but the consequences of changes in torso posture for belt interaction should also be investigated. Because occupant protection is more challenging when the range of postures is larger, systems that are able to reduce the range of pre-crash postures should continue to be studied.

5.3 Limitations

The analysis focused on excursions in the primary axes and only maximum excursions were subject to a scalar statistical analysis. However, the functional modeling showed that rebound motions could be as large or larger than the movement in the primary phase. Large rebound movements were generated by the turn-and-brake maneuver, frequently resulting in head locations outboard of the seat centerline. Forward reaching trials also produced large rebound motions as the vehicle acceleration stopped while the occupants were maintaining relatively large muscle exertions.

Rebound in these scenarios is caused primarily by lags in the passenger's motor control system. Specifically, the passenger's muscles tense to restrict movement during the vehicle acceleration event. The abrupt removal of the acceleration (vehicle comes to a stop in braking or straightens out in the lane-change maneuvers) causes the tensed muscles to accelerate the passenger's body

in the direction opposite of the initial motion until the motor control system can relax the agonist muscles and regain postural stability.

The consequences may be minimal if the passenger has rebounded close to the nominal posture when a crash occurs but rebound may have important consequences in a few situations. In left lane change, the inboard rebound can be larger than the initial outboard excursion, probably because the passenger activates their muscles to a large extent to prevent head contact with the vehicle interior. This inboard rebound can be larger than the inboard movement associated with a right lane change. The presence of contracted muscles also has the potential to change kinematics and internal tissue loading in certain crash scenarios, notably low-speed rear impact. More research is needed to assess the consequences of braking related excursions, including rebound, for the scenario of a rear-impact crash occurring during or immediately after the braking event.

One goal of the study was to gather data for the smallest front seat occupants, between 1,450 and 1,500 mm tall. Unfortunately, efforts to recruit individuals in this size range (typically children age 10 to 12) were not successful due to the timing of testing occurring during the summer. Future studies should address this group, who represent a small percentage of front-seat passengers but may be at greater risk.

Most crash avoidance maneuvers in the field have lower acceleration levels than those used in the current study. For example, Scanlon et al. (2015) reported an average braking deceleration in attempted avoidance of intersection crashes of 0.58 g. However, higher accelerations in attempted crash-avoidance maneuvers may become more common with increasing fleet penetration of automated crash-avoidance systems, notably automated braking. The effects of the vehicle acceleration level on the magnitude of head motions is unknown. Higher accelerations could be expected to produce higher excursions, but because the observed motions are mostly under the control of the passenger, it is possible that similar results would be observed with much lower accelerations.

The behaviors observed in the current study may not be representative of passengers who perceive an imminent crash. Anecdotal review of videos available online of crashes and near crashes suggest that occupants who detect a possible crash tend to move their bodies away from the expected crash location. However, the relationship between this behavior and the response due to vehicle motion is unknown. Importantly, the current data illustrate the range of head locations that are possible for alert, belted passengers.

Excursions could be larger in a wide range of scenarios. Poor belt fit or lack of belt use could increase excursions, as could higher accelerations due to vehicle contact with objects or furrowing in soft ground. Other factors with potential effects on excursions that could be addressed in future studies include:

Clothing – Heavy winter clothing would tend to increase slack in the belt system and could lead to larger excursions. However, we believe these effects would be small relative to the variance due to occupant body shape and behavior.

Seat Surface – We and others have conducted testing using relatively low-friction leather seat coverings. A higher-friction cloth surface might reduce excursions in lateral motions, but we anticipate that the effects would be small. Ghaffari et al. (2018) concluded from seat surface pressure measurements that pelvis motions during lane change and braking maneuvers were negligible.

Seat Bolstering – The contour of the seat back could influence responses in lateral accelerations. However, we believe that the range of bolstering across front seats is not large enough, relative to other factors such as passenger anthropometry, to be an important factor to study at this time. Holt et al. (2018) did not find inflatable bolsters to significantly affect lateral torso and head motions during oscillatory lateral accelerations.

Seat Orientation – Some concepts for highly automated vehicles have placed the seats oblique to the direction of travel. These conditions could alter the responses of occupants.

Pre-Pretensioning – Previous studies have shown significant reductions in excursions with pre-pretensioners. The current study did not find any effect of pre-locking of the retractor, suggesting that slack removal is needed to achieve a reduction in excursion; merely locking the belt to prevent spool-out is insufficient.

Vehicle Differences — The pilot study showed a difference in head excursion across vehicles, but data was similar in the two vehicles used in the full-scale study. Nonetheless, the data suggest that the relationship between the upper belt anchorage (D-ring) and the shoulder can influence kinematics. Since this can be affected by seat position as well as by vehicle design, more work is needed to determine if changes in belt geometry can be used to limit excursions. For example, seat-mounted belts might produce lower excursions. The current work does not suggest that differences in vehicle kinematics, for example in body roll during lane change, have important effects on excursions. However, these findings are limited to the vehicles used in testing, which did not include, for example, a large van.

This report focuses exclusively on the motion of the head CG, but other dependent measures could be analyzed using similar methods. Head orientation was obtained during the head tracking process. Head posture was analyzed in Reed et al. (2018) but no important findings were noted. Head and neck posture are determined by the passenger's acceptance of deviations from the nominal posture. Most participants maintained their heads in approximately the initial attitude, although some who entered the maneuver while looking at the questionnaire on their laps looked up and then back down at the paper. A qualitative review of the video from the trials shows that passengers tended to maintain a fairly constant relationship between the head and torso. That is, they tended to stiffen their necks during the event. During rebound, this sometimes resulted in the head pitching or rolling when the vehicle acceleration was removed. A subsequent analysis of head orientation and head posture relative to the torso would be most valuable for consideration of injury scenarios in low-speed rear-impact, for which neck and torso muscle exertions are known to have large effects on kinematics and may also influence injury risk.

Optical targets were applied to the belt. These targets can be tracked in three-dimensions using semi-automated methods, except in scenarios in which the targets were obscured by the participant's motion. Belt tracking data might be useful for tuning and validating computational models of occupant kinematics in pre-crash maneuvers.

6 REFERENCES

Bohman, K., Stockman, I., Jakobsson, L., Osvalder, A-L., Bostrom, O., & Arbogast, K. B. (2011). Kinematics and shoulder belt position of child rear seat passengers during vehicle maneuvers. *Annals of the Association for the Advancement of Automotive Medicine.* 55: 15–26.

Carlsson, S., & Davidsson, J. (2011, September 14-16). *Volunteer occupant kinematics during driver initiated and autonomous braking when driving in real traffic environments* (Conference report No. IRC-11-43). 11th International Research Council on Biomechanics of Injury Conference, Krakow, Poland.

Ejima, S., Zama, Y., Ono, K., Kaneoka, K., Shiina, I., & Asada, H. (2009, June 15-18). *Prediction of pre-impact occupant kinematic behavior based on the muscle activity during frontal collision* (Report 09-0913). 21st International Technical Conference on the Enhanced Safety of Vehicles, Stuttgart, Germany.

Faraway, J. J., & Reed, M. P. (2007). Statistics for digital human modeling in ergonomics. *Technometrics, 49*:262-276.

Faraway, J. J., Reed, M. P., & Wang, J. (2007). Modeling 3D trajectories using Bézier curves with application to hand motion. *Journal of the Royal Statistical Society Series C – Applied Statistics*, *56*(5):571-585

Hault-Dubrullea, A., Robachea, F., Pacauxa, M.-P., & Morvana, H. (2011). Determination of pre-impact occupant postures and analysis of consequences on injury outcome. Part I: A driving simulator study. *Accident Analysis and Prevention, 43*: 66–74

Ghaffari, G., Brolin, K., Bråse, D., Pipkorn, B., Svanberg, B., Jakobsson, L., & Davidsson, J. (2018, September 12-14). *Passenger kinematics in lane change and lane change with braking manoeuvres using two belt configurations: Standard and reversible pre-pretensioner* (Report No. IRC-18-80). 18th International Research Council on Biomechanics of Injury Conference, Athens, Greece.

Graci, V., Douglas, E.C., Seacrist, T., Kerrigan, J., Mansfield, J., Bolte, J., Sherony, R., Hallman,J .J., & Arbogast, K. B. (2018, September 12-14). *Effect of age on kinematics during pre-crash vehicle manoeuvres with sustained lateral acceleration* . (Report No. IRC-18-82). 18th International Research Council on Biomechanics of Injury Conference, Athens, Greece.

Holt, C., Douglas, E., Graci, V., Seacrist, T., Kerrigan, J., Kent, R., Balasubramanian, S., & Arbogast, K. (2018, September 12-14). *Effect of countermeasures on adult kinematics during pre-crash evasive swerving* (Report No. IRC-18-83). 18th International Research Council on Biomechanics of Injury Conference, Athens, Greece.

Huber, P., Kirschbichler, S., Prüggler, A., & Steidl, T. (2015, September 9-11). *Passenger kinematics in braking, lane change and oblique driving maneuvers* (Report No. IRC-15-89). 15th International Research Council on Biomechanics of Injury Conference, Lyon, France.

Iwamoto, M., Nakahira, Y., Kimpara, H., & Sugiyama, T. (2012). Development of a human body finite element model with multiple muscles and their controller for estimating occupant

motions and impact responses in frontal crash situations. *Stapp Car Crash Journal, 56*:231–268.

Kirschbichler, S., Huber, P., Prüggler, A., Steidl, T., Sinz, W., Mayer, C., & D`Addetta, G.A. (2014, September 10-12). *Factors influencing occupant kinematics during braking and lane change maneuvers in a passenger vehicle*. (Report No. IRC-14-70). 14th International Research Council on Biomechanics of Injury Conference, Berlin, Germany.

Morris, R., & Cross, G. (2005, June 6-9). *Improved understanding of passenger behavior during pre-impact events to aid smart restraint development* (Paper Number 05-0320). 19th International Technical Conference on the Enhanced Safety of Vehicles, Washington, DC.

Ólafsdóttir, J. M., Östh, J. K., Davidsson, J., & Brolin, K. B. (2013, September 11-13). *Passenger kinematics and muscle responses in autonomous braking events with standard and reversible pre-tensioned restraints*. (Report No. IRC-13-70). 13th International Research Council on Biomechanics of Injury Conference, Gothenburg, Sweden.

Östh, J., Brolin, K., & Bråse, D. (2014a) A human body model with active muscles for simulation of pre-tensioned restraints in autonomous braking interventions. *Traffic Injury Prevention, 16*(3):304–313.

Östh, J., Brolin, K., Carlsson, S., Wismans, J., & Davidsson, J. (2012). The occupant response to autonomous braking: A modeling approach that accounts for active musculature. *Traffic Injury Prevention, 13*(3):265–277.

Östh,. J., Brolin, K., & Happee, R. (2012). Active muscle response using feedback control of a finite element human arm model. *Computer Methods in Biomechanics and Biomedical Engineering, 15*(4):347–361.

Östh, J., Ólafsdóttir, J. M., Davidsson, J., & Brolin, K, (2013). Driver kinematic and muscle responses in braking events with standard and reversible pre-tensioned restraints: Validation data for human models. *Stapp Car Crash Journal*, *57*.

Östhmann, M., & Jakobsson, L. (2016, September 14-16). *An examination of pre-crash braking influence on occupant crash response using an active human body model*. (Report No. IRC-16-37). 16th International Research Council on Biomechanics of Injury Conference, Malaga, Spain.

Park, B.-K., Jones, M. L. H., Miller, C., Hallman, J., Sherony, R., & Reed, M. P. (2018). *In-vehicle occupant head tracking using a low-cost depth camera* (SAE Technical Paper 2018-01-1172). SAE International.

Ramsay, J., & Silverman, B. W. (2007). *Functional data analysis*. Springer, New York.

Reed, M. P., Ebert, S. M., & Hallman, J. J. (2013). Effects of driver characteristics on seat belt fit. *Stapp Car Crash Journal*, *57*:43-57.

Reed, M. P., Ebert, S. M., Park, B.-K. D., & Jones, M. L. H. (2018). Passenger kinematics during crash avoidance maneuvers (Technical Report UMTRI-2018-5). University of Michigan Transportation Research Institute.

Samuels, M. A., Reed, M. P., Arbogast, K. B., & Seacrist, T. (2015). Modeling spatial trajectories in dynamics testing using basis splines: application to tracking human

volunteers in low-speed frontal impacts. *Computer Methods in Biomechanics and Biomedical Engineering.* 10.1080/10255842.2015.1091886

Scanlon, J. M., Kusano, K. D., & Gabler, H. M. Analysis of driver evasive maneuvering prior to intersection crashes using event data recorders. *Traffic Injury Prevention. 16,* S182–S189, 2015.

Schneider, L. W., Robbins, D. H., Pflüg, M. A., & Snyder, R. G. (1983, December). Anthropometry of motor vehicle occupants: Development of anthropometrically based design specifications for an advanced adult anthropomorphic dummy family, Volume 1 (Report No. DOT HS 806 715). National Highway Traffic Safety Administration. Available at https://deepblue.lib.umich.edu/bitstream/handle/2027.42/259/72268.0001.001.pdf?sequence=2&isAllowed=y

Stockman, I. (2016). *Safety for children in cars – Focus on three point seatbelts in emergency events*. (Ph.D. dissertation). Chalmers University of Technology, Gothenburg, Sweden.

APPENDIX A: CUBIC BASIS SPLINE FITTING AND RECONSTRUCTION

Overview

The functional analysis of trajectory in this report employed standard methods described in Ramsay and Silverman (2005) and other work (see Faraway & Reed, 2007; Faraway et al., 2007; Samuels et al., 2015). Functional analysis differs from conventional statistical analysis in that the response is a function (e.g., of time or space) rather than a scalar value (for example, excursion vs time rather than maximum excursion).

A common first step in functional analysis is fitting a curve with a parametric spline. Splines enable both smoothing and a dramatic dimension reduction. The method used in the current work is described in detail in Samuels et al. (2015), though in the current work a single coordinate is fit.

Each curve was fitted using a weighted combination of the cubic spline basis functions depicted in Figure 99. Conceptually, each curve in Figure 99 is multiplied by a scalar weight such that the linear combination (weighted sum) approximates the curve. In the current case, 12 evenly spaced basis functions were used, resulting in each trajectory being reduced to a vector of 12 scalar values.

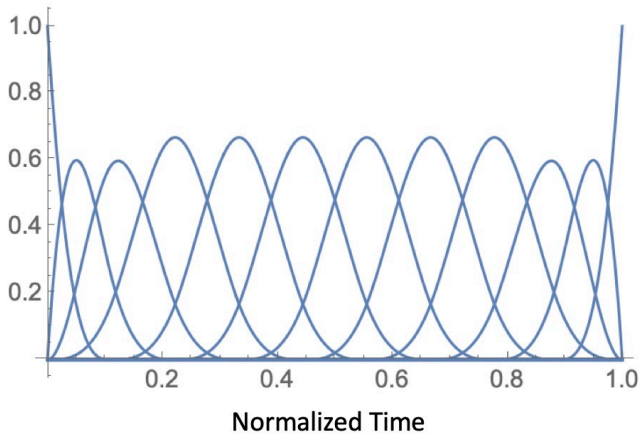

Figure 100. Twelve cubic spline basis functions.

As described in Appendices B and C, the vector of spline coefficients can be predicted by regression. The curve then must be reconstructed by multiplying the basis functions by their associated coefficients.

Mathematical Background

The k^{th} order (degree k-1) basis-spline (or b-spline $S(t)$ is a parametric curve composed of a linear combination of n+1 weights (coefficients) P and basis functions $N_i^k(t)$:

$$S(t) = \sum_{i=0}^{n} P_i N_i^k(t) \text{, where } 0 \leq t \leq 1$$

where $n - k + 2 > 0$. The b-spline curve is evaluated along the non-decreasing input parameter $t \in [0\ 1]$, or the normalized time vector in the case of these kinematic data. The vector T consists of $n + k + 1$ "knots" that locally control the shape of the b-spline curve. In the current work, the knots were evenly spaced from 0 to 1 in normalized time. (Due to the structure of the basis functions, it is necessary to duplicate knots at the beginning and end of the knot vector so that the approximating function interpolates the end points of the data. The knot vector used for the current fitting is {0, 0, 0, 0, 0.11.., 0.22.., …, 0.99…, 1, 1, 1, 1}).

The b-spline functions in Figure 99 are constructed by a recursive algorithm that utilizes the knot vector:

$$N_i^1(t) = \begin{cases} 1, T_i \le t \le T_{i+1} \\ 0, \text{otherwise} \end{cases}$$

$$N_i^k(t) = \frac{t - T_i}{T_{i+k-1} - T_i} \cdot N_i^{k-1}(t) + \frac{T_{i+k} - t}{T_{i+k} - T_{i+1}} \cdot N_{i+1}^{k-1}(t)$$

where the fraction is set to 0 if the numerator and denominator both equal 0. Note that many software packages provide the b-spline basis functions.

To fit the functions, the values of the function over time (K) are approximated by finding the set of n+1 coefficients P using linear least squares regression:

$$P = (N^T N)^{-1}(N^T K)$$

In implementation, a design matrix is constructed in which each of the spline functions is evaluated at each of 100 normalized time points. The function to be fit is evaluated at the same time point, then ordinary least squares regression is used to obtain the vector of coefficients.

The root-mean-square error (RMSE) of the resultant distance between the measured function K and the b-spline curve S was computed to assess goodness of fit:

$$RMSE = \sqrt{\frac{1}{k}\sum_{i=1}^{k}(S_i - K_i)^2}$$

where k is the length of t, K, and S.

Figure 100 shows an example head-CG excursion curve plotted in normalized time. Each of the basis functions in Figure 99 has been multiplied by a weight (coefficient) such that the sum of the functions approximates the data curve. (Note that these weights are negative, since the curve is below the horizontal axis.) In practice, the use of 12 basis functions is sufficient to produce median rms errors of below 5 mm in this dataset.

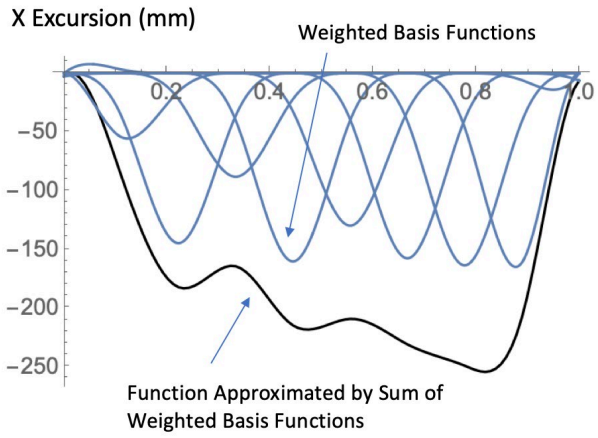

Figure 101. Approximating a function of time by weighted basis functions.

APPENDIX B: FUNCTIONAL REGRESSION EQUATIONS

The outcome of the functional trajectory analysis is a set of regression equations that predict principal component scores from initial conditions and anthropometric variables. Table B1 lists the variables and associated coding. Tables B2-B6 present the coefficients along with the residual root-mean-square error. Models are presented for the first four PCs. For consistency, the models use the same predictors; any predictor that was significant with $p<0.05$ for any of the first four PCs was included. To use the models, multiply each coefficient by the appropriate predictor value based on the coding in Table B1 and sum, adding in the intercept. The result is a principal component score. Assign zero to the remaining 8 PCs (which together account for less than 5 percent of the variance in the spline coefficients) to obtain a vector of 12 PC scores. These PC score vectors are then multiplied by the corresponding PC matrices — see Appendix C.

Table 35. Corridor Scenarios

Predictors	Values	Coding and Range
Seat Position	0	0 to 150 mm forward of full rear
Feet Flat	0	0 = feet on heels, 1 = feet flat
Forward Lean	0	0 = standard posture, 1 = forward lean
Recline	23	23-47 deg seat back angle (SAE J826 torso angle)
Age	45	20-80 years
BMI	26	20 to 35 kg/m2
Stature	1650	1510 to 1870 mm

Table 36. Regression Coefficients: Braking

Predictor	PC1	PC2	PC3	PC4
Seat Position	-0.877	0.149	0.206	0.040
Feet Flat	52.549	-27.206	1.843	-18.350
Forward Lean	-118.828	-3.518	25.238	-16.197
Recline	4.828	-1.168	3.962	1.456
Age	-1.915	-0.242	-0.099	-0.196
BMI				
Stature	-0.007	0.110	-0.088	0.004
Intercept	-11.7	-142.0	40.1	-29.7
R^2_{adj}	0.17	0.01	0.22	0.07
RMSE	165.9	101.9	49.1	48.3

Table 37. Regression Coefficients: Right Lane Change

Predictor	PC1	PC2	PC3	PC4
Seat Position	-0.174	0.120	0.274	-0.218
Feet Flat	0.929	56.630	21.671	2.647
Forward Lean	183.134	-8.533	-34.068	-10.726
Recline	-2.727	-4.074	0.597	-0.438
Age	-0.338	-0.884	-0.157	-0.090
BMI	0.541	2.057	3.068	1.012
Stature				
Intercept	51.3	74.4	-89.7	-4.6
R^2_{adj}	0.29	0.11	0.13	0.03
RMSE	109.8	106.9	70.2	43.4

Table 38. Regression Coefficients: Left Lane Change

Predictor	PC1	PC2	PC3	PC4
Seat Position				
Feet Flat	76.399	-32.262	12.325	10.398
Forward Lean	37.854	38.323	8.945	34.593
Recline	-3.937	-0.459	-2.726	0.159
Age				
BMI				
Stature				
Intercept	91.7	10.5	60.4	-11.1
R^2_{adj}	0.09	0.05	0.08	0.07
RMSE	126.6	72.5	60.2	39.6

Table 39. Regression Coefficients: Turn and Brake X

Predictor	PC1	PC2	PC3	PC4
Seat Position	-0.676	0.044	0.308	0.020
Feet Flat	-4.981	26.159	-40.116	8.837
Forward Lean	-231.228	-40.148	-86.925	19.049
Recline				
Age	-1.336	0.418	0.615	0.063
BMI				
Stature				
Intercept	94.5	-19.9	-11.9	-8.4
R^2_{adj}	0.28	0.03	0.22	0
RMSE	133.1	93.8	65.2	46.3

Table 40. Regression Coefficients: Turn and Brake Y

Predictor	PC1	PC2	PC3	PC4
Seat Position				
Feet Flat				
Forward Lean	282.835	-5.975	3.775	71.011
Recline	-4.716	0.556	-1.034	2.089
Age				
BMI				
Stature				
Intercept	87.2	-11.4	20.8	-65.2
R^2_{adj}	0.25	0	0	0.18
RMSE	179.6	95.4	77.7	55.7

APPENDIX C: PRINCIPAL COMPONENT ANALYSIS

Overview

A principal component analysis (PCA) of the spline coefficients was conducted for each analysis. When a set of variables is correlated, as is the case with the spline coefficients, most of the variance in the dataset can be represented by a smaller number of mutually orthogonal (independent) linear combinations of the original variables. These vectors in the space of the original data variables are called principal components (PCs) and typically are ordered from the direction in the data of greatest variance to least. For the current analysis, the PCs were computed as the eigenvectors of the covariance matrix. The associated eigenvalues are equal to the variance for each PC. The total of the eigenvalues is equal to the total variance in the dataset.

In the current study, 95 percent of the variance in the spline coefficients was accounted for by four or fewer PCs. Consequently, the regression analysis focused on the first four PCs. The regression analysis described in Appendix B produces a vector of PC scores (that is, coordinate values on each PC, if the PCs are visualized as a geometric space). To reconstruct a curve, the PC scores are multiplied by the PC matrix (eigenvectors) and the result added to the mean of the spline coefficients to obtain a coefficient vector. These coefficients are then multiplied by the basis functions, as described in Appendix A, to obtain the predicted curve.

This appendix presents the PC matrices M (columns are PCs) and mean vectors V for each of the analyses presented in Section 4.8. For each vector of PC scores S, compute

$$M.S + V = C$$

where C is a vector of spline coefficients.

Tables C1-C5 contain the principal component matrices. In these matrices, the PCs are in columns (verify that the norm of each column is unity). Right-multiply these matrices by a vector of PC scores obtained from the regression functions, then add the corresponding mean vector from Table C6 to obtain a predicted set of spline coefficients. Use these to reconstruct an excursion curve using the methods in Appendix A.

Table 41. Principal Component Matrix: Braking

PC1	PC2	PC3	PC4	PC5	PC6	PC7	PC8	PC9	PC10	PC11	PC12
-0.01030	-0.00965	0.04190	0.01099	-0.00714	0.03856	-0.01423	0.00562	-0.02472	-0.07929	-0.15833	-0.98193
0.04321	0.02884	-0.14898	-0.08449	0.01338	-0.18751	0.06962	-0.05599	0.12695	0.37681	0.85503	-0.18833
-0.06170	-0.24431	0.54262	0.29846	-0.64507	0.18980	0.11122	0.20468	-0.09235	0.03586	0.19153	0.00979
-0.27443	-0.07739	0.54800	-0.00951	0.66848	0.06958	0.28314	0.05629	-0.15057	-0.15697	0.18951	0.00692
-0.27747	-0.21934	0.15856	-0.12170	0.07897	0.00657	-0.71327	0.21295	0.50690	-0.10491	0.08117	0.00433
-0.33832	-0.17926	0.15744	0.03974	-0.00550	-0.13868	0.18698	-0.42804	0.32320	0.61002	-0.33617	-0.00127
-0.36470	-0.09850	-0.11818	-0.19221	-0.00904	-0.22595	-0.21066	0.41009	-0.61979	0.38490	-0.10190	-0.00485
-0.36527	-0.20624	-0.11837	0.01276	-0.14292	0.00712	-0.21986	-0.67678	-0.35455	-0.34755	0.19095	0.00778
-0.37715	-0.06593	-0.14513	-0.32523	-0.25123	-0.42418	0.46088	0.21178	0.25492	-0.40148	-0.00937	0.00199
-0.40192	-0.12721	-0.50968	0.48604	0.11968	0.46319	0.17311	0.22182	0.12103	0.01591	0.05715	-0.00831
-0.32167	0.78541	0.13899	0.40343	-0.06908	-0.26425	-0.14303	-0.01226	0.02437	-0.03712	0.01999	-0.00261
-0.23189	0.40438	0.05701	-0.58763	-0.16677	0.62275	0.05603	-0.05285	0.02448	0.10450	0.03242	0.00458

Table 42. Principal Component Matrix: Right Lane Change

PC1	PC2	PC3	PC4	PC5	PC6	PC7	PC8	PC9	PC10	PC11	PC12
0.00441	-0.01086	-0.02218	-0.01379	-0.03433	0.02332	0.01530	-0.00814	-0.01441	0.15616	-0.00130	0.98619
-0.03511	0.01858	0.07666	0.03677	0.10849	-0.04878	-0.10808	0.05477	0.07066	-0.96470	0.00244	0.16345
-0.02909	-0.19953	-0.35425	-0.21023	-0.62215	0.54004	0.20788	0.12788	-0.15026	-0.16756	-0.00961	-0.02525
-0.41362	-0.33447	-0.08952	-0.11925	-0.20404	-0.07443	-0.60757	-0.49242	0.18591	0.03028	0.02231	-0.00754
-0.60730	-0.28000	-0.02065	-0.01101	0.48701	0.34040	0.08154	0.40793	0.13782	0.07622	-0.03657	-0.00008
-0.49955	-0.10261	0.23038	-0.12566	-0.26054	-0.53745	0.45775	-0.02159	-0.31937	-0.04769	-0.00629	0.00377
-0.28031	0.46458	0.59477	0.22842	-0.19220	0.46592	-0.06701	-0.18255	-0.08583	0.02086	0.00496	0.00021
-0.15309	0.49290	-0.27034	-0.56896	0.22552	0.07016	0.27441	-0.37923	0.23446	-0.04144	-0.07234	0.00078
-0.17644	0.44736	-0.09724	-0.15853	-0.31907	-0.25156	-0.34598	0.60451	0.25869	0.07029	0.10986	-0.00070
-0.16003	0.26674	-0.40227	0.09441	0.21287	0.00512	-0.30041	-0.00776	-0.77235	-0.01723	-0.00674	-0.00075
-0.15670	0.13615	-0.32114	0.53839	-0.13220	-0.09586	0.12946	-0.06715	0.23195	-0.00947	-0.67977	0.00160
-0.15861	0.10159	-0.32462	0.47364	-0.03010	-0.02591	0.23034	-0.15523	0.19259	-0.02030	0.72012	0.00284

Table 43. Principal Component Matrix: Left Lane Chang

PC1	PC2	PC3	PC4	PC5	PC6	PC7	PC8	PC9	PC10	PC11	PC12
0.00519	-0.00818	0.01121	0.00999	-0.01959	-0.01215	0.00938	0.00817	0.00303	-0.15593	0.00529	0.98724
-0.00946	0.01525	-0.03237	0.00002	0.04970	0.05492	-0.09284	-0.04668	-0.09156	0.97281	0.05396	0.15711
0.13439	-0.22932	0.21932	0.39812	-0.62197	-0.23924	0.50141	0.01311	-0.13202	0.09455	0.02265	-0.01407
0.10251	0.03166	0.55350	-0.03472	-0.09456	-0.34522	-0.52829	0.52167	-0.00008	0.01740	0.03450	-0.00907
0.04647	0.11228	0.52987	0.08659	-0.24209	0.50729	-0.24478	-0.52509	0.20801	-0.02640	-0.03775	-0.00271
-0.03270	0.28719	0.52679	-0.40439	0.34190	-0.17138	0.51667	-0.12385	-0.21204	0.02899	-0.03172	0.00685
-0.32805	0.78226	-0.07445	0.50291	-0.03097	-0.07051	-0.01782	0.06119	-0.10563	-0.01981	-0.02138	-0.00055
-0.46068	0.06312	-0.02565	-0.43808	-0.45405	0.43627	0.11655	0.41081	-0.10558	0.01455	-0.03176	0.00231
-0.53327	-0.05208	-0.02152	-0.19972	-0.17687	-0.50561	-0.04681	-0.30799	0.51358	0.05273	0.14842	0.00386
-0.45000	-0.33278	0.07293	0.09454	0.05693	-0.10226	-0.27067	-0.28390	-0.69608	-0.09130	-0.10951	-0.00909
-0.30699	-0.26932	0.19062	0.30494	0.30240	0.11813	0.16061	0.23017	0.32964	0.07612	-0.63648	0.01258
-0.25909	-0.22165	0.19435	0.28726	0.30457	0.24156	0.13702	0.18287	0.08180	-0.03205	0.74319	-0.00868

Table 44. Principal Component Matrix: Turn and Brake X Excursion

PC1	PC2	PC3	PC4	PC5	PC6	PC7	PC8	PC9	PC10	PC11	PC12
-0.00168	0.00653	0.01959	0.00690	-0.00641	-0.00433	0.03070	0.08842	-0.00963	-0.02955	-0.18228	-0.97802
0.00513	-0.02602	-0.07795	-0.02201	0.01418	-0.00707	-0.11140	-0.33989	0.01172	0.11747	0.89868	-0.20734
0.03052	0.02080	0.20137	0.05521	-0.13377	0.16103	0.47629	0.71643	-0.15156	-0.09738	0.37183	0.01952
-0.30596	-0.08865	-0.26838	0.03528	0.56919	-0.39412	-0.19531	0.31606	0.10249	-0.42884	0.11602	0.00559
-0.25291	-0.06775	-0.26098	0.07619	0.11217	-0.09859	0.63450	-0.38668	-0.51538	-0.11244	-0.06968	0.00141
-0.30387	-0.25330	-0.28280	-0.00360	0.20290	0.13122	-0.07464	0.26382	-0.11102	0.78469	-0.04339	-0.00179
-0.28289	-0.16097	-0.13990	-0.03724	-0.18640	-0.03279	0.44202	-0.08726	0.79599	0.02523	-0.00617	-0.00375
-0.29172	-0.27905	-0.17867	-0.03815	-0.08678	0.77021	-0.21483	-0.03484	-0.05409	-0.39060	-0.00456	-0.00476
-0.30302	-0.26338	-0.09501	-0.16210	-0.70211	-0.43276	-0.23382	0.11460	-0.22253	-0.07468	0.01805	0.00633
-0.41244	-0.30879	0.81813	0.02730	0.19289	-0.04877	-0.01469	-0.14925	-0.03023	0.03829	-0.00135	-0.00039
-0.43089	0.67022	0.05494	-0.59345	0.01954	0.08362	-0.00313	0.01049	-0.02601	0.04063	0.01093	-0.00053
-0.36934	0.45226	-0.00230	0.77930	-0.17694	0.02803	-0.13059	-0.00525	0.02674	0.04066	0.01361	0.00153

Table 45. Principal Component Matrix: Turn and Brake Y Excursion

PC1	PC2	PC3	PC4	PC5	PC6	PC7	PC8	PC9	PC10	PC11	PC12
0.00219	0.00608	-0.02107	0.05743	-0.01335	-0.01304	-0.04539	-0.00996	0.04561	0.00915	-0.20076	-0.97532
-0.01184	-0.02234	0.06720	-0.21521	0.05558	0.02222	0.14295	0.00087	-0.15003	-0.02707	0.92365	-0.21940
0.00198	0.14899	-0.21762	0.88410	-0.04428	-0.14346	-0.22923	-0.04651	-0.04277	-0.01011	0.26342	0.01504
-0.45528	-0.00270	-0.19005	-0.12066	0.41608	0.17827	-0.38363	-0.41992	0.38207	0.24625	0.08267	0.01319
-0.37078	0.01439	-0.13843	0.10796	0.25428	0.32163	0.28224	-0.12093	-0.73705	0.02888	-0.15770	-0.01281
-0.39666	-0.03372	-0.07748	-0.05239	0.16291	-0.17081	-0.12098	0.25236	0.06987	-0.83288	-0.01304	-0.00127
-0.37868	0.00448	-0.10861	0.19554	-0.15114	0.22674	0.62900	0.29791	0.47642	0.14022	0.03530	-0.00391
-0.38008	-0.02103	0.01803	-0.10318	0.01881	-0.51284	-0.21188	0.52703	-0.19317	0.46987	-0.00484	0.00000
-0.35412	-0.01305	-0.17869	-0.14852	-0.77730	-0.16461	-0.03930	-0.41739	-0.10198	-0.05268	0.01384	0.00505
-0.10939	-0.87902	0.38596	0.23010	-0.00319	-0.02201	-0.00815	-0.11298	0.00288	0.00829	0.00577	0.00038
-0.21665	0.41987	0.72412	0.11788	0.11361	-0.29114	0.20468	-0.30714	0.04739	-0.02483	-0.04208	0.00002
-0.15997	0.16221	0.41113	0.04479	-0.30025	0.62257	-0.44661	0.30866	-0.05034	-0.00438	0.04510	-0.00386

Table 46. Mean Spline Coefficient Vectors

Braking	Left LC	Right LC	T&BX	T&BY
-0.8	-2.4	2.3	-0.7	-4.2
-0.7	5.8	-4.7	2.4	13.9
-110.1	-62.6	67.6	-15.6	-71.0
-123.0	-116.3	92.9	13.0	-129.6
-103.6	-110.5	79.4	5.6	-105.7
-134.2	-84.5	48.4	-16.4	-97.0
-111.0	47.7	-44.6	-28.0	-92.4
-131.8	78.7	-76.8	-39.0	-90.6
-142.0	64.4	-73.9	-52.6	-90.5
-158.5	38.8	-43.9	-64.7	11.5
-29.6	12.1	-19.2	-42.9	22.5
-7.8	7.4	-13.0	-31.0	0.7

APPENDIX D: EXCURSION CORRIDORS

This appendix presents mean excursion corridors for some typical scenarios. Table D1 lists the conditions for each corridor. Note that the standard deviation (SD) at each time point is independent of the mean prediction, so it may be used with any other prediction made using the models in this report. Not all of the predictors are used in the regression model for every event, so when a predictor is missing from the regression model its value does not affect the corridor.

Table 47. Corridor Scenarios

Predictors	Values	Coding and Range
Seat Position	0	0 to 150 mm forward of full rear
Feet Flat	0	0 = feet on heels, 1 = feet flat
Forward Lean	0	0 = standard posture, 1 = forward lean
Recline	23	23-47 deg seat back angle (SAE J826 torso angle)
Age	45	20-80 years
BMI	26	20 to 35 kg/m2
Stature	1650	1510 to 1870 mm

Table 48. Excursion Corridors for Braking and Lane Change

Braking			Right	Lane	Change	Left	Lane	Change
Time (s)	Mean (mm)	SD	Time (s)	Mean (mm)	SD	Time (s)	Mean (mm)	SD
0.000	-1.7	5.3	0.000	-2.7	3.7	0.000	2.0	3.0
0.022	-2.3	2.5	0.028	-1.3	2.1	0.028	1.4	2.2
0.044	-5.7	6.4	0.057	-1.9	4.7	0.057	2.5	4.9
0.067	-11.4	9.3	0.085	-4.4	6.9	0.085	5.1	7.2
0.089	-19.1	11.4	0.113	-8.4	8.7	0.113	9.1	9.3
0.111	-28.3	13.3	0.141	-13.7	10.8	0.141	14.0	11.5
0.133	-38.6	15.4	0.170	-20.1	13.5	0.170	19.8	13.9
0.156	-49.6	17.9	0.198	-27.2	16.6	0.198	26.1	16.6
0.178	-60.9	21.0	0.226	-34.7	20.2	0.226	32.8	19.4
0.200	-72.1	24.4	0.255	-42.6	23.9	0.255	39.5	22.2
0.222	-82.8	27.8	0.283	-50.3	27.5	0.283	46.1	24.9
0.244	-92.5	30.9	0.311	-57.8	30.9	0.311	52.4	27.2
0.267	-101.0	33.7	0.339	-64.7	33.8	0.339	58.0	29.0
0.289	-108.2	36.0	0.368	-71.1	36.3	0.368	63.0	30.3
0.311	-114.2	38.0	0.396	-76.9	38.7	0.396	67.5	31.4
0.333	-119.1	39.9	0.424	-82.1	40.8	0.424	71.4	32.1
0.356	-123.0	41.7	0.453	-86.8	43.0	0.453	74.8	32.7

Braking			Right	Lane	Change	Left	Lane	Change
Time (s)	Mean (mm)	SD	Time (s)	Mean (mm)	SD	Time (s)	Mean (mm)	SD
0.378	-126.0	43.5	0.481	-90.9	45.1	0.481	77.7	33.3
0.400	-128.1	45.3	0.509	-94.4	47.3	0.509	80.1	33.8
0.422	-129.4	47.0	0.537	-97.4	49.6	0.537	82.1	34.3
0.444	-130.0	48.6	0.566	-99.9	51.8	0.566	83.6	34.8
0.467	-130.0	50.1	0.594	-101.8	54.0	0.594	84.8	35.3
0.489	-129.5	51.3	0.622	-103.2	56.2	0.622	85.5	35.7
0.511	-128.6	52.3	0.651	-104.0	58.1	0.651	85.9	36.0
0.533	-127.3	52.9	0.679	-104.4	59.9	0.679	86.0	36.3
0.556	-125.7	53.4	0.707	-104.3	61.6	0.707	85.8	36.5
0.578	-123.9	53.7	0.735	-103.9	63.0	0.735	85.3	36.6
0.600	-122.1	53.9	0.764	-103.2	64.4	0.764	84.6	36.8
0.622	-120.3	54.1	0.792	-102.2	65.6	0.792	83.6	36.9
0.644	-118.6	54.3	0.820	-101.0	66.6	0.820	82.4	37.0
0.667	-117.2	54.5	0.848	-99.6	67.4	0.848	81.0	37.2
0.689	-116.0	54.8	0.877	-98.2	68.0	0.877	79.5	37.2
0.711	-115.2	55.0	0.905	-96.7	68.4	0.905	77.8	37.2
0.733	-114.9	55.3	0.933	-95.3	68.5	0.933	76.0	37.2
0.756	-115.2	55.5	0.962	-93.9	68.3	0.962	74.1	37.1
0.778	-115.9	55.7	0.990	-92.5	67.9	0.990	72.0	36.9
0.800	-117.0	56.0	1.018	-90.9	67.3	1.018	69.8	36.8
0.822	-118.4	56.2	1.046	-89.2	66.5	1.046	67.3	36.7
0.844	-120.0	56.6	1.075	-87.2	65.5	1.075	64.5	36.7
0.867	-121.6	56.9	1.103	-84.7	64.5	1.103	61.5	36.8
0.889	-123.3	57.3	1.131	-81.8	63.3	1.131	58.0	36.9
0.911	-124.7	57.8	1.160	-78.3	62.1	1.160	54.2	37.2
0.933	-126.0	58.2	1.188	-74.1	60.8	1.188	49.9	37.6
0.956	-126.9	58.7	1.216	-69.1	59.5	1.216	45.1	38.0
0.978	-127.4	59.1	1.244	-63.3	58.3	1.244	39.8	38.5
1.000	-127.4	59.4	1.273	-56.5	57.1	1.273	33.9	39.2
1.022	-126.9	59.6	1.301	-48.8	56.1	1.301	27.5	40.0
1.044	-126.1	59.9	1.329	-40.6	55.5	1.329	20.8	41.1
1.067	-125.0	60.1	1.358	-31.9	55.2	1.358	13.8	42.5
1.089	-123.7	60.4	1.386	-22.8	55.3	1.386	6.6	44.3
1.111	-122.3	60.8	1.414	-13.6	55.7	1.414	-0.6	46.2
1.133	-120.8	61.1	1.442	-4.3	56.5	1.442	-7.8	48.2
1.156	-119.5	61.5	1.471	4.7	57.4	1.471	-14.8	50.3
1.178	-118.3	61.9	1.499	13.5	58.4	1.499	-21.5	52.1
1.200	-117.3	62.3	1.527	21.7	59.2	1.527	-27.8	53.7

Braking			Right	Lane		Left	Lane	
Time (s)	Mean (mm)	SD	Time (s)	Mean (mm)	SD	Time (s)	Mean (mm)	SD
1.222	-116.6	62.7	1.556	29.3	59.9	1.556	-33.7	54.9
1.244	-116.4	63.0	1.584	36.1	60.1	1.584	-39.0	55.6
1.267	-116.5	63.2	1.612	42.1	60.1	1.612	-43.7	56.0
1.289	-116.9	63.5	1.640	47.5	59.9	1.640	-47.9	56.0
1.311	-117.6	63.8	1.669	52.1	59.5	1.669	-51.6	56.0
1.333	-118.6	64.1	1.697	56.0	59.2	1.697	-54.9	55.9
1.356	-119.7	64.5	1.725	59.4	59.0	1.725	-57.7	55.8
1.378	-121.0	64.8	1.754	62.1	58.8	1.754	-60.1	56.0
1.400	-122.5	65.2	1.782	64.3	58.8	1.782	-62.1	56.3
1.422	-124.0	65.6	1.810	66.1	58.9	1.810	-63.7	56.8
1.444	-125.5	65.9	1.838	67.3	59.0	1.838	-65.1	57.4
1.467	-127.0	66.1	1.867	68.2	59.1	1.867	-66.1	58.2
1.489	-128.4	66.2	1.895	68.7	59.1	1.895	-66.9	58.9
1.511	-129.8	66.2	1.923	68.8	59.0	1.923	-67.4	59.7
1.533	-131.2	66.3	1.952	68.7	58.8	1.952	-67.7	60.4
1.556	-132.5	66.3	1.980	68.2	58.5	1.980	-67.7	61.1
1.578	-133.8	66.3	2.008	67.5	58.1	2.008	-67.6	61.7
1.600	-135.0	66.5	2.036	66.6	57.6	2.036	-67.2	62.3
1.622	-136.2	66.6	2.065	65.6	57.1	2.065	-66.6	62.8
1.644	-137.4	66.9	2.093	64.4	56.5	2.093	-65.8	63.3
1.667	-138.6	67.1	2.121	63.1	55.8	2.121	-64.9	63.7
1.689	-139.8	67.4	2.149	61.8	55.1	2.149	-63.8	64.0
1.711	-141.0	67.6	2.178	60.5	54.3	2.178	-62.5	64.2
1.733	-142.2	67.7	2.206	59.1	53.3	2.206	-61.1	64.3
1.756	-143.2	67.8	2.234	57.7	52.3	2.234	-59.5	64.2
1.778	-143.9	67.9	2.263	56.3	51.2	2.263	-57.8	64.0
1.800	-144.1	68.0	2.291	54.8	50.0	2.291	-56.0	63.8
1.822	-143.8	68.1	2.319	53.2	48.9	2.319	-54.0	63.4
1.844	-142.7	68.1	2.347	51.6	47.8	2.347	-52.0	62.9
1.867	-140.7	68.1	2.376	49.7	46.7	2.376	-49.8	62.2
1.889	-137.6	68.0	2.404	47.8	45.7	2.404	-47.6	61.5
1.911	-133.3	67.9	2.432	45.6	44.7	2.432	-45.3	60.6
1.933	-127.6	67.8	2.461	43.2	43.7	2.461	-42.9	59.5
1.956	-120.5	67.8	2.489	40.6	42.6	2.489	-40.4	58.3
1.978	-111.7	68.1	2.517	37.7	41.6	2.517	-37.9	56.9
2.000	-101.6	68.8	2.545	34.7	40.6	2.545	-35.3	55.5
2.022	-90.6	70.0	2.574	31.5	39.7	2.574	-32.8	53.9
2.044	-79.0	71.5	2.602	28.4	39.1	2.602	-30.3	52.3

Braking			Right	Lane	Change	Left	Lane	Change
Time (s)	Mean (mm)	SD	Time (s)	Mean (mm)	SD	Time (s)	Mean (mm)	SD
2.067	-67.1	72.8	2.630	25.3	38.6	2.630	-27.9	50.8
2.089	-55.4	73.6	2.659	22.4	38.3	2.659	-25.5	49.3
2.111	-44.2	73.6	2.687	19.7	38.1	2.687	-23.4	47.8
2.133	-33.9	72.3	2.715	17.3	38.0	2.715	-21.3	46.3
2.156	-24.7	70.0	2.743	15.3	38.0	2.743	-19.5	44.9
2.178	-17.2	67.4	2.772	13.8	37.9	2.772	-17.9	43.6
2.200	-11.6	66.3	2.800	12.9	37.8	2.800	-16.5	42.5

Table 49. Excursion Corridors for Turn and Brake

Turn	& Brake	X	Turn	& Brake	Y
Time (s)	Mean (mm)	SD	Time (s)	Mean (mm)	SD
0.000	-0.6	3.1	0.000	-4.9	5.0
0.035	0.0	1.0	0.035	-0.8	1.6
0.071	0.1	2.6	0.071	0.2	4.1
0.106	-0.2	3.7	0.106	-1.4	6.1
0.141	-0.7	4.1	0.141	-5.2	7.6
0.177	-1.5	4.5	0.177	-10.8	9.6
0.212	-2.4	5.1	0.212	-17.9	12.5
0.247	-3.4	6.3	0.247	-26.1	16.1
0.283	-4.5	7.9	0.283	-34.8	20.3
0.318	-5.5	9.7	0.318	-43.9	24.7
0.354	-6.4	11.6	0.354	-52.7	28.9
0.389	-7.2	13.3	0.389	-61.1	32.7
0.424	-7.7	14.9	0.424	-68.5	36.1
0.460	-8.1	16.6	0.460	-75.1	39.1
0.495	-8.2	18.6	0.495	-80.9	42.1
0.530	-8.3	21.0	0.530	-85.8	45.3
0.566	-8.2	23.7	0.566	-90.0	48.6
0.601	-8.1	26.7	0.601	-93.6	52.2
0.636	-7.8	29.9	0.636	-96.4	56.0
0.672	-7.6	33.0	0.672	-98.7	59.8
0.707	-7.3	36.0	0.707	-100.4	63.6
0.742	-7.1	38.7	0.742	-101.6	67.0
0.778	-6.9	40.9	0.778	-102.4	70.0
0.813	-6.7	42.6	0.813	-102.7	72.3
0.848	-6.7	43.8	0.848	-102.7	73.9

Turn	& Brake	X	Turn	& Brake	Y
Time (s)	Mean (mm)	SD	Time (s)	Mean (mm)	SD
0.884	-6.7	44.5	0.884	-102.4	75.1
0.919	-6.8	45.0	0.919	-101.8	75.7
0.955	-7.1	45.2	0.955	-101.0	75.9
0.990	-7.5	45.2	0.990	-100.0	75.7
1.025	-8.0	45.1	1.025	-98.9	75.3
1.061	-8.6	44.9	1.061	-97.7	74.8
1.096	-9.4	44.8	1.096	-96.5	74.1
1.131	-10.4	44.6	1.131	-95.3	73.5
1.167	-11.5	44.6	1.167	-94.1	72.8
1.202	-12.8	44.6	1.202	-93.1	72.3
1.237	-14.2	44.6	1.237	-92.1	71.9
1.273	-15.8	44.8	1.273	-91.3	71.6
1.308	-17.5	45.0	1.308	-90.5	71.4
1.343	-19.3	45.4	1.343	-89.8	71.4
1.379	-21.1	45.8	1.379	-89.2	71.4
1.414	-22.9	46.2	1.414	-88.6	71.5
1.449	-24.6	46.6	1.449	-88.1	71.6
1.485	-26.4	47.0	1.485	-87.6	71.8
1.520	-28.0	47.3	1.520	-87.2	72.0
1.556	-29.6	47.4	1.556	-86.8	72.1
1.591	-31.0	47.4	1.591	-86.4	72.1
1.626	-32.3	47.2	1.626	-86.1	72.1
1.662	-33.5	46.9	1.662	-85.8	72.1
1.697	-34.7	46.5	1.697	-85.5	72.1
1.732	-35.7	46.1	1.732	-85.2	72.1
1.768	-36.7	45.7	1.768	-85.0	72.1
1.803	-37.7	45.4	1.803	-84.8	72.1
1.838	-38.6	45.2	1.838	-84.6	72.1
1.874	-39.5	45.0	1.874	-84.4	72.1
1.909	-40.5	44.9	1.909	-84.3	72.1
1.944	-41.4	44.9	1.944	-84.3	72.0
1.980	-42.4	45.0	1.980	-84.2	71.8
2.015	-43.4	45.1	2.015	-84.2	71.6
2.051	-44.4	45.4	2.051	-84.2	71.4
2.086	-45.5	45.8	2.086	-84.3	71.2
2.121	-46.6	46.3	2.121	-84.3	71.0
2.157	-47.7	46.9	2.157	-84.4	70.9
2.192	-48.7	47.5	2.192	-84.5	70.9

Turn	& Brake	X	Turn	& Brake	Y
Time (s)	Mean (mm)	SD	Time (s)	Mean (mm)	SD
2.227	-49.8	48.2	2.227	-84.7	71.0
2.263	-50.9	48.8	2.263	-84.8	71.2
2.298	-52.0	49.3	2.298	-84.9	71.4
2.333	-53.0	49.8	2.333	-85.1	71.6
2.369	-54.0	50.1	2.369	-85.2	71.8
2.404	-55.0	50.3	2.404	-85.3	72.0
2.439	-56.0	50.5	2.439	-85.2	72.2
2.475	-56.9	50.8	2.475	-84.9	72.4
2.510	-57.8	51.0	2.510	-84.2	72.5
2.545	-58.7	51.3	2.545	-83.2	72.6
2.581	-59.5	51.7	2.581	-81.8	72.5
2.616	-60.2	52.2	2.616	-79.8	72.2
2.652	-60.9	52.7	2.652	-77.2	71.6
2.687	-61.6	53.3	2.687	-74.0	70.9
2.722	-62.2	53.9	2.722	-69.9	69.8
2.758	-62.7	54.6	2.758	-65.1	68.6
2.793	-63.1	55.4	2.793	-59.6	67.3
2.828	-63.5	56.3	2.828	-53.6	66.1
2.864	-63.8	57.3	2.864	-47.1	65.2
2.899	-63.9	58.4	2.899	-40.4	64.5
2.934	-64.0	59.4	2.934	-33.6	64.0
2.970	-63.9	60.2	2.970	-26.9	63.5
3.005	-63.6	60.8	3.005	-20.3	63.0
3.040	-63.3	61.0	3.040	-14.1	62.1
3.076	-62.7	61.0	3.076	-8.3	60.7
3.111	-61.9	60.6	3.111	-3.2	58.8
3.146	-61.0	60.3	3.146	1.3	56.6
3.182	-59.9	60.3	3.182	4.9	54.6
3.217	-58.7	61.0	3.217	7.7	53.4
3.253	-57.3	62.5	3.253	9.7	53.2
3.288	-55.9	64.4	3.288	10.9	54.0
3.323	-54.3	66.4	3.323	11.3	55.3
3.359	-52.8	68.2	3.359	10.7	56.5
3.394	-51.2	69.6	3.394	9.3	57.0
3.429	-49.6	70.7	3.429	7.1	56.4
3.465	-48.0	72.2	3.465	3.8	55.1
3.500	-46.5	75.8	3.500	-0.3	54.4

DOT HS 812 997
February 2021

U.S. Department
of Transportation

**National Highway
Traffic Safety
Administration**

14909-022621-v6